Supplementary Table 1. Nomenclature for fat traits and adjustment models.

Abbreviation	Trait Name
Fat Volume Traits	
SAT	Subcutaneous adipose tissue volume
VAT	Visceral adipose tissue volume
VATadjBMI	Visceral adipose tissue volume adjusted for BMI
PAT	Pericardial fat volume
PATadjHtWt	Pericardial fat volume adjusted for height and weight
Fat Attenuation Traits	
SATHU	Subcutaneous adipose tissue attenuation
VATHU	Visceral adipose tissue attenuation
Relative Fat Distribution Traits	
VAT/SAT ratio	Ratio of visceral to subcutaneous adipose tissue volume
VAT/SAT ratio adjBMI	Ratio of visceral to subcutaneous adipose tissue volume adjusted for BMI

Supplementary Table 2a. Ectopic fat assessment methods by cohort for subcutaneous and visceral adipose tissue.

Cohort	Modality	Units	Slice Number	Slice Thickness (mm)	Level of image
AGES	CT	cm^2	1	10	L4-L5
DHS	CT	cm^3	4	2.5	L4-L5
FamHS	CT	cm^2	2	5	L4-L5
FELS	MRI	cm^3	24	10	T1-S1
FHS	CT	cm^3	25	5	125mm above S1
GENOA	CT	cm^3	24	2.5	L3-S1
HABC	CT	cm^2	1	10	L4-L5
JHS	CT	cm^3	24	2.5	L3-S1
MESA	CT	cm^2	2	6	L4-L5
MRCOB	CT	cm^3	3	3	L3
PIVUS	MRI	cm^2	1	10	L4-L5
SHIP-2	MRI	cm^3	64	3-4	Whole abdomen
SHIPTREND	MRI	cm^3	64	3-4	Whole abdomen

Supplementary Table 2b. Ectopic fat assessment methods by cohort for pericardial adipose tissue.

Cohort	Modality	Units	Slice Number	Slice Thickness (mm)	Level of image
Amish	CT	cm^3	1	3	Full length of heart
DHS	CT	cm^3	18	2.5	1.5cm and 3.0cm below superior extend of left main coronary artery
FamHS	CT	cm^3	18	2.5	1.5cm and 3.0cm below superior extend of left main coronary artery
FHS	CT	cm^3	48	2.5	Full length of heart
GENOA		cm^3	1	45	Full length of heart
MESA	CT	cm^3	18	2.5	1.5cm and 3.0cm below superior extend of left main coronary artery

Supplementary Table 3a. Characteristics for cohorts contributing to subcutaneous adipose tissue volume (SAT) and visceral adipose tissue volume (VAT) analyses by strata (overall, women and men).

Study	Ancestry	SAT	VAT	Women	Age (years)		BMI (kg/m^2)		SAT (cm^2 or $*cm^3$)		VAT (cm^2 or $*cm^3$)	
		N	N	%	mean	SD	mean	SD	mean	SD	mean	SD
OVERALL												
AGES	EA	3172	3172	57.8	76.4	5.4	27.1	4.4	257.6	113.2	172.7	80.7
DHS*	EA	445	448	53.5	62.1	9.3	31.8	6.5	708.6	313.4	442.6	174.7
FamHS	EA	2659	2659	55.3	57.2	13.3	28.8	5.7	286.0	132.0	167.0	91.0
FELS*	EA	578	578	52.6	44.7	17.8	26.8	5.7	4620.3	2970.3	2514.1	2046.6
FHS*	EA	3336	3336	48.2	52.8	11.8	27.8	5.2	2884.6	1389.8	1820.6	1033.3
GENOA*	AA	552	552	75.0	69.1	8.0	32.5	7.2	2319.8	985.6	906.0	392.8
HABC	AA	1041	1041	56.9	73.4	2.9	28.4	5.0	313.6	136.7	129.0	59.6
HABC	EA	1567	1567	47.1	73.8	2.8	26.6	4.1	266.3	101.9	153.4	69.5
JHS*	AA	1631	1631	63.8	59.3	10.9	31.8	6.4	2413.2	1026.6	837.3	382.6
MESA	AA	243	245	46.9	62.4	10.2	24.2	3.0	141.7	53.8	127.5	58.6
MESA	EA	664	744	49.3	62.8	9.8	27.8	4.8	208.3	98.8	176.4	92.0
MRCOB*	EA	423	423	59.8	42.9	15.8	32.6	8.8	84.9	47.8	48.4	30.3
PIVUS	EA	287	287	48.4	70.0	0.1	26.9	4.4	253.2	97.2	130.7	67.7
SHIP-2*	EA	783	783	35.9	52.9	12.1	27.3	3.9	7391.3	3078.7	4531.2	2311.2
SHIPTREND*	EA	866	866	56.1	50.3	13.5	27.2	4.3	7792.5	3394.3	3746.1	2321.2
TOTAL		**18247**	**18332**									
WOMEN												
AGES	EA	1835	1835	100.0	76.3	5.5	27.2	4.8	296.1	115.2	149.2	66.9
DHS*	EA	237	239	100.0	61.7	9.3	32.5	7.3	822.3	300.1	419.4	159.0
FamHS	EA	1189	1189	100.0	56.7	13.4	29.3	4.7	249.0	108.0	203.0	94.0
FELS*	EA	304	304	100.0	44.6	17.5	26.5	5.9	4932.9	3136.4	1687.5	1306.4
FHS*	EA	1608	1608	100.0	54.1	11.3	27.1	5.8	3149.9	1519.9	1367.1	833.2
GENOA*	AA	416	416	100.0	69.0	7.9	33.6	7.5	2586.5	916.0	894.3	382.2

Study	Ancestry	SAT	VAT	Women	Age (years)		BMI (kg/m^2)		SAT (cm^2 or $*cm^3$)		VAT (cm^2 or $*cm^3$)	
		N	N	%	mean	SD	mean	SD	mean	SD	mean	SD
HABC	AA	592	592	100.0	73.4	3.0	29.2	5.4	372.2	131.6	128.5	58.0
HABC	EA	739	739	100.0	73.7	2.8	26.1	4.4	311.3	104.9	134.3	62.0
JHS*	AA	1040	1040	100.0	59.7	10.9	32.9	6.9	2766.8	972.6	814.7	367.2
MESA	AA	115	115	100.0	62.4	9.7	24.3	3.2	165.3	48.4	111.6	48.1
MESA	EA	328	358	100.0	63.0	9.3	27.4	5.6	227.3	111.3	130.8	72.5
MRCOB*	EA	253	253	100.0	43.5	15.5	33.7	9.3	92.8	48.2	42.7	29.1
PIVUS	EA	139	139	100.0	70.0	0.1	26.9	4.8	286.6	106.3	110.2	58.3
SHIP-2*	EA	281	281	100.0	46.5	8.9	26.3	4.7	8622.3	3805.2	2455.8	1722.9
SHIPTREND*	EA	486	486	100.0	50.6	13.0	26.8	4.8	8794.8	3737.8	2684.5	1747.4
TOTAL		**9562**	**9594**									
MEN												
AGES	EA	1337	1337	0.0	76.5	5.3	26.9	3.8	204.6	85.8	205.1	86.5
DHS*	EA	208	209	0.0	62.5	9.3	30.9	5.4	579.1	276.4	469.0	188.1
FamHS	EA	1470	1470	0.0	57.6	13.1	28.5	6.3	315.0	142.0	138.0	78.0
FELS*	EA	274	274	0.0	44.7	18.2	27.2	5.4	4273.4	2738.5	3431.3	2313.8
FHS*	EA	1728	1728	0.0	51.5	12.2	28.5	4.5	2637.8	1205.7	2242.6	1022.8
GENOA*	AA	136	136	0.0	69.6	7.6	29.4	5.1	1505.2	704.8	941.7	423.2
HABC	AA	449	449	0.0	73.9	2.8	27.2	4.2	236.3	100.0	129.7	61.7
HABC	EA	828	828	0.0	73.9	2.9	27.1	3.7	226.1	80.1	170.3	71.6
JHS*	AA	591	591	0.0	58.5	10.8	29.8	4.9	1791.0	798.3	877.1	405.7
MESA	AA	128	130	0.0	62.5	10.7	24.2	2.9	120.5	49.7	141.6	63.5
MESA	EA	336	386	0.0	62.6	10.2	28.2	4.0	189.8	80.8	218.6	87.9
MRCOB*	EA	170	170	0.0	42.0	16.4	31.0	7.7	72.4	42.9	57.1	30.3
PIVUS	EA	148	148	0.0	70.0	0.1	26.8	3.9	221.8	87.8	150.0	75.5
SHIP-2*	EA	502	502	0.0	56.5	13.5	27.8	3.4	6702.3	2585.3	5693.0	2582.2
SHIPTREND*	EA	380	380	0.0	50.0	14.1	27.6	3.6	6510.5	2896.0	5103.8	2894.1
TOTAL		**8685**	**8738**									

Abbreviations: Please see Supplementary Table 9 for complete listing of cohort names and abbreviations

AA - African Ancestry; EA - European Ancestry

BMI - Body Mass Index

SAT - Subcutaneous Adipose Tissue Volume

VAT - Visceral Adipose Tissue Volume

N - Sample Size

SD - Standard Deviation

Supplementary Table 3b. Characteristics for cohorts contributing to pericardial adipose tissue volume (PAT) analysis

Study	Ancestry	PAT	Women	Age (years)		BMI (kg/m^2)		PAT (cm^2)	
		N	%	mean	SD	mean	SD	mean	SD
OVERALL									
Amish	EA	542	54.2	56.2	12.8	27.8	4.7	89.4	40.5
DHS	EA	541	53.5	62.1	9.3	31.8	6.5	131.5	55.6
FamHS	EA	892	52.8	62.7	11.3	29.1	5.5	82.4	43.9
FHS	EA	3336	48.2	52.8	11.8	27.8	5.2	113.9	45.0
GENOA	AA	552	75.0	69.1	8.0	32.5	7.2	66.2	27.6
MESA	AA	1609	44.6	62.0	10.0	30.2	5.9	68.0	34.9
MESA	AS	768	51.0	62.4	10.4	24.0	3.3	74.1	31.6
MESA	EA	2519	52.6	62.8	10.1	27.7	5.1	85.4	46.1
MESA	HS	1445	52.0	61.4	10.3	29.4	5.1	88.6	43.7
TOTAL		**12204**							
WOMEN									
Amish	EA	294	100.0	55.8	12.3	28.7	5.4	86.1	36.3
DHS	EA	302	100.0	61.7	9.3	32.5	7.3	117.9	45.1
FamHS	EA	421	0.0	64.7	10.0	28.7	6.1	97.0	51.1
FHS	EA	1608	100.0	54.1	11.3	27.1	5.8	101.2	39.0
GENOA	AA	416	100.0	69.0	7.9	33.6	7.5	64.8	26.4
MESA	AA	868	100.0	62.0	9.9	31.4	6.5	61.5	29.2
MESA	AS	390	100.0	60.8	10.1	23.9	3.5	70.0	20.6
MESA	EA	1317	100.0	62.7	10.3	27.5	5.8	70.5	34.8
MESA	HS	746	100.0	60.7	10.3	29.5	5.4	76.0	35.4
TOTAL		**6362**							
MEN									
Amish	EA	248	0.0	56.6	13.3	26.7	3.5	93.2	44.7
DHS	EA	239	0.0	62.5	9.3	30.9	5.4	148.6	62.5

Study	Ancestry	PAT	Women	Age (years)		BMI (kg/m^2)		PAT (cm^2)	
FamHS	EA	471	100.0	60.5	12.3	29.6	4.7	69.4	30.8
FHS	EA	1728	0.0	51.5	12.2	28.5	4.5	125.8	46.9
GENOA	AA	136	0.0	69.6	7.6	29.4	5.1	70.6	30.6
MESA	AA	741	0.0	62.1	10.2	28.8	4.8	76.0	39.5
MESA	AS	378	0.0	61.6	10.3	24.1	3.1	78.0	35.0
MESA	EA	1202	0.0	62.9	10.0	27.9	4.1	101.8	51.2
MESA	HS	699	0.0	60.4	10.3	28.6	4.1	101.0	47.7
TOTAL		**5842**							

Abbreviations: Please see Supplementary Table 9 for complete listing of cohort names and abbreviations
AA - African Ancestry; AS - Chinese Ancestry; EA - European Ancestry; HS - Hispanic Ancestry
BMI - Body Mass Index
PAT - Pericardial Adipose Tissue Volume
N - Sample Size
SD - Standard Deviation

Supplementary Table 3c. Characteristics for cohorts contributing to subcutaneous and visceral adipose tissue attenuation (SATHU and VATHU) analyses

Study	Ancestry	SATHU	VATHU	SAT HU (HU)		VAT HU (HU)	
		N	N	mean	SD	mean	SD
OVERALL							
AGES	EA	3172	3172	-99.0	5.9	-86.2	7.3
FamHS	EA	2659	2659	-101.5	6.5	-92.9	8.0
FHS	EA	3336	3336	-100.9	5.0	-93.9	4.6
HABC	AA	1041	1041	-97.2	10.7	-85.3	10.3
HABC	EA	1567	1567	-96.9	8.1	-88.3	9.2
MESA	EA	664	744	-92.8	9.9	-62.8	23.2
TOTAL		**12439**	**12519**				
WOMEN							
AGES	EA	1835	1835	-100.6	5.3	-85.7	7.4
FamHS	EA	1189	1189	-99.6	5.9	-95.0	6.9
FHS	EA	1608	1608	-102.3	5.1	-92.5	4.4
HABC	AA	592	592	-100.6	8.1	-87.2	8.6
HABC	EA	739	739	-100.5	7.4	-88.4	9.6
MESA	EA	328	358	-96.7	8.7	-57.9	25.2
TOTAL		**6291**	**6321**				
MEN							
AGES	EA	1337	1337	-96.7	5.9	-87.0	7.2
FamHS	EA	1470	1470	-103.1	6.5	-91.2	8.4
FHS	EA	1728	1728	-99.6	4.4	-95.2	4.5
HABC	AA	449	449	-92.7	10.7	-82.8	11.6
HABC	EA	828	828	-93.7	7.4	-88.2	8.8
MESA	EA	336	386	-89.0	9.6	-67.4	20.2
TOTAL		**6149**	**6199**				

Abbreviations: Please see Supplementary Table 9 for complete listing of cohort names and abbreviations

AA - African Ancestry; EA - European Ancestry

BMI - Body Mass Index

SATHU - Subcutaneous Adipose Tissue Attenuation

VATHU - Visceral Adipose Tissue Attenuation

HU - Hounsfield Units

N - Sample Size

SD - Standard Deviation

Supplementary Table 3d. Characteristics for cohorts contributing to ratio of visceral to subcutaneous adipose tissue volume ratio (VAT/SAT ratio) analysis

Study	Ancestry	VAT/SAT ratio	Women	VAT/SAT ratio	
		N	%	mean	SD
OVERALL					
AGES	EA	3172	57.8	0.8	0.4
DHS	EA	433	53.5	0.7	0.4
FamHS	EA	2658	55.3	0.7	0.4
FELS	EA	578	52.6	0.6	0.4
FHS	EA	3158	48.2	0.7	0.4
GENOA	AA	552	75.0	0.4	0.2
HABC	AA	1039	56.9	0.5	0.3
HABC	EA	1567	47.1	0.6	0.3
JHS	AA	1621	63.8	0.4	0.2
MESA	AA	317	46.9	1.0	0.5
MESA	EA	662	49.3	0.9	0.5
MRCOB	EA	412	59.8	0.7	0.4
PIVUS	EA	373	48.4	0.6	0.2
SHIP-2	EA	783	35.9	0.7	0.1
SHIPTREND	EA	866	56.1	0.5	0.1
TOTAL		**18191**			
WOMEN					
AGES	EA	1835	100.0	0.5	0.3
DHS	EA	229	100.0	0.5	0.2
FamHS	EA	1469	100.0	0.5	0.3
FELS	EA	304	100.0	0.3	0.2
FHS	EA	1516	100.0	0.4	0.2
GENOA	AA	416	100.0	0.4	0.2
HABC	AA	591	100.0	0.4	0.2

Study	Ancestry	VAT/SAT ratio	Women	VAT/SAT ratio	
		N	%	mean	SD
HABC	EA	739	100.0	0.5	0.2
JHS	AA	1031	100.0	0.3	0.1
MESA	AA	167	100.0	0.7	0.2
MESA	EA	326	100.0	0.6	0.3
MRCOB	EA	253	100.0	0.5	0.3
PIVUS	EA	180	100.0	0.4	0.2
SHIP-2	EA	281	100.0	0.3	0.1
SHIPTREND	EA	486	100.0	0.3	0.1
TOTAL		**9823**			
MEN					
AGES	EA	1337	0.0	1.1	0.4
DHS	EA	204	0.0	0.9	0.4
FamHS	EA	1189	0.0	0.9	0.4
FELS	EA	274	0.0	0.8	0.4
FHS	EA	1642	0.0	0.9	0.4
GENOA	AA	136	0.0	0.7	0.3
HABC	AA	448	0.0	0.6	0.3
HABC	EA	828	0.0	0.8	0.3
JHS	AA	590	0.0	0.5	0.2
MESA	AA	150	0.0	1.2	0.5
MESA	EA	336	0.0	1.2	0.5
MRCOB	EA	165	0.0	0.9	0.5
PIVUS	EA	193	0.0	0.7	0.3
SHIP-2	EA	502	0.0	0.9	0.3
SHIPTREND	EA	380	0.0	0.8	0.3
TOTAL		**8374**			

Abbreviations: Please see Supplementary Table 9 for complete listing of cohort names and abbreviations

AA - African Ancestry; EA - European Ancestry
BMI - Body Mass Index
SAT - Subcutaneous Adipose Tissue Volume
VAT - Visceral Adipose Tissue Volume
VAT/SAT ratio - Visceral to Subcutaneous Adipose Tissue Volume Ratio
N - Sample Size
SD - Standard Deviation

Supplementary Table 4. Cohort Genotyping Information

Study	Array type	Genotype calling	Quality control filters for genotyped SNPs used for imputation	No of SNPs used for imputation	Imputation	Imputation Backbone for phased CEU haplotypes (NCBI build)	Filtering of imputed genotypes	Data management and statistical analysis
AGES	Illumina Hu370CNV	Illumina BeadStudio	call rate <97%; genotype sex mismatch: mismatch previous genotypes	324,603	MACH+Mini Mac	HapMap release 22 (build 36)	none	R, PLINK, ProbABEL
Amish	Affymetrix 500K, Affymetric 6.0	Affymetrix	SNP call rate >95%, MAF >0, and HWE (at P>0.0001)	373,825	MACH version 1.0.15	HapMap release 22 (build 36)	none	Mixed Model Analysis in Pedigrees (MMAP)
DHS	Genome-Wide Human SNP Array 5.0	Affymetrix	call rate > 0.95, HWE_pval >0.0001, MAF>0.01	361,574	IMPUTE v2.2.2	HapMap release 22 (build 36)	none	SOLAR
FamHS	Illumina 550K, Illumina 610K, and Illumina 1M	BeadStudio-GenCall v3.0	MAF <1% or >99%; p≤10-6; callrate <98%	824,714	MACH version 1.0.16	HapMap release 22 (build 36)	none	R mixed model with kinship matrix

Study	Array type	Genotype calling	Quality control filters for genotyped SNPs used for imputation	No of SNPs used for imputation	Imputation	Imputation Backbone for phased CEU haplotypes (NCBI build)	Filtering of imputed genotypes	Data management and statistical analysis
FELS	Illumina Human 610 Quad v1_B	Illumina's GenomeStudio (v1.5.16)	pHWE<1e-6, call rate<90%, MAF<0.01, Mendelian errors (Simwalk)	542,711	MACH version 1.0	HapMap release 21 (build 35)	none	Pedsys, R, SOLAR
FHS	Affymetrix 500K Affymetrix 50K supplemental	Affymetrix	pHWE<1e-6, call rate<97%, mishap (non random missingness by haplotype) p<1e-9, MAF<0.01, Mendelian errors>100, SNPs not in Hapmap or strandedness issues merging with Hapmap	378,163	MACH version 1.0.15	HapMap release 22 (build 36)	none	R, linear mixed effect models and GEE models, robust variance option to account for relatedness

Study	Array type	Genotype calling	Quality control filters for genotyped SNPs used for imputation	No of SNPs used for imputation	Imputation	Imputation Backbone for phased CEU haplotypes (NCBI build)	Filtering of imputed genotypes	Data management and statistical analysis
GENOA	Affymetrix 6.0 & Illumina 1M	Birdseed & GenomeStudio	call rate < 95%; MAF<0.01; SNPs not in HapMap	Affymetrix 6.0: 550,325 Illumina 1M: 780,147 ARIC Affymetrix 6.0: 565,043	MACH 1.0.16	HapMap release 22 (build 36); combined CEU+YRI reference panel	none	MMAP
HABC (European Ancestry)	Illumina Human 1M-Duo BeadChip	BeadStudio version 3.3.7	SNPs with minor allele frequency ≥ 1%, call rate ≥97% and HWE p≥10-6 were used for imputation.	914,263	MACH	HapMap release 22 (build 36)	none	R
HABC (African Ancestry)	Illumina Human 1M-Duo BeadChip	BeadStudio version 3.3.7	SNPs with minor allele frequency ≥ 1%, call rate ≥97% and HWE p≥10-6 were used for imputation.	1,007,948	MACH	HapMap release 22 (build 36)	none	R

Study	Array type	Genotype calling	Quality control filters for genotyped SNPs used for imputation	No of SNPs used for imputation	Imputation	Imputation Backbone for phased CEU haplotypes (NCBI build)	Filtering of imputed genotypes	Data management and statistical analysis
JHS	Affymetrix Genome-Wide Human SNP Array 6.0	Birdseed v1.33	SNP level callrate > 90%, sample level callrate >95%, MAF >0.01, HWE > 1E-06	832,508	MACH and Minimac	HapMap release 22 (build 36)	none	MACH2QTL
MESA	Affymetrix Genome-Wide Human SNP Array 6.0	Affymetrix	pHWE<1e-6, call rate<95%, MAF<0.01,	888,666	IMPUTE2	HapMap release 22 (build 36)	none	SAS, SNPTEST2, R

Study	Array type	Genotype calling	Quality control filters for genotyped SNPs used for imputation	No of SNPs used for imputation	Imputation	Imputation Backbone for phased CEU haplotypes (NCBI build)	Filtering of imputed genotypes	Data management and statistical analysis
MRCOB/ TOPS	Affymetrix Genome-Wide Human SNP 6.0 arrays Affymetrix 50K supplemental	Genotype Console 3.2	pHWE<1e-8, call rate<95%, >2 alleles called, fewer than 5 copies of minor allele, SNPs not in Hapmap or strandedness issues merging with Hapmap	869,222	Impute2/SHAPEIT/MERLIN	HapMap release 22 (build 36)	none	SOLAR, variance components models including random effect of kinship
PIVUS	Human Omni Express and Metabochip	Illumina	For SNPs with MAF >=0.05: pHWE<1e-6, call rate<95%; For SNPs with MAF <0.05: pHWE<1e-6, call rate<99%; MAF<0.01	738,879	IMPUTE version 2.1.2	HapMap release 22 (build 36)	none	SNPTEST

Study	Array type	Genotype calling	Quality control filters for genotyped SNPs used for imputation	No of SNPs used for imputation	Imputation	Imputation Backbone for phased CEU haplotypes (NCBI build)	Filtering of imputed genotypes	Data management and statistical analysis
SHIP-2	Affymetrix Genome-Wide Human SNP Array 6.0	Birdseed2	none	869,224	IMPUTE v0.5.0	HapMap release 22 (build 36)	none	quicktest v0.95
SHIP-TREND	Illumina Omni 2.5	GenCall	pHWE <= 0.0001 or CallRate <= 0.9 or monomorphic SNPs	1,782,967	IMPUTE v2.1.2.3	HapMap release 22 (build 36)	none	quicktest v0.95

Supplementary Table 5. Heritability estimates of ectopic fat traits in the Framingham Heart Study in the overall cohort (N=3,312) and stratified by sex (N_{WOMEN}=1,593 and N_{MEN}=1,719). Heritability estimates were calculated using variance components estimation in SOLAR[1].

	ALL				WOMEN				MEN			
TRAIT	**N**	**H^2_r**	**P**	**SE**	**N**	**H^2_r**	**P**	**SE**	**N**	**H^2_r**	**P**	**SE**
SAT	3312	0.59*	6.4E-55	0.04	1593	0.64	8.8E-22	0.07	1719	0.71#	2.3E-26	0.07
SATHU	3312	0.29#	7.6E-17	0.04	1593	0.30#	2.8E-06	0.07	1719	0.40#	2.6E-12	0.07
VAT	3312	0.39	1.5E-32	0.04	1593	0.55*	1.9E-16	0.07	1719	0.51	5.5E-17	0.07
VATHU	3312	0.31	9.9E-19	0.04	1593	0.38	5.9E-09	0.07	1719	0.39	5.5E-10	0.07
VAT/SAT ratio	3312	0.55	6.0E-54	0.04	1593	0.55	8.6E-16	0.07	1719	0.61	1.0E-22	0.07
VAT/SAT ratio adjBMI	3299	0.55	5.2E-05	0.04	1584	0.56	3.9E-16	0.07	1715	0.59	4.9E-21	0.07

* Kurtosis is moderate
# Kurtosis is very high

Abbreviations:
- N - Sample Size
- H^2_r - Heritability
- P - P-value
- SE - Standard Error
- SAT - Subcutaneous Adipose Tissue Volume
- SATHU - Subcutaneous Adipose Tissue Attenuation
- VAT - Visceral Adipose Tissue Volume
- VATHU - Visceral Adipose Tissue Attenuation
- VAT/SAT ratio - Visceral to Subcutaneous Adipose Tissue Volume Ratio
- adjBMI - Adjusted for Body Mass Index

Supplementary Table 6. Pairwise genetic correlations between ectopic fat depots and body mass index (BMI) among 3,336 participants from the Framingham Heart Study. Bottom diagonal is the genetic correlation (RhoG) between traits with P-value testing for overlapping genetic correlations (RhoG=0), and the top diagonal is the P-value testing for non-overlapping genetic correlations (absolute value [RhoG]=1).

		Non-overlapping genetic correlation, P (abs(RhoG)=1)					
		SAT	**SATHU**	**VAT**	**VATHU**	**VAT/SAT ratio**	**BMI**
Genetic correlation estimate (RhoG), P (RhoG=0)	**SAT**	--	P=1.0E-9	P=1.7E-28	P=3.6E-17	P=2.6E-32	P=6.7E-40
	SATHU	-0.54, P=9.4E-10	--	P=1.2e=11	P=4.5E-11	P=4.2E-11	P=1.8E-11
	VAT	0.67, P=3.7E-24	-0.35, P=3.2E-4	--	P=2.0E-14	P=2.8E-35	P=5.3E-23
	VATHU	-0.40, P=5.9E-7	0.52, P=6.3E-6	-0.74, P=4.7E-16	--	P=1.4E-16	P=9.8E-16
	VAT/SAT ratio	-0.43, P=1.9E-12	0.21, P=0.019	0.35, P=4.7E-7	-0.41, P=6.0E-7	--	P=3.2E-37
	BMI	0.87, P=2.5E-42	-0.27, P=2.5E-3	0.76, P=3.8E-28	-0.45, P=2.6E-8	-0.19, P=3.9E-4	--

Supplementary Table 7. Pearson correlation coefficients for ectopic fat traits in the Framingham Heart Study.[2-5] Correlation coefficients for women in gray and men in white.

		MEN					
		SAT	SATHU	VAT	VATHU	VAT/SAT ratio	BMI
WOMEN	SAT	--	-0.56	0.58	-0.40	-0.43	0.83
	SATHU	-0.49	--	-0.42	NA	0.17	-0.34
	VAT	0.71	-0.36	--	-0.72	0.42	0.71
	VATHU	-0.51	NA	-0.75	--	-0.38	-0.42
	VAT/SAT ratio	-0.11	0.04	0.53	-0.49	--	-0.14
	BMI	0.88	-0.30	0.75	-0.51	0.06	--

Supplementary Table 8a. Imputation quality for *UBE2E2*, *RREB1*, *ATXN1*, *GRAMD3* and *GSDMB* by cohort

Cohort	Ancestry	rs7374732 (*UBE2E2*)	rs2842895 (*RREB1*)	rs2237199 (*ATXN1*)	rs10060123 (*GRAMD3*)	rs2123685 (*GSDMB*)
AGES	EU	1.00	0.93	0.99	0.92	0.99
DHS	EU	1.00	NA	0.90	NA	0.99
FamHS	EU	1.00	0.94	1.00	0.95	0.97
FELS	EU	1.00	0.94	NA	0.96	0.97
FHS	EU	0.97	0.94	0.89	0.96	0.99
GENOA	AF	1.00	NA	NA	0.92	NA
HABC	AF	1.00	0.94	0.98	0.98	1.00
HABC	EU	1.00	0.95	1.00	0.97	0.97
JHS1	AF	1.00	0.92	NA	0.94	NA
JHS2	AF	1.00	0.92	NA	0.96	NA
MESA	AF	1.00	0.91	0.82	0.95	NA
MESA	EU	1.00	0.87	0.87	0.93	0.98
MRCOB	EU	0.96	0.88	NA	0.97	1.19
PIVUS	EU	1.00	0.88	NA	0.95	0.98
SHIP2	EU	1.00	0.88	NA	0.95	1.19
SHIP-TREND	EU	1.00	0.95	NA	0.95	1.19

Ancestry abbreviations: EA - European ancestry, AA - African ancestry, AS - Asian ancestry, HS - Hispanic ancestry

Supplementary Table 8b. Imputation quality for *EBF1* and *ENSA* by cohort.

Cohort	Ancestry	rs1650505 (*EBF1*)	rs6587515 (*ENSA*)
Amish	EU	0.85	0.99
DHS	EU	0.97	0.97
FamHS	EU	1.00	1.00
FHS	EU	0.95	1.01
MESA	EU	0.96	0.99
GENOA	AF	0.85	NA
MESA	AF	1.00	0.94
MESA	AS	0.99	1.01
MESA	HS	0.97	0.97

Ancestry abbreviations: EA - European ancestry, AF - African ancestry, AS - Asian ancestry, HS - Hispanic ancestry

Supplementary Table 9. Ancestry-specific association results of lead SNPs from newly identified ectopic fat loci from a sample size weighted fixed effects meta-analysis implemented in METAL.[6,7]

Locus[1]	Traits	Strata	Ancestry[2]	Lead SNP	A1[3]	A2[4]	FreqA1[5]	N	Z score	P-value[6]
Fat Volume Traits[8]										
ENSA	PATadjHtWt	ALL	EU	rs6587515	a	g	0.10	7425	-5.00	4.8E-07
			AF				0.02	1442	-1.30	1.9E-01
			AS				0.20	761	-2.80	5.9E-03
			HS				0.06	1399	-1.70	8.5E-02
GRAMD3	VATadjBMI	WOMEN	EU	rs10060123	a	c	0.26	7403	4.80	1.3E-06
			AF				0.14	2220	2.60	1.1E-02
EBF1	PATadjHtWt	ALL	EU	rs1650505	a	g	0.22	7412	-4.50	6.7E-06
			AF				0.22	1994	-3.40	7.8E-04
			AS				0.31	761	-2.30	2.3E-02
			HS				0.29	1399	-1.50	1.3E-01
RREB1	VATadjBMI	ALL	EU	rs2842895	c	g	0.58	14295	5.80	5.8E-09
			AF				0.11	3002	1.00	3.0E-01
GSDMB[7]	SAT	WOMEN	EU	rs2123685	t	c	0.94	7137	5.52	3.4E-08
Fat Quality Traits[8]										
ATXN1	SATHU	MEN	EU	rs2237199	a	g	0.11	5331	5.30	1.4E-07
			AF				0.11	449	2.20	2.8E-02
Relative Fat Distribution Traits[8]										
UBE2E2	VAT/SAT ratio	ALL	EU	rs7374732	t	c	0.63	14674	-5.10	2.9E-07
			AF				0.90	3531	-3.80	1.3E-04

1 Conventional locus name based on closest gene in the region
2 Ancestry abbreviations: EU - European ancestry, AF - African ancestry, AS - Asian ancestry, HS - Hispanic ancestry
3 A1 is the coded allele
4 A2 is the non-coded allele
5 FreqA1 is the allele frequency of the coded allele
6 P-values are double GC corrected
7 rs2123685 near *GSDMB* was observed only in European ancestry cohorts and therefore the multiethnic meta-analyses reflect the ancestry-specifc meta-analysis

8 European and African ancestry cohorts contributed to all ectopic fat traits; Chinese and Hispanic ancestry cohorts contributed only to pericardial volume traits.

Abbreviations:

N - Sample Size

PATadjHtWt - Pericardial Adipose Tissue Volume Adjusted for Height and Weight

VATadjBMI - Visceral Adipose Tissue Volume Adjusted for Body Mass Index

SAT - Subcutaneous Adipose Tissue Volume

SATHU - Subcutaneous Adipose Tissue Attenuation

VAT/SAT ratio - Visceral to Subcutaneous Adipose Tissue Volume Ratio

Supplementary Table 10. Association of newly identified loci with other ectopic fat traits within VATGen* (using the sample size weighted fixed effects meta-analysis method implemented in METAL[6,7]) and with BMI and WHR from the GIANT Consoritum.[8,9]

A. *GSDMB*

	Trait	Strata	Direction	P-value	N
VATGen	**SAT**	ALL	+	9.5E-06	14230
		WOMEN	**+**	**3.4E-08**	**7137**
		MEN	+	0.61	6681
	VAT	WOMEN	+	4.8E-04	7167
	VATSAT	WOMEN	-	0.17	7136
GIANT	BMI	WOMEN	+	2.0E-03	131549
	WHRadjBMI	WOMEN	-	0.75	86317

B. *RREB1*

	Trait	Strata	Direction	P-value	N
VATGen	**VATadjBMI**	**ALL**	**+**	**1.1E-08**	**17297**
		WOMEN	+	1.8E-03	9207
		MEN	+	1.5E-06	8090
	VAT	ALL	+	4.8E-05	17312
	SAT	ALL	+	0.87	17209
	VATSATadjBMI	ALL	+	8.9E-06	17193
GIANT	BMI	ALL	+	0.01	235260
	WHRadjBMI	ALL	+	1.4E-04	142019

C. *GRAMD3*

	Trait	Strata	Direction	P-value	N
VATGen	**VATadjBMI**	ALL	+	2.2E-04	17849
		WOMEN	**+**	**4.5E-08**	**9623**
		MEN	-	0.85	8226
	VAT	WOMEN	+	1.1E-06	9634
	SAT	WOMEN	+	0.11	9590
	VATSATadjBMI	WOMEN	+	3.2E-04	9578
GIANT	BMI	WOMEN	+	0.43	131761
	WHRadjBMI	WOMEN	+	0.66	85564

D. *EBF1*

	Trait	Strata	Direction	P-value	N
VATGen	**PATadjHtWt**	**ALL**	**-**	**1.0E-09**	**11566**
		WOMEN	-	1.8E-07	6101
		MEN	-	1.0E-04	5465
	SAT	ALL	+	0.06	16576
	VAT	ALL	+	0.98	16682
	VATSAT	ALL	-	0.09	16575
GIANT	BMI	ALL	-	0.33	236156
	WHRadjBMI	ALL	+	0.88	142655

E. *ENSA*

	Trait	Strata	Direction	P-value	N
VATGen	**PATadjHtWt**	**ALL**	**-**	**2.8E-09**	**11027**
		WOMEN	-	4.0E-06	5691
		MEN	-	2.0E-05	5336
	SAT	ALL	+	0.05	15264
	VAT	ALL	+	0.21	15347
	VATSAT	ALL	+	0.68	15263
GIANT	BMI	ALL	+	0.13	236166
	WHRadjBMI	ALL	-	0.33	142737

F. *ATXN1*

	Trait	Strata	Direction	P-value	N
VATGen	**SATHU**	ALL	+	1.9E-03	12255
		WOMEN	-	0.36	6475
		MEN	**+**	**1.4E-08**	**5780**
	VATHU	Men	+	8.0E-06	5830
	SAT	Men	-	3.9E-04	7771
	VAT	Men	-	2.7E-03	7831
GIANT	BMI	Men	+	0.96	99228
	WHRadjBMI	Men	+	0.65	51038

G. *UBE2E2*

	Trait	Strata	Direction	P-value	N
VATGen	**VATSAT**	**ALL**	**-**	**3.1E-10**	**18205**
		WOMEN	**-**	**5.8E-08**	**9826**
		MEN	-	8.8E-04	8379
	VATSATadjBMI	ALL	-	1.7E-08	18190
	VAT	ALL	-	1.4E-03	18312
	SAT	ALL	+	0.32	18206
GIANT	BMI	ALL	+	0.83	236146
	WHRadjBMI	ALL	-	0.04	142752

* The trait and strata in which the locus was originally identified in is bolded.

Abbreviations

N - Sample Size
SAT - Subcutanous Adipose Tissue Volume
VAT - Visceral Adipose Tissue Volume
BMI - Body Mass Index
WHR - Waist to Hip Ratio
adjBMI - Adjusted for BMI
SATHU - Subcutaneous Adipose Tissue Attenuation
VATHU - Visceral Adipose Tissue Attenuation
PAT - Pericardial Adipose Tissue Volume
adjHtWt - Adjusted for Height and Weight

Supplementary Table 11. Summary of direction concordant associations for 97 body mass index (BMI - top) and 49 waist-hip ratio (WHR - bottom) GWAS SNPs in association with listed ectopic fat traits. Direction consistent indicates the number of SNPs with an effect estimate that is concordant with Locke et al.[9] and Shungin et al.[8] for all SNPs. SAT was the only trait with a significant number of concordant associations for BMI, and thus was evaluated for only those associations attaining nominal significance for ectopic fat (P_{SAT}<0.05). P-values calculated using a 1-sided binomial distribution. No other ectopic fat traits had a significant number of concordant associations for BMI SNPs and no ectopic fat traits had a significant number of concordant associations for WHR SNPs.

BMI SNPS	All Associations (N=97)		Associations with P<0.05		
Trait	# Direction Consistent	1-sided Binomial P	Total	# Direction Consistent	1-sided Binomial P
SAT	87	8.9E-17	27	27	7.5E-09
VAT	51	0.34	-	-	-
VATadjBMI	43	0.89	-	-	-
SATHU	55	0.11	-	-	-
VATHU	49	0.50	-	-	-
VAT/SAT ratio	42	0.92	-	-	-
VAT/SAT ratio adjBMI	41	0.95	-	-	-

WHR SNPs	All Associations (N=49)		Associations with P<0.05		
Trait	# Direction Consistent	1-sided Binomial P	Total	# Direction Consistent	1-sided Binomial P
SAT	22	0.80	-	-	-
VAT	28	0.20	-	-	-
VATadjBMI	29	0.13	-	-	-
SATHU	21	0.87	-	-	-
VATHU	24	0.61	-	-	-
VAT/SAT ratio	27	0.28	-	-	-
VAT/SAT ratio adjBMI	28	0.20	-	-	-

Supplementary Table 12. Association between newly discovered SNPs and previously published GWAS of cardio-metabolic risk factors.

			MAGIC (Meta-Analyses of Glucose and Insulin Consortium)[10]							
					Fasting Glucose adjusted for BMI (N=58,074)			Fasting Insulin adjusted for BMI (N=51,750)		
Trait	**Locus**	**rsID**	**A1/A2**	**A1_AF**	**BETA**	**SE**	**P**	**BETA**	**SE**	**P**
PATadjHtWt	*ENSA*	rs6587515	A/G	0.13	0.003	0.005	0.58	-0.011	0.005	0.01
VATadjBMI	*GRAMD3*	rs10060123	A/C	0.24	-0.001	0.004	0.90	-0.005	0.003	0.11
PATadjHtWt	*EBF1*	rs1650505	A/G	0.27	0.003	0.004	0.53	0.007	0.003	0.03
VATadjBMI	*RREB1*	rs2842895	C/G	0.59	-0.007	0.003	0.03	0.000	0.003	0.90
SAT	*GDSMB*	rs2123685	T/C	0.95	0.001	0.008	0.93	0.011	0.007	0.11
SATHU	*ATXN1*	rs2237199	A/G	0.12	-0.001	0.005	0.81	-0.004	0.004	0.44
VATSAT	*UBE2E2*	rs7374732	T/C	0.63	0.001	0.003	0.85	0.005	0.003	0.11

			DIAGRAM (DIAbetes Genetics Replication And Meta-analysis)[11]			
			Type 2 Diabetes (N_{cases}=26,488 and $N_{controls}$=83,964)			
Trait	**Locus**	**rsID**	**A1/A2**	**OR**	**95%CI**	**P**
PATadjHtWt	*ENSA*	rs6587515	A/G	1.00	0.96-1.04	0.97
VATadjBMI	*GRAMD3*	rs10060123	A/C	0.98	0.95-1.01	0.21
PATadjHtWt	*EBF1*	rs1650505	A/G	1.04	1.01-1.07	0.11
VATadjBMI	*RREB1*	rs2842895	C/G	0.98	0.94-1.01	0.15
SAT	*GDSMB*	rs2123685	T/C	1.03	0.95-1.13	0.44
SATHU	*ATXN1*	rs2237199	A/G	0.99	0.96-1.02	0.50
VATSAT	*UBE2E2*	rs7374732	T/C	0.94	0.92-0.96	1.3E-6

			GLGC (Global Lipids Genetics Consortium)[12]										
					Triglycerides (N=91,013)			High Density Lipoprotein Cholesterol (N=94,311)			Total Cholesterol (N=94,595)		
Trait	**Locus**	**rsID**	**A1/A2**	**A1_AF**	**BETA**	**SE**	**P**	**BETA**	**SE**	**P**	**BETA**	**SE**	**P**
PATadjHtWt	*ENSA*	rs6587515	G/A	0.92	0.003	0.008	0.89	0.007	0.008	0.55	0.008	0.009	0.45
VATadjBMI	*GRAMD3*	rs10060123	A/C	0.26	0.007	0.006	0.43	-0.004	0.006	0.82	-0.014	0.006	0.07
PATadjHtWt	*EBF1*	rs1650505	A/G	0.20	0.019	0.006	6.7E-4	-0.022	0.006	2.1E-4	0.008	0.006	0.22
VATadjBMI	*RREB1*	rs2842895	G/C	0.46	0.000	0.005	0.84	0.004	0.005	0.42	-0.001	0.005	0.76
SAT	*GSDMB*	rs2123685	T/C	0.96	0.011	0.012	0.50	-0.014	0.012	0.11	0.007	0.013	0.80
SATHU	*ATXN1*	rs2237199	A/G	0.12	0.003	0.008	0.96	-0.007	0.008	0.97	-0.004	0.008	0.63
VATSAT	*UBE2E2*	rs7374732	T/C	0.65	0.005	0.005	0.19	0.005	0.005	0.32	0.003	0.005	0.44

165

			Coronary Artery Disease									
			CARDIoGRAM[29] (N_{cases}=21,846, $N_{controls}$=62,200)					C4D[30] (N_{cases}=15,396, $N_{controls}$=15,046)				
Trait	**Locus**	**rsID**	**A1/A2**	**A1_AF**	**OR**	**95%CI**	**P**	**A1/A2**	**A1_AF**	**OR**	**95%CI**	**P**
PATadjHtWt	*ENSA*	rs6587515	A/G	0.10	1.00	0.94-1.04	0.89					
VATadjBMI	*GRAMD3*	rs10060123	A/C	0.28	1.01	0.97-1.04	0.55					
PATadjHtWt	*EBF1*	rs1650505	A/G	0.22	1.01	0.97-1.04	0.45	G/A	0.28	0.99	0.95-1.02	0.62
VATadjBMI	*RREB1*	rs2842895	G/C	0.41	0.99	0.96-1.01	0.50					
SAT	*GSDMB*	rs2123685	T/C	0.92	1.01	0.94-1.07	0.80					
SATHU	*ATXN1*	rs2237199	A/G	0.12	1.02	0.97-1.06	0.43	G/A	0.18	0.99	0.94-1.03	0.54
VATSAT	*UBE2E2*	rs7374732	T/C	0.63	1.00	0.97-1.02	0.99	C/T	0.33	1.02	0.98-1.05	0.28

166
167
168
169
170
171
172

			ICBP (International Consortium for Blood Pressure)[13]							
					Systolic Blood Pressure (N=69,788)			Diastolic Blood Pressure (N=69,783)		
Trait	**Locus**	**rsID**	**A1/A2**	**A1_AF**	**BETA**	**SE**	**P**	**BETA**	**SE**	**P**
PATadjHtWt	*ENSA*	rs6587515	G/A	0.92	0.032	0.166	0.85	0.098	0.106	0.35
VATadjBMI	*GRAMD3*	rs10060123	C/A	0.74	0.044	0.116	0.70	0.068	0.074	0.35
PATadjHtWt	*EBF1*	rs1650505	G/A	0.80	0.167	0.122	0.17	0.086	0.076	0.26
VATadjBMI	*RREB1*	rs2842895	G/C	0.46	0.053	0.101	0.60	0.003	0.064	0.96
SAT	*GSDMB*	rs2123685	T/C	0.96	0.583	0.253	0.02	0.235	0.160	0.14
SATHU	*ATXN1*	rs2237199	G/A	0.88	0.160	0.164	0.33	0.059	0.103	0.57
VATSAT	*UBE2E2*	rs7374732	T/C	0.65	0.017	0.101	0.86	0.030	0.064	0.64

Abbreviations

N - Sample Size
A1/A2 - Coded Allele/Non-Coded Allele
A1_AF - 1000 Genomes Project Allele Frequency
SE - Standard Error
P - P-value
OR - Odds Ratio
95%CI - 95% Confidence Interval
PATadjHtWt - Pericardial Adipose Tissue adjusted for Height and Weight
VATadjBMI - Visceral Adipose Tissue adjusted for Body Mass Index
SAT - Subcutaneous Adipose Tissue
SATHU - Subcutaneous Adipose Tissue Attenuation
VATSAT - Visceral to Subcutaneous Adipose Tissue Ratio

187 **Supplementary Table 13**. SNP specific background information for newly discovered loci
188

SNP name	SNP location	GWAS Catalog	HaploReg[14]			Regulome DB[15]	
		traits associated with SNP	Promoter	Enhancer	DHS	Score	In adipose tissue?
rs6587515	6.8kb 5' of *ENSA*	NA	NA	ESC, ESDR, IPSC, BLD	BLD	5	NA
rs12045807	*ENSA*	NA	BLD	ESDR, ESC, LNG, FAT, STRM, BRST, BLD, MUS, BRN, SKIN, LIV, GI, ADRL, PLCNT, THYM, HRT, PANC, SPLN, CRVX, VAS, BONE	BLD, PLCNT	5	Possible enhancer in adipose derived mesnchymal stem cells and adipose nuclei
rs138805506	*ENSA*	NA	LNG, FAT, STRM, BLD, MUS, SKIN, BRN, GI, HRT, CRVX, LIV, BRST, VAS, BONE	ESDR, BRST, BLD, SKIN, FAT, VAS, LIV, BRN, GI, ADRL, PANC, MUS, PLCNT, HRT, SPLN	ESDR,LNG,BRST, BLD SKIN,HRT,KID,LNG,MUS,THYM,GI,OVRY,PANC,CRVX, LIV,VAS, BRN,	4	Possible enhancer in adipose nuclei and flanking active transcription start site in adipose derived mesnchymal stem cells and
rs10060123	12kb 5' of *GRAMD3*	NA	NA	NA	NA	7	NA
rs6877526	7.8kb 5' of GRAMD3	NA	NA	ESDR, LNG, FAT, STRM, BRST, MUS, SKIN, GI, CRVX, VAS, BLD	NA	5	Possible enhancer in adipose derived mesnchymal stem cells
rs1549189	7.5kb 5' of GRAMD3	NA	NA	ESDR, LNG, FAT, STRM, BRST, MUS, SKIN, ADRL, GI, CRVX, VAS	NA	6	Possible enhancer in adipose derived mesnchymal stem cells
rs6595695	6.7kb 5' of GRAMD3	NA	NA	LNG, FAT, STRM, BRST, MUS, SKIN, BRN, ADRL, PLCNT,	MUS	5	Possible enhancer in adipose derived mesnchymal stem cells

SNP name	SNP location	GWAS Catalog	HaploReg[14]			Regulome DB[15]	
		traits associated with SNP	Promoter	Enhancer	DHS	Score	In adipose tissue?
				GI, CRVX, VAS, BONE			
rs2080	6.4kb 5' of GRAMD3	NA	NA	ESDR, LNG, FAT, STRM, BRST, BLD, MUS, SKIN, GI, CRVX, VAS, BRN, BONE	NA	5	Possible enhancer in adipose derived mesnchymal stem cells
rs1650505	93kb 3' of *EBF1*	Age related hearing impairment	NA	NA	NA	7	NA
rs890945	31kb 3' of RP11-32D16.1	NA	NA	BLD, FAT	NA	4	Possible enhancer in adipose nuclei
rs2963474	37kb 3' of RP11-32D16.1	NA	NA	FAT	NA	7	NA
rs2914224	37kb 3' of RP11-32D16.1	NA	NA	FAT	NA	7	NA
rs2963471	39kb 3' of RP11-32D16.1	NA	NA	FAT	NA	6	Possible enhancer in adipose nuclei
rs1428443	39kb 3' of RP11-32D16.1	NA	NA	FAT	NA	5	Possible enhancer in adipose nuclei
rs1428442	39kb 3' of RP11-32D16.1	NA	NA	FAT	NA	5	Possible enhancer in adipose nuclei
rs2963470	40kb 3' of RP11-32D16.1	NA	NA	FAT	NA	7	NA
rs748510	65kb 3' of RP11-32D16.1	NA	NA	ESDR,FAT,BLD,SKIN,BRN,LNG,THYM	NA	7	NA
rs890939	65kb 3' of RP11-32D16.1	NA	NA	ESDR, FAT, BLD,SKIN, BRN, MUS, THYM,LNG	NA	7	NA
rs890940	65kb 3' of RP11-32D16.1	NA	NA	ESDR, FAT, BLD,SKIN, BRN, MUS, THYM,LNG	NA	7	NA

SNP name	SNP location	GWAS Catalog	HaploReg[14]			Regulome DB[15]	
		traits associated with SNP	Promoter	Enhancer	DHS	Score	In adipose tissue?
rs2842895	1.5kb 5' of *RREB1*	NA	BLD	ESDR,ESC,IPSC,BLD,THYM,LIV	LNG,BLD	4	NA
rs11759956	*RREB1*	NA	ESC, ESDR, LNG, IPSC, FAT, STRM, BRST, BLD, MUS, BRN, SKIN, VAS, LIV, GI, ADRL, KID, PANC, PLCNT, THYM, HRT, OVRY, SPLN, CRVX, BONE	BRN	BLD,KID,GI,THYM, MUS, LIV	2b	Possible enhancer in adipose derived mesnchymal stem cells and adipose nuclei
rs7451690	*RREB1*	NA	ESC, ESDR, LNG, IPSC, FAT, STRM, BRST, BLD, MUS, BRN, SKIN, VAS, LIV, GI, ADRL, KID, PANC, PLCNT, THYM, HRT, OVRY, SPLN, CRVX, BONE	BLD, BRN	ESDR, BLD, SKIN, HRT, KID,MUS, GI, THYM, OVRY	2b	Active transcription site in adipose nuclei and adipose derived mesnchymal stem cells
rs148697759	*RREB1*	NA	ESC, ESDR, IPSC, STRM, BLD, MUS, SKIN, GI, HRT, PANC, LNG,	ESC, ESDR, LNG, IPSC, FAT, BRST, BLD, BRN, SKIN, LIV, GI, KID, MUS, PLCNT, THYM, HRT,	ESDR, BRST, BLD, SKIN, LNG, PLCNT, GI, LIV, BRST	4	Possible enhancer in adipose nuclei and adipose derived mesnchymal stem cells

SNP name	SNP location	GWAS Catalog	HaploReg[14]			Regulome DB[15]	
		traits associated with SNP	Promoter	Enhancer	DHS	Score	In adipose tissue?
			LIV, BRST	OVRY, BONE			
rs4960289	*RREB1*	NA	ESC, IPSC, BRST, BLD, SKIN, GI, KID, THYM, PANC, MUS, LNG	ESC, ESDR, LNG, IPSC, FAT, STRM, BLD, MUS, BRN, SKIN, VAS, LIV, GI, ADRL, HRT, PLCNT, SPLN, BONE	ESC,BRST,SKIN,HRT,GI,KID,LNG,PLCNT, THYM,PANC,MUS, LIV,BLD	3a	Possible enhancer in adipose nuclei and adipose derived mesnchymal stem cells
rs2123685	7kb 3' of *GSDMB*	NA	NA	NA	NA	7	NA
rs112599791	*GSDMB*	NA	GI	FAT, LIV, GI, BLD	GI,LIV	6	
rs113894104	*GSDMB*	NA	GI	FAT, LIV, GI, BLD	BLD,GI, LIV	2b	possible enhancer in adipose nuclei
rs3859186	*GSDMB*	NA	NA	BLD, SKIN, FAT, LIV, GI, PLCNT, THYM, SPLN	NA	2b	Strong transcription in adipose derived mesnchymal stem cells and genic enhancer in adipose nuclei
rs112260932	*GSDMB*	NA	BLD	BLD, FAT, LIV, GI, MUS, PLCNT, THYM, SPLN	BLD, ADRL,GI, THYM,OVRY,LIV	6	Possible enhancer in adipose nuclei
rs3169572	*ORMDL3*	NA	BLD	BLD, SKIN, FAT, LIV, GI, ADRL, MUS, PLCNT, THYM, SPLN	BLD	4	Strong transcription in adipose derived mesnchymal stem cells and genic enhancer in adipose nuclei
rs3169574	*ORMDL3*	NA	BLD	BLD, SKIN, FAT, LIV, GI, ADRL, MUS, PLCNT, THYM, SPLN	BLD	2b	Strong transcription in adipose derived mesnchymal stem cells and genic enhancer in adipose nuclei
rs78199107	*ORMDL3*	NA	BLD	BLD, SKIN, FAT, LIV, GI, ADRL, MUS, PLCNT, THYM, SPLN	BLD, PLCNT, LIV	2b	Strong transcription in adipose derived mesnchymal stem cells and genic enhancer in

SNP name	SNP location	GWAS Catalog	HaploReg[14]			Regulome DB[15]	
		traits associated with SNP	Promoter	Enhancer	DHS	Score	In adipose tissue?
							adipose nuclei
rs2237199	intronic *ATXN1*	NA	NA	BRN, GI	NA	7	NA
rs6809615		NA	NA	FAT, MUS, SKIN, BLD, VAS, LNG	NA	6	Possible enhancer in adipose derived mesnchymal stem cells
rs7374732	29kb 5' of *UBE2E2*	NA	BLD	FAT, BLD, SKIN, LNG, BRN	ESDR, BLD, SKIN	2b	Possible enhancer in adipose derived mesnchymal stem cells

*Abbreviations:

DHS DNAse Hypersensitivity Site
BLD Blood
BRN Brain
ESC Embryonic Stem Cells
ESDR Embryonic Stem Derived Cultured Cells
FAT Adipose Tissue
GI Digestive Tract
IPSC Induced Pluripotent Stem Cells
LIV Liver
LNG Lung
SKIN Epithelial
THYM Thymus

202 **Supplementary Table 14.** Gene-specific background information on newly identified loci.

Gene Name	Gene information
ENSA	A total of 32 genes are found within 500 kb of the lead marker, rs6587515. *ENSα* (endosulfine alpha, 1q21) is located 7 kb upstream from our lead marker. *ENSα* encodes protein that belongs to a highly conserved cAMP-regulated phosphoprotein (ARPP) family. This protein was identified as an endogenous ligand for the sulfonylurea receptor, *ABCC8*/*SUR1*. ABCC8 is the regulatory subunit of the ATP-sensitive potassium (KATP) channel, which is located on the plasma membrane of pancreatic beta cells and plays a key role in the control of insulin release from pancreatic beta cells. SUR system seems also to be involved in human adipose tissue. The expression of *SUR2B* gene was higher in subcutaneous compared with omental adipose tissue and was not affected by weight loss (Gabrielsson et al. 2004).[16] There are also two genes involved in development of obesity, *CTSS* and *CTSK* (Naour et al. 2010, Xiao et al. 2006).[17,18] *CTSS* (cathepsin K) is located at 94 kb downstream of our leader marker. *CTSS* plays a central role in extracellular matrix remodeling by stimulating adipocyte differentiation through degrading fibronectin. *CTSK* (cathepsin K) is located at 160 kb downstream of our leader marker. It encodes a lysosomal cysteine proteinase involved in extracellular matrix remodeling and could be one of the determinants of adipocyte differentiation. *CTSK* may be involved in the pathogenesis of obesity by promoting adipocyte differentiation (Xiao et al. 2006).[18] In addition, there are several biologically relevant genes within 1000 kb of the lead marker for regulatory role in Golgi complex (*GOLPH3L*), apoptosis (*MCL1*), cell cycle regulation (*HORMAD1*), transcriptional regulation (*MIR4257, ECM1, ARNT, SETBD1, MRPS21, CIART*, and *GABPB2*), threonine-tRNA ligase activity (*TARS2*), among others. GWA studies have reported associations within the 1Mb region of rs6587515 for fat body mass adjusted by lean body mass (rs2230061: p=4E-8, Pei et al. 2014),[19] BMI (rs4357530: p=7.03E-14, Winkler et al. 2015),[20] height (rs956796: p=1.7E-10, Wood et al. 2014),[21] LDL cholesterol (rs267733: p=5E-9, Willer et al. 2013),[12] prostate cancer (rs17599629: p=6E-23, Al Olama et al. 2014),[22] melanoma (rs7412746: p=6E-23, Macgregor et al. 2014),[23] rhegmatogenous retinal detachment (rs267738: p=1E-7, Kirin et al. 2013),[24] and chronic kidney disease (rs267734: p=1E-12, Köttgen et al. 2010).[25] All of these markers appear to be independent of our lead SNP (r2<0.15).
GRAMD3	A total of five genes are found within 500 kb of the lead marker, rs10060123. *GRAMD3* (GRAM domain containing 3, 5q23.2) is located 11.9 kb upstream from rs10060123. At 193.6 kb downstream of this lead marker is located *ALDH7A1* (5q31) gene, which encodes a member of subfamily 7 in the aldehyde dehydrogenase gene family. This enzyme degrades and detoxifies acetaldehyde generated by alcohol metabolism (cf. Guo et al. 2011).[26] A significant GWA has been reported between osteoporosis with *ALDH7A1*-rs13182402 (p=2E-09, Guo et al. 2011)[26] that is in low LD with rs10060123 (r2=0.006). In addition, suggestive evidence of GWA has been found between *GRAMD3* region with diabetic retinopathy (rs1073203: p=9E-06, Grassi et al. 2011),[27] QT interval (rs1546498: p=5E-06, Smith et al. 2012),[28] cognitive outcomes in Parkinson's disease (rs959573: p=2E-06, Chung et al. 2012),[29] and cognitive tests (rs13169113: p=9E-06, Cirulli et al. 2010).[30]

Gene Name	Gene information
EBF1	The *EBF1* (early B-cell factor 1, 5q34) is located 93 kb downstream from rs1650505. The *EBF1* is the only gene located within 500 kb of this lead marker. *EBF1* is a transcriptional activator, expressed in early B lymphocytes, adipocytes, and olfactory neurons (Hagman et al. 2012, Milatovich et al. 1994).[31,32] *EBF1* negatively regulates estrogen receptors (ER) at the protein level (Le et al. 2013).[33] It seems that *EBF1* suppresses the expression and activity of ER, which consequently facilitates adipogenesis by up regulating adipogenic genes as well as by releasing *PPARγ* from the inhibition exerted by estrogen signaling (cf. Le et al. 2013).[33] Recently, a significant *EBF1*-psychosocial stress interaction GWA for hip circumference was reported (rs17056278: p=3E-8, Singh et al. 2015),[34] but the SNP is in low LD with the leader markers (rs17056278 with rs1650505 or with rs2434264: r2<0.1). Additional GWA studies have shown association with blood pressure (rs11953630: p=3E-11 for systolic, and rs11953630: p=4E-13 for diastolic Ehret et al. 2011,[13] and rs9313772: p=1E-11 for mean arterial pressure, Wain et al. 2011),[35] longevity (90 years and older, rs2149954: p=2E-8, Deelen et al. 2014),[36] breast cancer (rs1432679: p=2E-14, Michailidou et al. 2013),[37] neutropenia/ leucopenia response to anthracycline-based drugs (rs10040979: p=5E-7, Low et al. 2013),[38] hypospadias (rs4563609: p=3E-7, Geller et al. 2014),[39] eotaxin (rs13170526: p=4E-06, Comuzzie et al. 2012),[38] and metabolite levels (dihydroxy docosatrienoic acid, rs11957368: p=4E-6, Yu et al. 2013).[40]
RREB1	A total of eight genes are found within 500 kb of the lead marker, rs2842895. *RREB1* (6p25), located 1.5 kb upstream from rs2842895, encodes a zinc finger transcription factor that binds to RAS-responsive elements (RREs) of gene promoters, including the calcitonin gene promoter. Another biological relevant gene located at 175 kb downstream from rs2842895 is the *SSR1* (signal sequence receptor, alpha, 6p24.3). *SSR1* encodes a glycosylated endoplasmic reticulum membrane receptor associated with protein translocation across the ER membrane. The association between rs2842895 with visceral adipose tissue adjusted for BMI was previously reported but did not reach a genomewide significance level (p=4E-6, Fox et al. 2012).[41] There is also evidence of GWA between waist-hip ratio with rs1294421 (p=2E-10, Berndt et al. 2013, p=2E-17, Heid et al. 2010)[42,43] and with rs1294410 (p=2E-18, Locke et al. 2015),[9] which are not in LD with the lead marker rs2842895 (r2=0.0). Several other loci from GWA studies have been reported on 6p24-6p25 region associated with body mass index (p=3E-8, Liu et al. 2013),[44] type 2 diabetes (rs9502570: p=1E-9, Mahajan et al. 2014),[11] BMI-adjusted-fasting glucose (rs17762454: p=9.6E-9, Scott et al. 2012),[45] fasting glucose-related traits interaction with BMI (rs11755724: p=3E-7, Manning et al. 2012),[10] height (p=4.6E-14, Wood et al. 2014),[21] interstitial lung disease (rs2076295: p=1E-19, Fingerlin et al. 2013),[46] urate levels (rs675209: p=1E-23, Köttgen et al. 2013, rs675209: p=1E-9, Yang et al. 2010),[47,48] multiple sclerosis (rs11755724: p=3E-6, Sawcer et al. 2011),[49] age-related macular degeneration (rs11755724: p=1E-6, Neale et al. 2010),[50] mammographic density non-dense area (rs1294438: p=1E-6, Lindström et al. 2014),[51] and major depressive disorder (rs2326810: p=7E-6, Shyn et al. 2011).[52]

Gene Name	Gene information
GSDMB	A total of 31 genes are found within 500 kb of the lead marker, rs2123685. *GSDMB* (gasdermin B, 17q12) is located 7 kb downstream from rs2123685. *GSDMB* and other genes on 17q12-q21 have shown association with inflammatory diseases, cancers, hematological parameters and/or metabolic traits. Five of the more biologically relevant genes that lie within the association signal region are *ERBB2, NR1D1, THRα, RARα*, and *MED1*. *ERBB2* (erb-b2 receptor tyrosine kinase 2, 17q12) is located 169 kb downstream from rs2123685. *ERBB2* encodes a member of the epidermal growth factor receptor (*EGFR*) family of receptor tyrosine kinases. Experimental studies have indicated that up-regulation of signaling via ERBB2 and *EGFR* by leptin contributes to vascular dysfunction as seen in obesity, metabolic syndrome, and diabetes (cf., Bełtowski et al. 2014).[53] *NR1D1* (nuclear receptor subfamily 1, group D, member 1) is located 195 kb downstream from rs2123685. The encoded protein is a ligand-sensitive transcription factor that regulates circadian rhythm and metabolism, influences adipocyte differentiation, and may also be involved in regulating genes that function in metabolic, inflammatory and cardiovascular processes (Wang et al. 2008, Fontaine et al. 2003).[54,55] *THRα* (thyroid hormone receptor, alpha, 17q11.2), located at 165 kb upstream from rs2123685, encodes a nuclear hormone receptor for triiodothyronine. It is one of the several receptors for thyroid hormone, and has been shown to mediate the biological activities of thyroid hormone. *THRα* is associated with obesity development (Fernández-Real et al. 2013),[56] and may contribute to subcutaneous adipose tissue expandability in obese subjects (Ortega et al. 2009).[57] There is also a suggestion that differential interaction of *NCoR1* (nuclear receptor corepressor) with thyroid hormone receptor (TR) isoforms accounted for the TR isoform-dependent regulation of adipogenesis, and that aberrant interaction of *NCoR1* with TR could underlie the pathogenesis of lipid disorders in hypothyroidism (Zhu et al. 2011).[58] *RARα* (retinoic acid receptor, alpha) is located 412 kb upstream from rs2123685. The encoded protein, retinoic acid receptor alpha, regulates transcription in a ligand-dependent manner. *RARα* plays a role in regulation of development, differentiation, apoptosis, granulopoeisis, and transcription of clock genes. Obesity was suggested to be associated with an inverse relationship between *PPARγ* (peroxisome proliferator-activated receptor gamma) and *RARα* expressions in human subcutaneous adipose tissue (Redonnet et al. 2002).[59] *MED1* (mediator complex subunit 1) is located 446 kb from rs2123685. The activation of gene transcription is a multistep process that is triggered by factors that recognize transcriptional enhancer sites in DNA (cf. Chen et al. 2009).[60] The protein encoded by this gene is a subunit of the *CRSP* (cofactor required for SP1 activation) complex, which, along with *TFIID*, is required for efficient activation by *SP1*. This protein is also a component of other multisubunit complexes, e.g. TR- associated proteins which interact with TR and facilitate TR function on DNA templates in conjunction with initiation factors and cofactors. In addition, *MED1/TRAP220* is the nuclear receptor-interacting subunit of the *MED* and is required for *PPARγ* -stimulated adipogenesis (Ge et al. 2002).[61] Several GWA studies have reported associations within the 1Mb region of rs2123685 for asthma (e.g., rs8069176: p=6E-23, Bønnelykke et al. 2014, rs11078927: p=2E-16, Torgerson et al. 2011),[62,63] fractional exhaled nitric oxide in childhood (rs8069176: p=2E-8, van der Valk et al. 2014),[64] self-reported allergy (rs9303280: p=9E-9, Hinds et al. 2013),[65] Crohn's disease (rs2872507: p=2E-09, Franke et al. 2010, rs2872507: p=5E-09, Barrett et al. 2008),[66,67] type 1 diabetes (rs2290400: p=6E-13, Barrett et al. 2009),[68] ulcerative colitis (rs2872507: p=5E-11, Anderson et al. 2011, rs2305480: p=3E-8, McGovern et al. 2010),[69,70] rheumatoid arthritis (rs1877030: p=2E-8, Okada et al. 2014),[71] primary biliary cirrhosis (rs9303277: p=4E-9, Nakamura et al. 2012, rs9303277: p=2E-9, Liu et al. 2010),[72,73] inflammatory bowel disease (rs12946510: p=4E-38, Jostins et al. 2012),[74] cervical cancer (rs2872507: p=9E-10, Shi et al. 2013),[75] white blood cell count (e.g., rs4065321: p=1E-12, Crosslin et al. 2012, rs4065321: p=9E-35, Nalls et al. 2011, rs4065321: p=3E-14, Kamatani et al. 2010, rs17609240: p=9E-9, Soranzo et al. 2009),[76-79] and HDL cholesterol (e.g., rs11869286: p=3E-17, Willer et al. 2013).[12]

Gene Name	Gene information
ATXN1	A total of 3 genes are found within 500 kb of the lead marker, rs2237199. This marker is located within an intron in *ATXN1* (6p22). Expansion of a CAG repeat in the coding region of *ATXN1* causes spinocerebellar ataxia type 1 (SCA1) which belongs to the autosomal dominant cerebellar ataxias. Longer expansions of CAG result in earlier onset and more severe clinical manifestations of the disease characterized by progressive degeneration of the cerebellum that may lead to optic atrophy, ophthalmoplegia, bulbar and extrapyramidal signs, peripheral neuropathy and dementia. However, the function of the ataxins is not known. GWA studies have shown association between variants on 6p22 with blood metabolite levels (p=2E-16, Shin et al. 2014),[80] electrocardiographic measure (QT interval: p=3E-10, Arking et al. 2014),[81] and cholesterol levels (total: p=2E-17, and LDL: p=2E-17, Willer et al. 2013).[12] Additional suggestive evidences of GWA have been reported between *ATXN1* with disordered gambling (p=5E-06, Lind et al. 2013),[82] major depressive disorder (p=1E-06, GENDEP Investigators et al. 2009),[83] and amyotrophic lateral sclerosis (p=4E-06, Landers et al. 2009).[84]
UBE2E3	The *UBE2E2* (3p24.2) is located 41 kb upstream from rs7374732, and the only gene located within 500 kb of this lead marker. *UBE2E2* encodes the ubiquitin-conjugating enzyme E2E2, which expression in human pancreas, liver, muscle and adipose tissue (Yamauchi et al. 2010).[85] GWA studies have reported association between *UBE2E2* region with type 2 diabetes (rs6780569: p=4E-07, Hara et al. 2014, rs7612463: p=7E-09, Mahajan et al. 2014, and rs7612463: p=2.3E-09, Yamauchi et al. 2014)[11,85,86] but the markers are in low LD with rs7374732 (with rs6780569: r^2=0.034, and with rs7612463: r^2=0.005). Additional suggestive evidence of GWA for *UBE2E2* have also been reported with atypical psychosis (rs4619807: p=2E-06, Kanazawa et al. 2013),[87] colorectal cancer (rs4591517: p=3E-06, Jiao et al. 2014),[88] chronic kidney disease (rs9310709: p=2E-06, Gudbjartsson et al. 2010).[89]

203

Supplementary Table 15. Mean variance explained by each newly identified ectopic fat locus. Variance explained was approximated using the following formula $R^2 = \beta^2 var(SNP)/var(ectopic\ fat\ trait)$, where β^2 is the estimated effect of the SNP on the ectopic fat trait, and $var(SNP)=2*MAF_{SNP}*(1-MAF_{SNP})$. Because sample-size weighted fixed-effect meta-analysis does not estimate effect sizes, the beta-coefficient for the association between the SNP and ectopic fat trait and the variance of the ectopic fat trait were obtained from cohort level analysis per contributing study.

Trait	Locus	rsID	Variance Explained
PATadjHtWt	*ENSA*	rs6587515	0.28%
VATadjBMI	*GRAMD3*	rs10060123	0.23%
PATadjHtWt	*EBF1*	rs1650505	0.53%
VATadjBMI	*RREB1*	rs2842895	0.15%
SAT	*GDSMB*	rs2123685	0.62%
SATHU	*ATXN1*	rs2237199	0.57%
VATSAT	*UBE2E2*	rs7374732	4.42%

Supplementary Table 16. Results from eQTL analysis of newly identified ectopic fat SNPs. Index SNPs and SNPs in LD with the index SNP (r^2>0.8) across all ancestries available in the 1000 Genomes Project pilot (SNAP[90]). A general overview of the larger collection of more than 50 eQTL studies from which the adipose-related datasets (omental, visceral and subcutaneous adipose,[91-95]).

LOCUS	SNPID	Tissue	P-value	Transcript
ENSA	rs12045807	Subcutaneous adipose tissue [93]	4.53E-05	*MRPS21*
ENSA	rs2134688	Omental adipos tissue [92]	9.17E-15	*CTSK*
ENSA	rs7517	Subcutaneous adipose tissue [93]	4.27E-05	*MRPS21*
ENSA	rs7521445	Omental adipose tissue [92]	9.48E-34	*LASS2*
ENSA	rs7521445	Subcutaneous adipose tissue [92]	4.78E-23	*LASS2*

Supplementary Table 17. Primer sequences used in qPCR analysis of murine adipose tissue.

Gene	Forward Primer Sequence	Reverse Primer Sequence
Ube2e2	ACTGAGGCGCAGAGAGTTGA	GCTGAACTTGTTCTCGATCAGG
Atxn1	CTCCCAAGAAACGTGAGATCC	CCATTCCTTGTAAACCATGCTCC
Rreb1	GCACTCTGGCGAGAGGCCTTAC	GCTGCAGCTGTAGTACTGTTG
Ebf1	GCATCCAACGGAGTGGAAG	GATTTCCGCAGGTTAGAAGGC

Supplementary Figure 1a. Regional association plot for the *ENSA* locus in up to 12,204 women and men. P-values for association were obtained using a sample-size weighted fixed-effects meta-analysis implemented in METAL.[6,7] Pairwise linkage disequilibrium estimates were obtained from SNAP.[90] Plot was created using the gap R package (https://www.jstatsoft.org/article/view/v023i08).

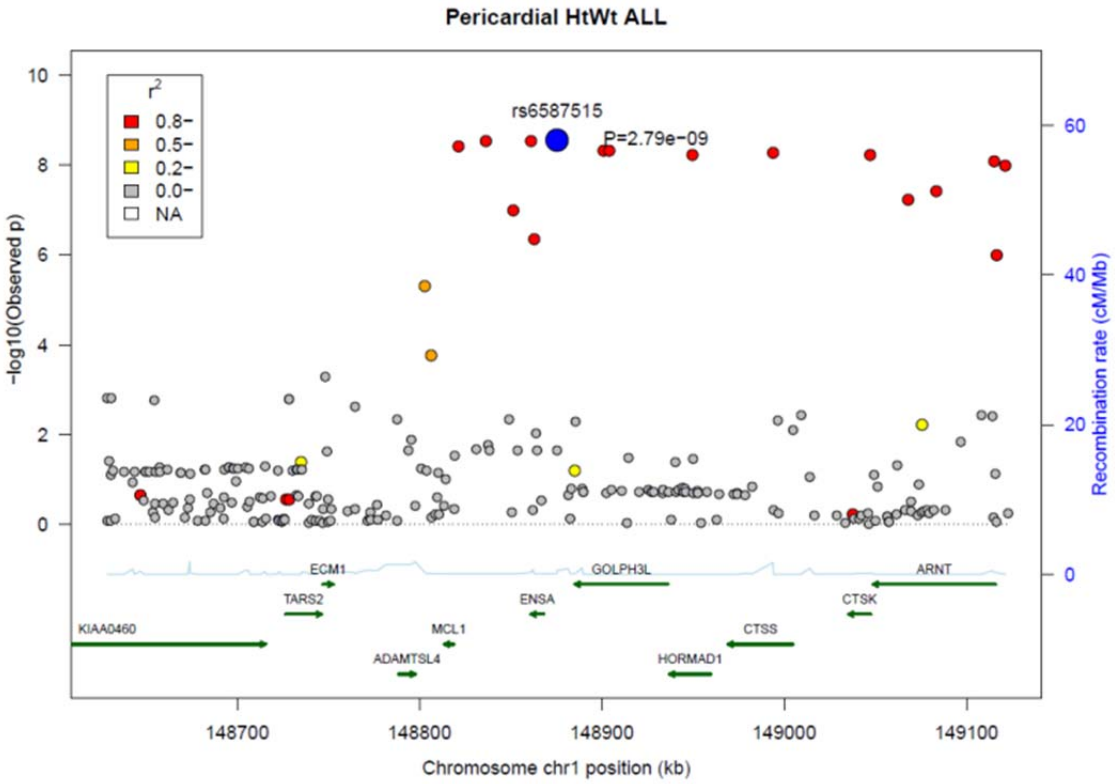

Supplementary Figure 1b. Regional association plot for the *GRAMD3* locus in up to 9,594 women. P-values for association were obtained using a sample-size weighted fixed-effects meta-analysis implemented in METAL.[6,7] Pairwise linkage disequilibrium estimates were obtained from SNAP.[90] Plot was created using the gap R package (https://www.jstatsoft.org/article/view/v023i08).

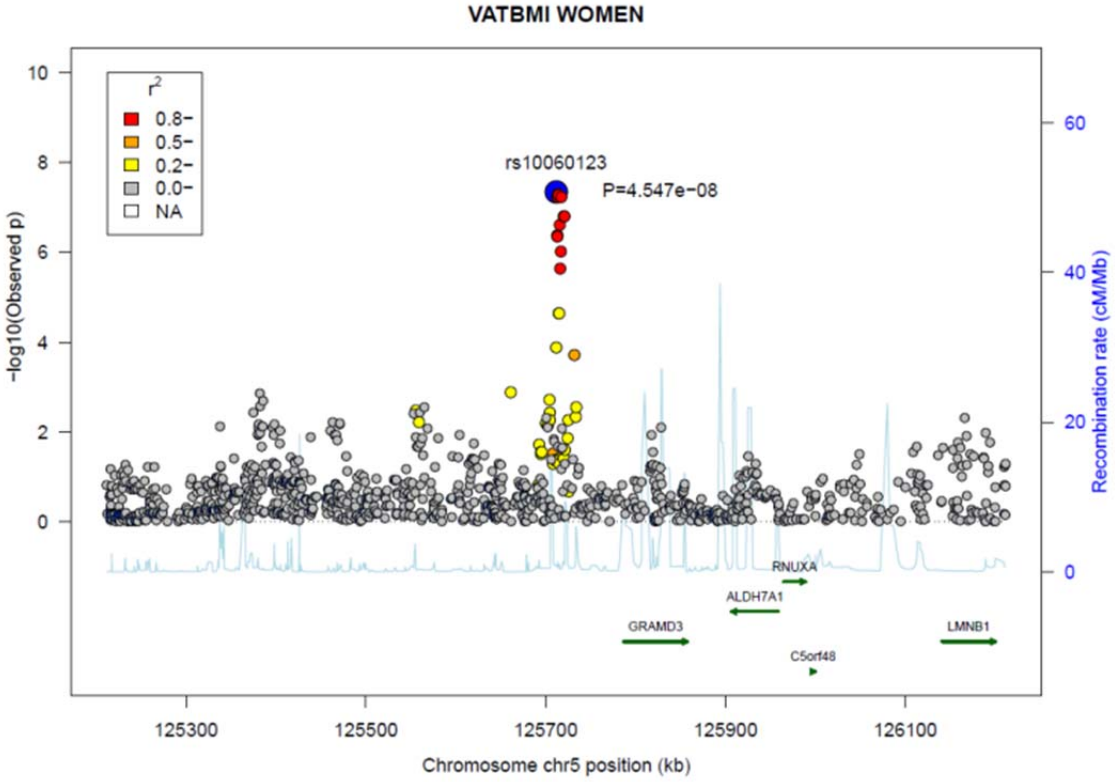

Supplementary Figure 1c. Regional association plot for the *EBF1* locus in up to 12,204 women and men. P-values for association were obtained using a sample-size weighted fixed-effects meta-analysis implemented in METAL.[6,7] Pairwise linkage disequilibrium estimates were obtained from SNAP.[90] Plot was created using the gap R package (https://www.jstatsoft.org/article/view/v023i08).

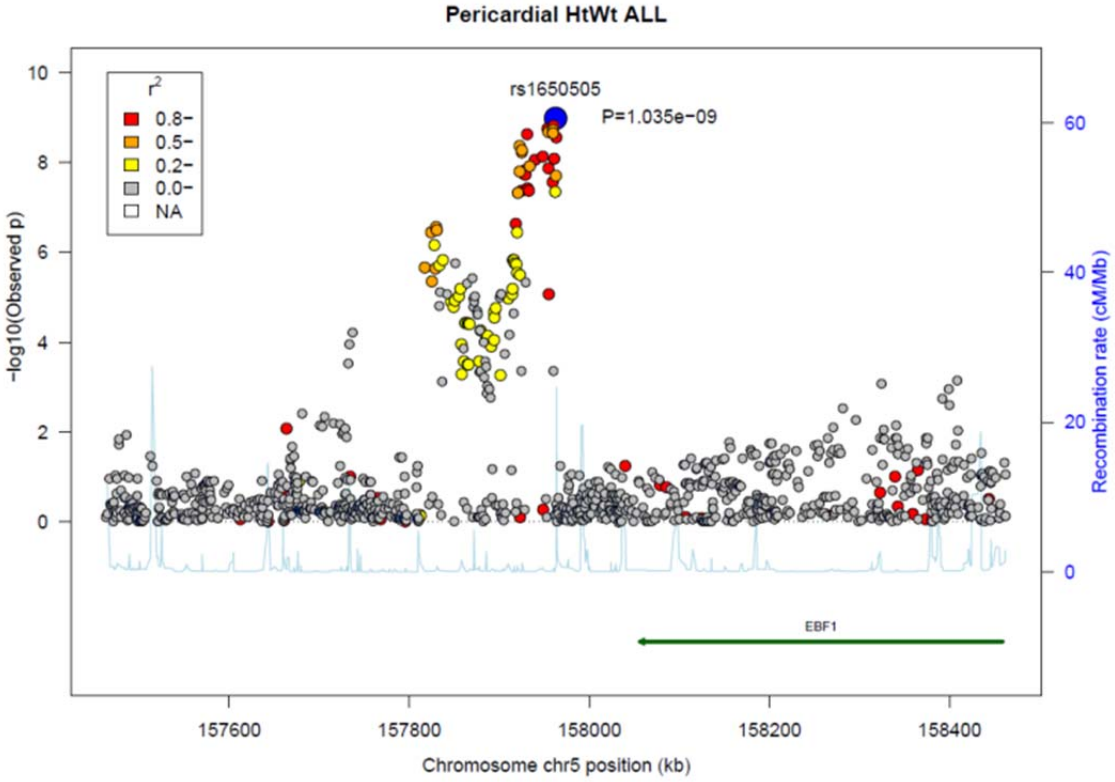

Supplementary Figure 1d. Regional association plot for the *RREB1* locus in up to 18,332 women and men. P-values for association were obtained using a sample-size weighted fixed-effects meta-analysis implemented in METAL.[6,7] Pairwise linkage disequilibrium estimates were obtained from SNAP.[90] Plot was created using the gap R package (https://www.jstatsoft.org/article/view/v023i08).

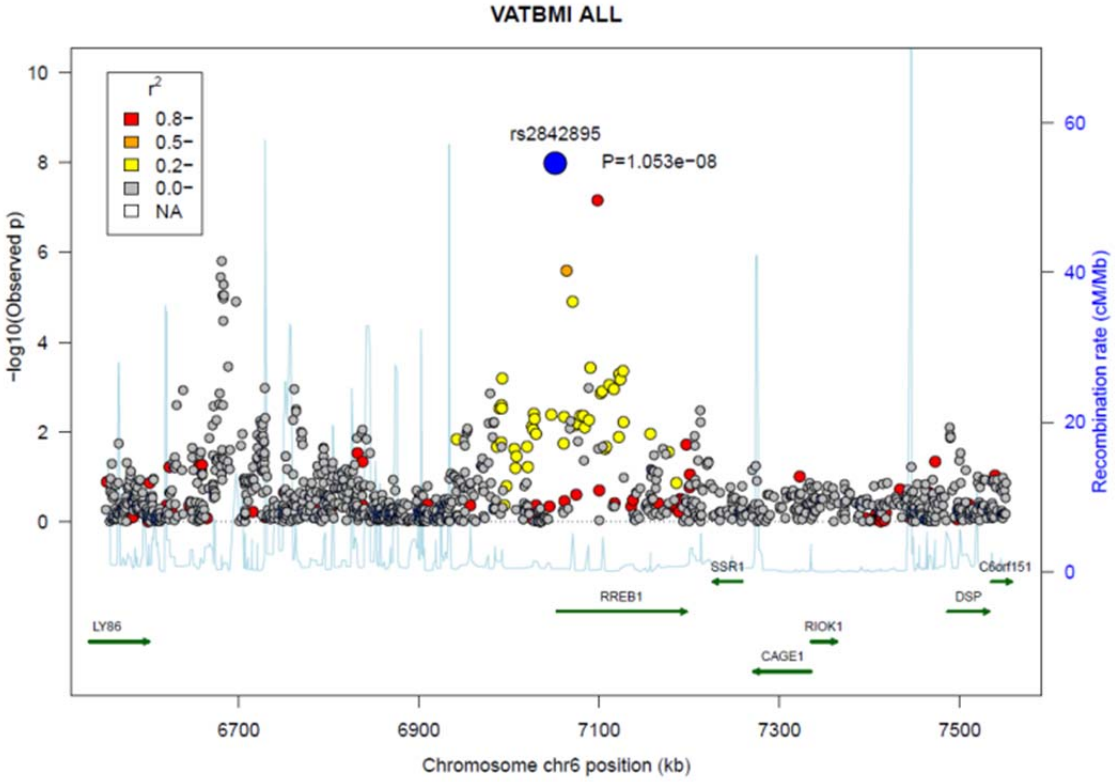

Supplementary Figure 1e. Regional association plot for the *GSDMB* locus in up to 9,562 women. P-values for association were obtained using a sample-size weighted fixed-effects meta-analysis implemented in METAL.[6,7] Pairwise linkage disequilibrium estimates were obtained from SNAP.[90] Plot was created using the gap R package (https://www.jstatsoft.org/article/view/v023i08).

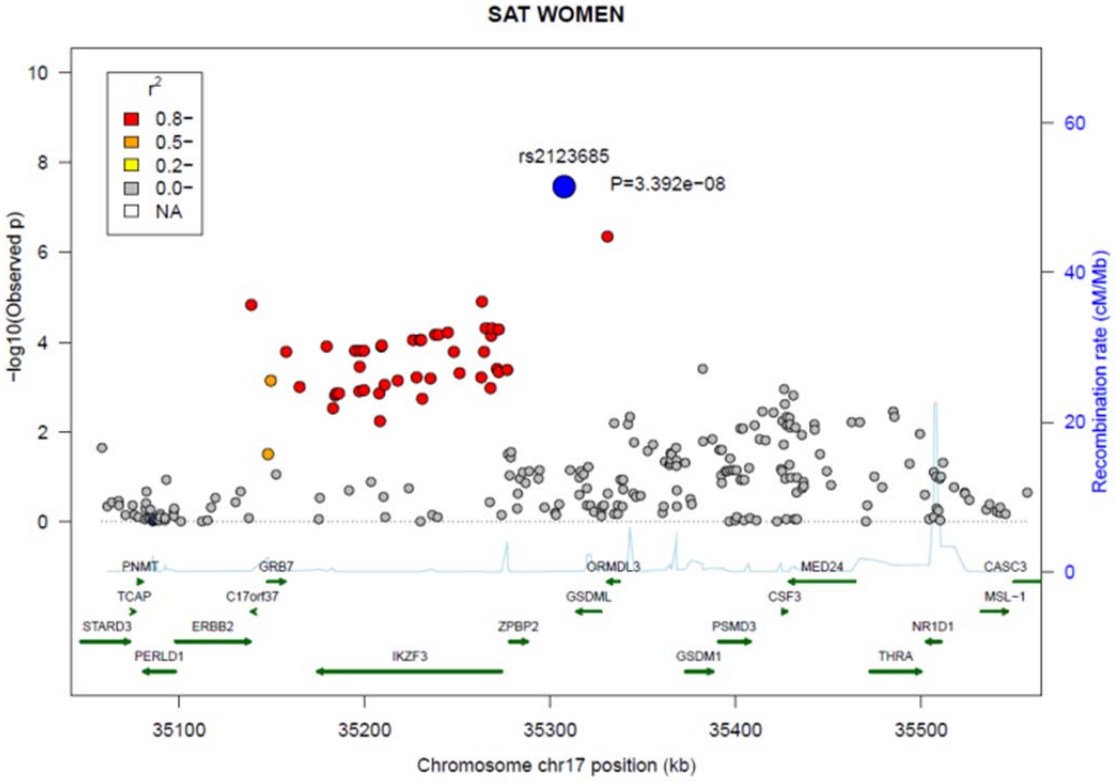

Supplementary Figure 1f. Regional association plot for the *ATXN1* locus in up to 6,149 men. P-values for association were obtained using a sample-size weighted fixed-effects meta-analysis implemented in METAL.[6,7] Pairwise linkage disequilibrium estimates were obtained from SNAP.[90] Plot was created using the gap R package (https://www.jstatsoft.org/article/view/v023i08).

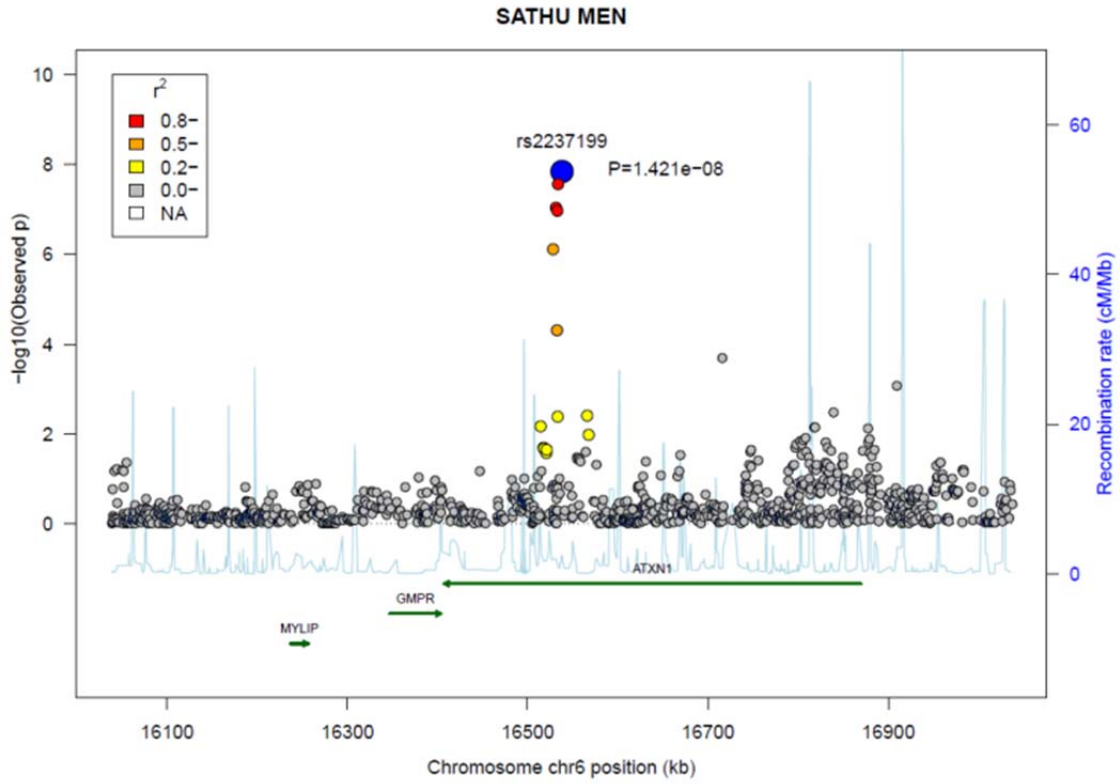

Supplementary Figure 1g. Regional association plot for the *UBE2E2* locus in up to 18,191 women and men. P-values for association were obtained using a sample-size weighted fixed-effects meta-analysis implemented in METAL.[6,7] Pairwise linkage disequilibrium estimates were obtained from SNAP.[90] Plot was created using the gap R package (https://www.jstatsoft.org/article/view/v023i08).

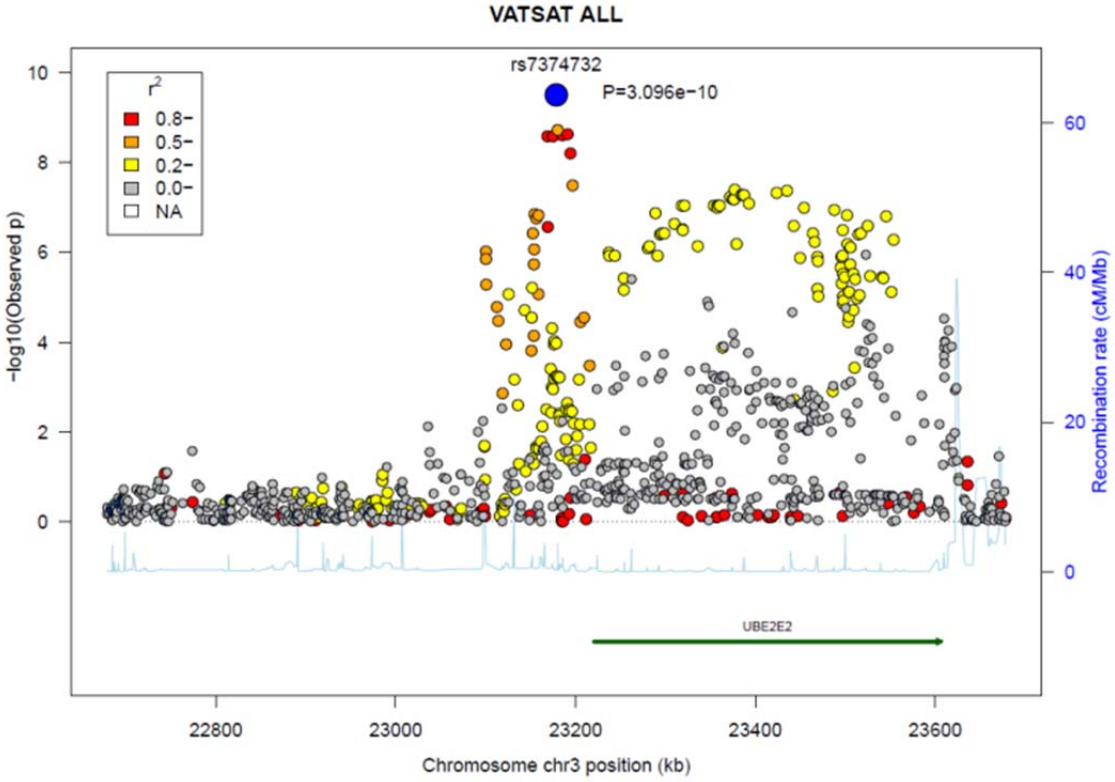

Supplementary Figure 2a. Forest plots of Z-scores for rs6587515 (*ENSA*, pericardial fat locus) among combined sample of 11,027 women and men ($N_{European\ Ancestry}$=7,425; $N_{African\ Ancestry}$=1,442; $N_{Asian\ Ancestry}$=761; $N_{Hispanic\ Ancestry}$=1,399).

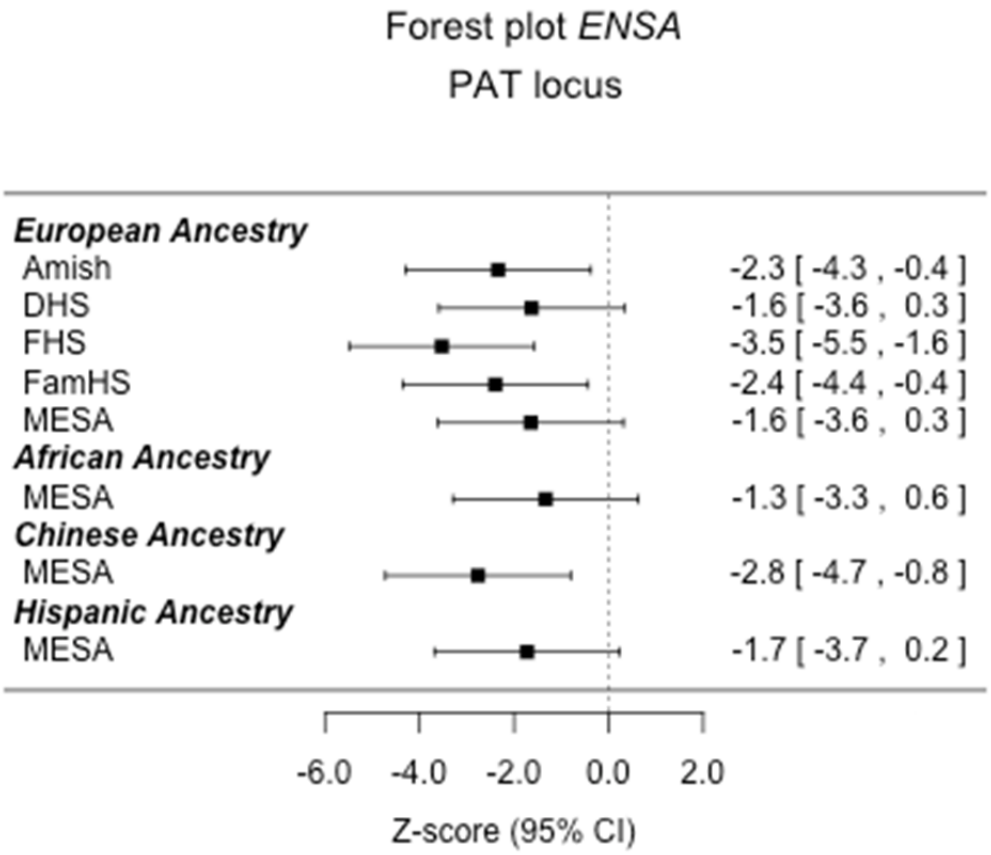

Supplementary Figure 2b. Forest plots of Z-scores for rs10060123 (*GRAMD3*, visceral fat locus) among 9,623 women ($N_{European\ Ancestry}$=7,403; $N_{African\ Ancestry}$=2,220).

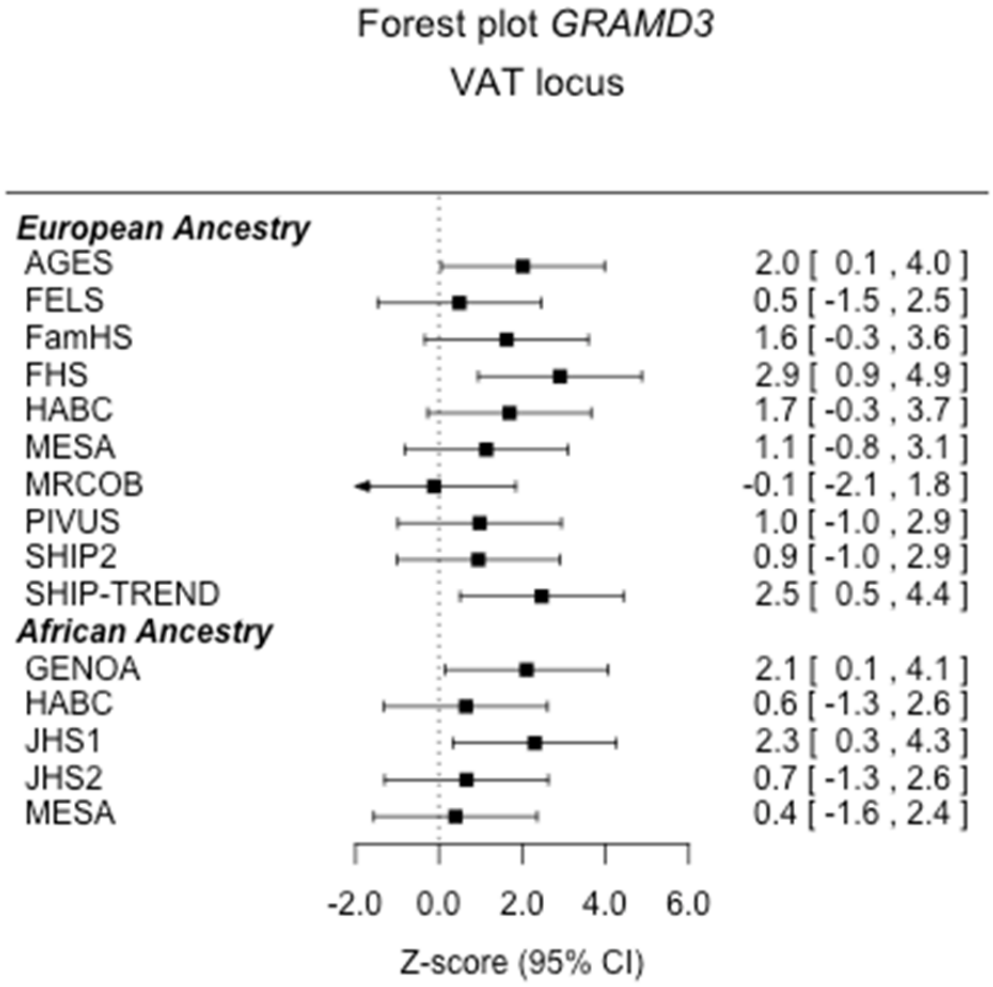

Supplementary Figure 2c. Forest plots of Z-scores for rs1650505 (*EBF1*, pericardial fat locus) among a combined sample of 11,566 women and men ($N_{European\ Ancestry}$=7,412; $N_{African\ Ancestry}$=1,994; $N_{Asian\ Ancestry}$=761; $N_{Hispanic\ Ancestry=}$1,399).

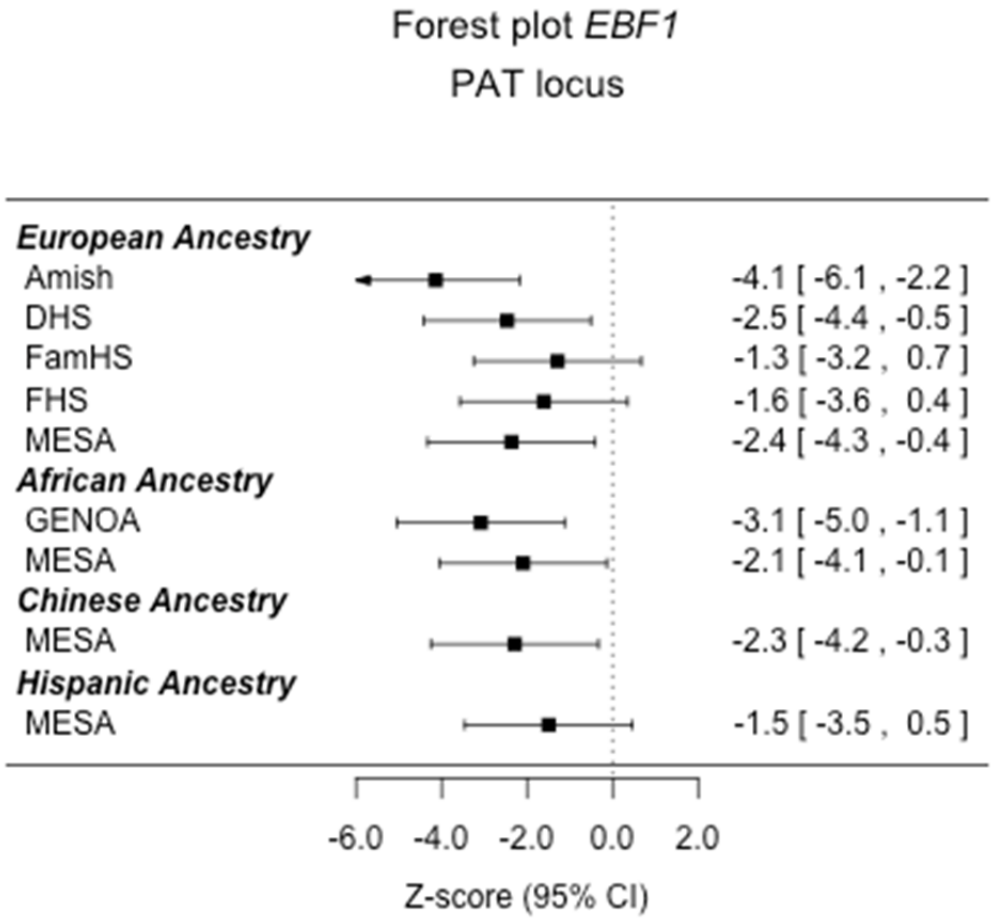

Supplementary Figure 2d. Forest plots of Z-scores for rs2842895 (*RREB1*, visceral fat locus) among a combined sample of 17,297 women and men ($N_{European\ Ancestry}$=14,295; $N_{African\ Ancestry}$=3,002). Associations are calculated among the overall combined sample of women and men among family based studies unless otherwise indicated. * indicates association among women in population-based study, + indicates association among men among population-based study.

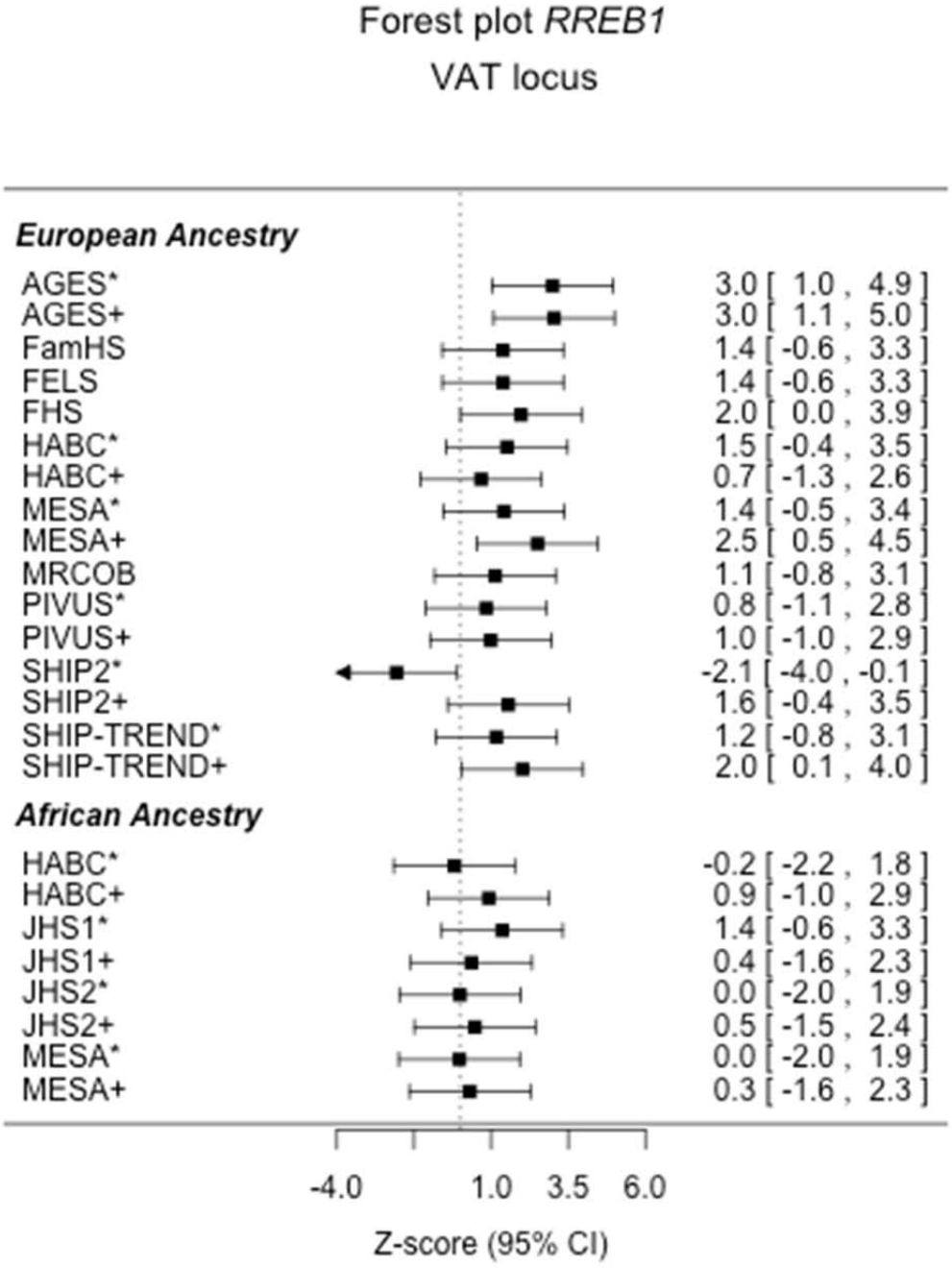

Supplementary Figure 2e. Forest plots of Z-scores for rs2123685 (*GSDMB*, subcutaneous fat locus) among 7,137 women ($N_{European\ Ancestry=}$7,137).

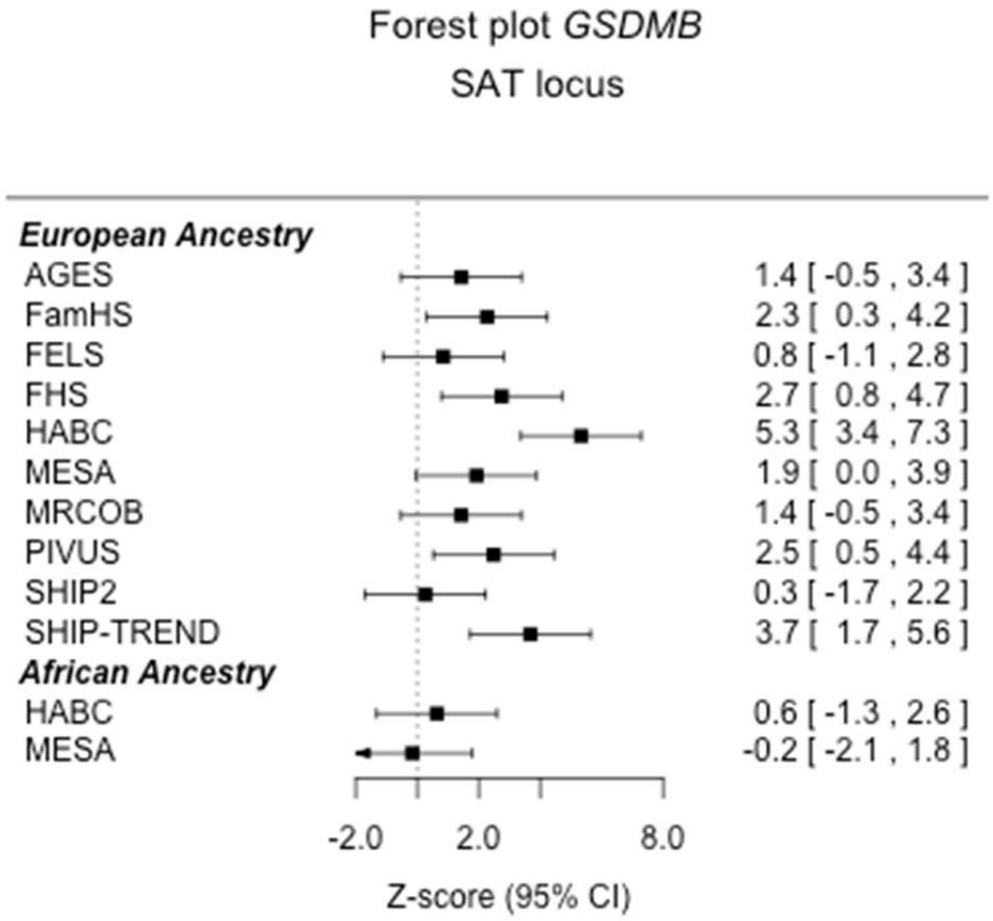

Supplementary Figure 2f. Forest plots of Z-scores for rs2237199 (*ATXN1*, subcutaneous fat attenuation locus) among 5,780 men ($N_{European\ Ancestry}$=5,331; $N_{African\ Ancestry}$=499).

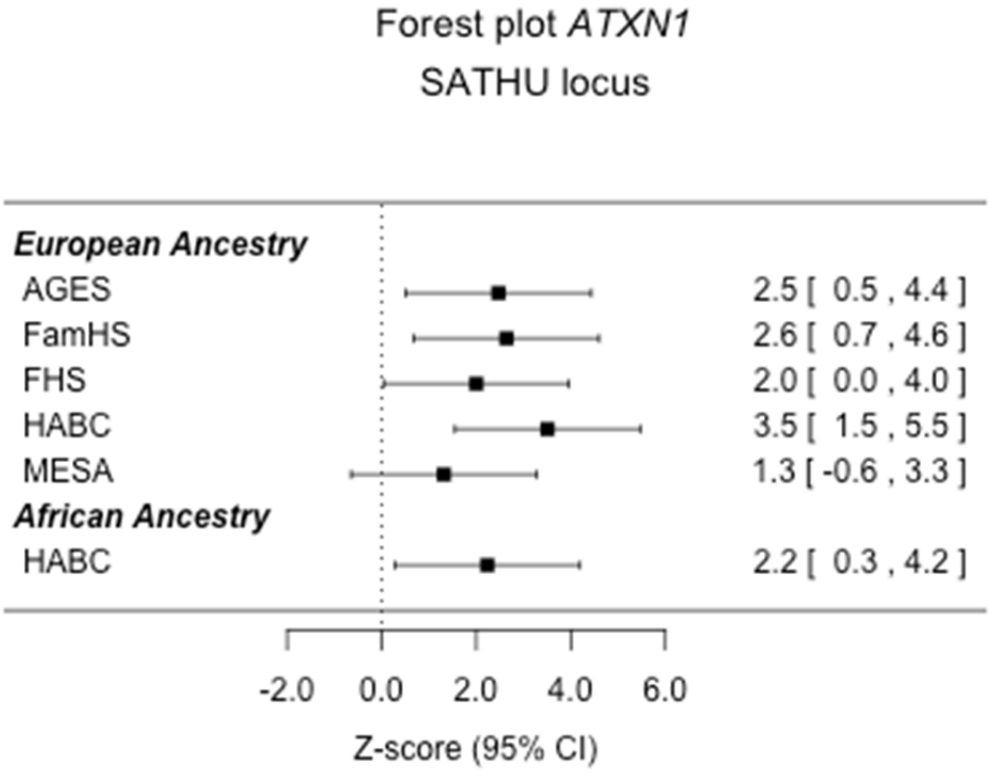

Supplementary Table 2g. Forest plots of Z-scores for rs7374732 (*UBE2E2*, ratio of visceral-to-subcutaneous fat locus) among a combined sample of 18,205 women and men ($N_{European\ Ancestry}$=14,674; $N_{African\ Ancestry}$=3,531). Associations are calculated among the overall combined sample of women and men among family based studies unless otherwise indicated. * indicates association among women in population-based study, + indicates association among men among population-based study.

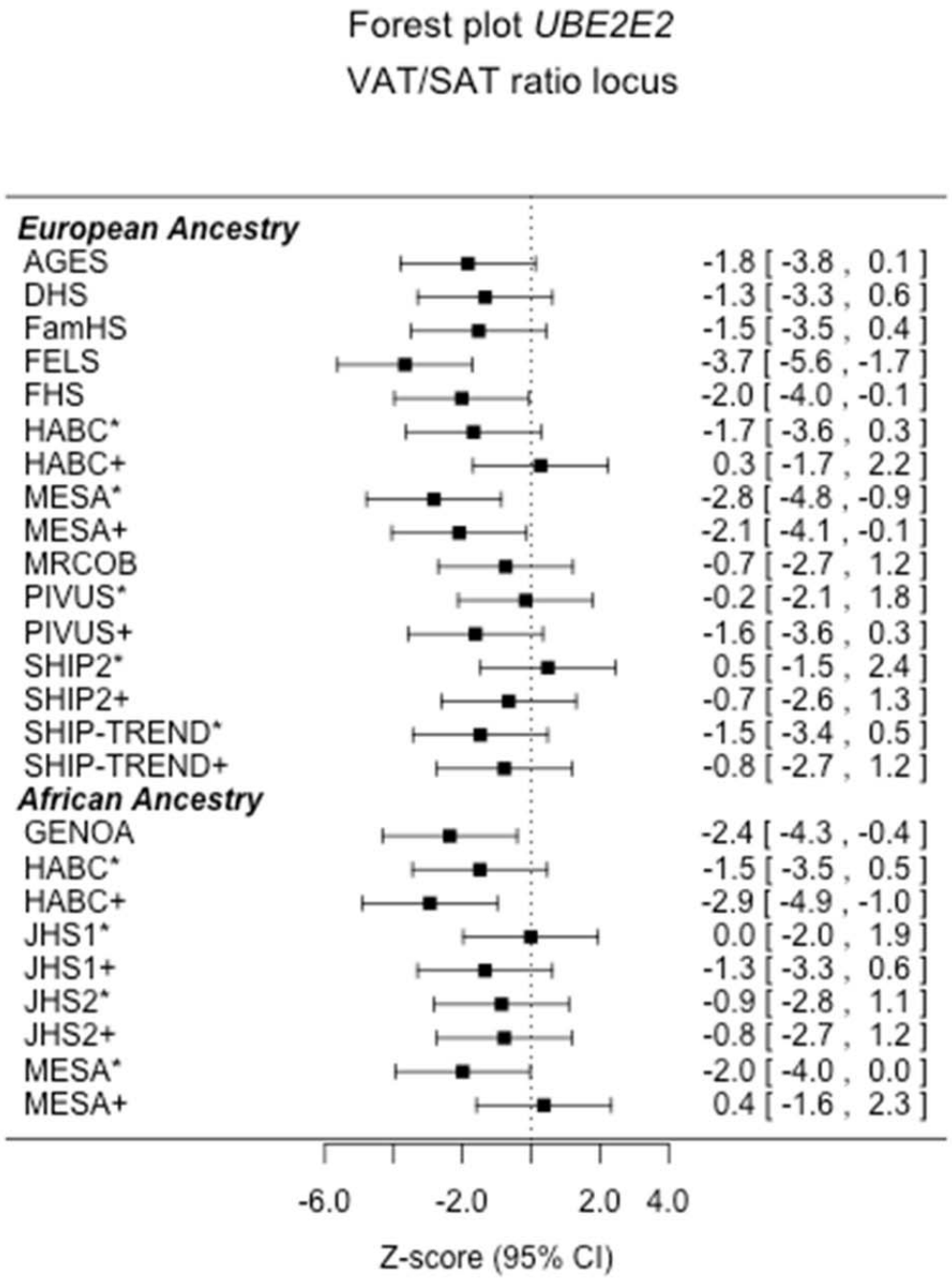

Supplementary Figure 3a. Linkage disequilibrium (LD) plots and genes within 500KB of rs6587515 (index SNP at the *ENSA* locus). LD information obtained from HapMap2 CEU (top) and JPT+CHB (bottom). SNAP[90] was used to create the LD plots and LD information was obtained from HapMap2.

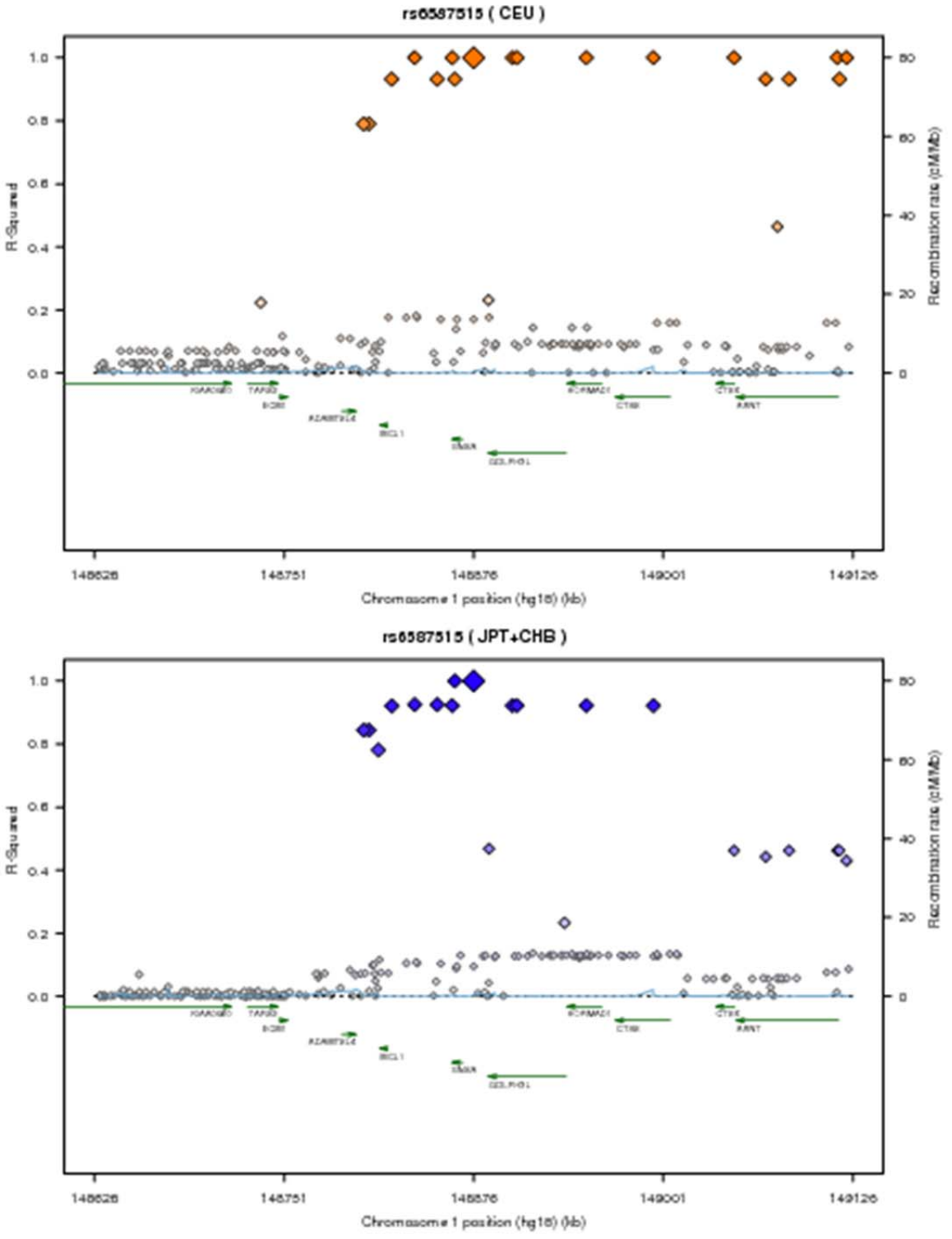

Supplementary Figure 3b. Linkage disequilibrium (LD) plots and genes within 500KB of rs10060123 (index SNP at the *GRAMD3* locus). LD information obtained from HapMap2 CEU (top) and YRI (bottom). SNAP[90] was used to create the LD plots and LD information was obtained from HapMap2.

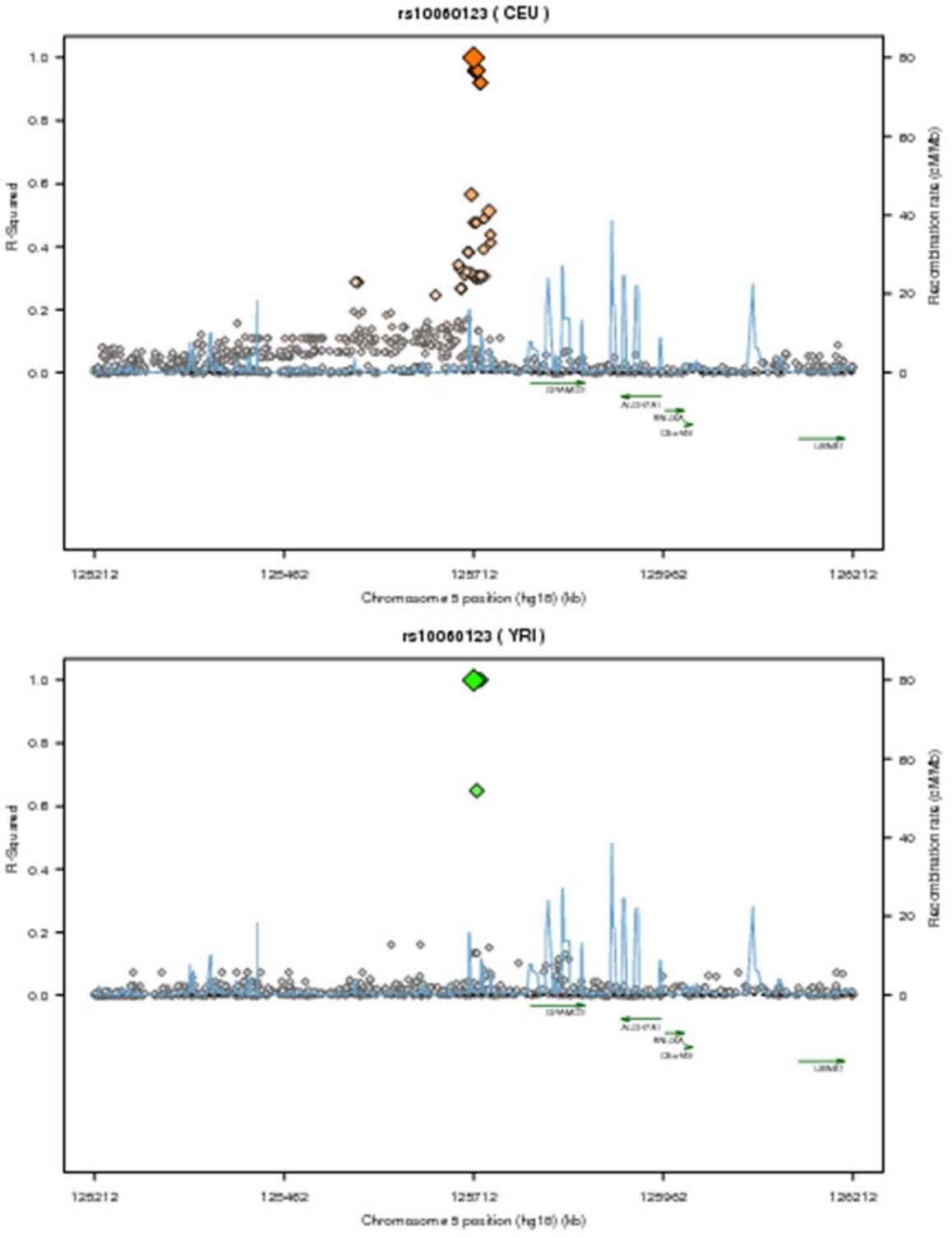

Supplementary Figure 3c. Linkage disequilibrium (LD) plots and genes within 500KB of rs1650505 (index SNP at the *EBF1* locus). LD information obtained from HapMap2 CEU (top), YRI (middle), JPT+CHB (bottom). SNAP[90] was used to create the LD plots and LD information was obtained from HapMap2.

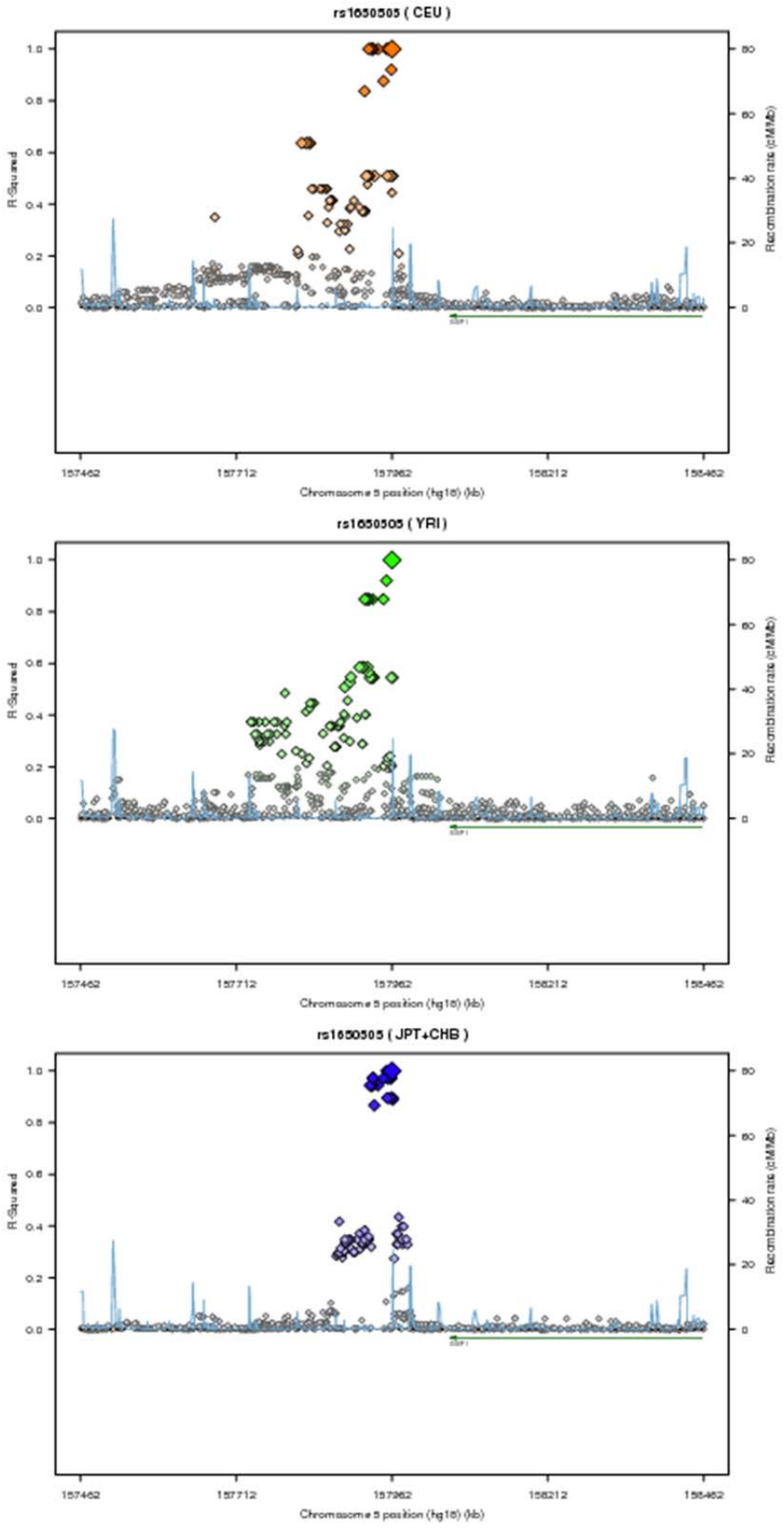
rs1650505 (CEU)
R-Squared
Recombination rate (cM/Mb)
157462
157712
157962
158212
158462
Chromosome 5 position (hg18) (kb)
rs1650505 (YRI)
R-Squared
Recombination rate (cM/Mb)
157462
157712
157962
158212
158462
Chromosome 5 position (hg18) (kb)
rs1650505 (JPT+CHB)
R-Squared
Recombination rate (cM/Mb)
157462
157712
157962
158212
158462
Chromosome 5 position (hg18) (kb)

337
338

Supplementary Figure 3d. Linkage disequilibrium (LD) plots and genes within 500KB of rs2842895 (the index SNP at the *RREB1* locus). LD information obtained from HapMap2 CEU. SNAP[90] was used to create the LD plots and LD information was obtained from HapMap2.

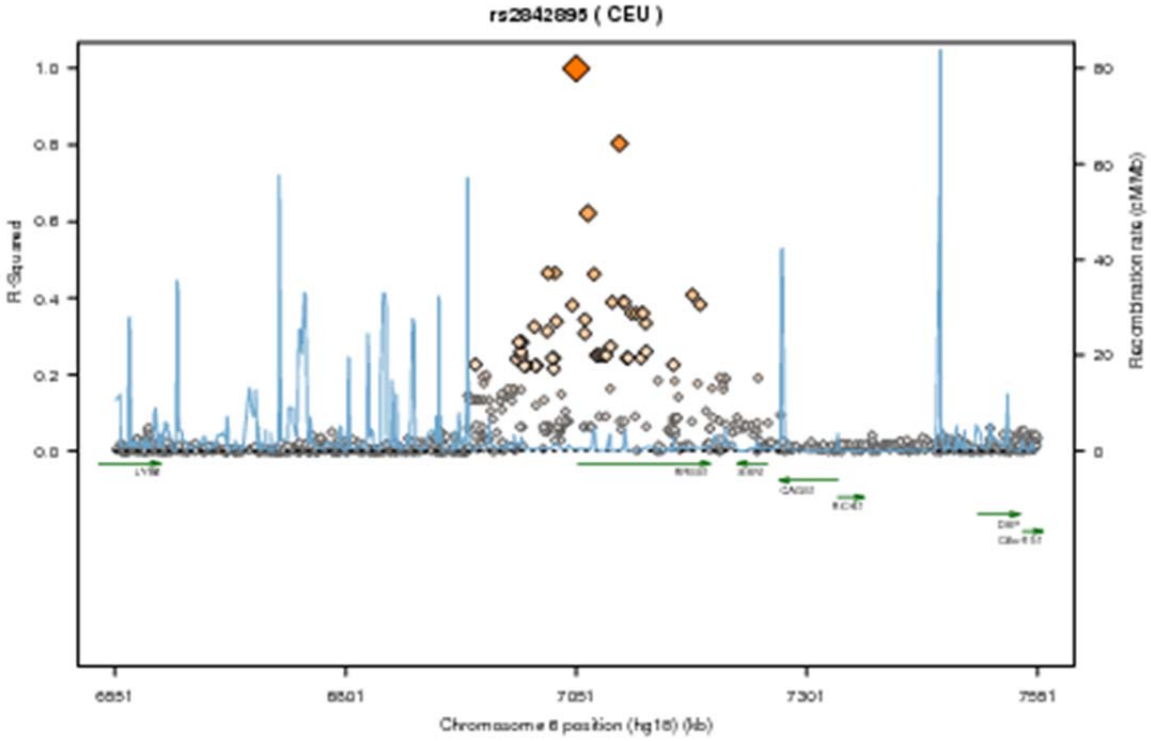

Supplementary Figure 3e. Linkage disequilibrium (LD) plots and genes within 500KB of rs2123685 (index SNP at the *GSDMB* locus). LD information obtained from HapMap2 CEU. SNAP[90] was used to create the LD plots and LD information was obtained from HapMap2.

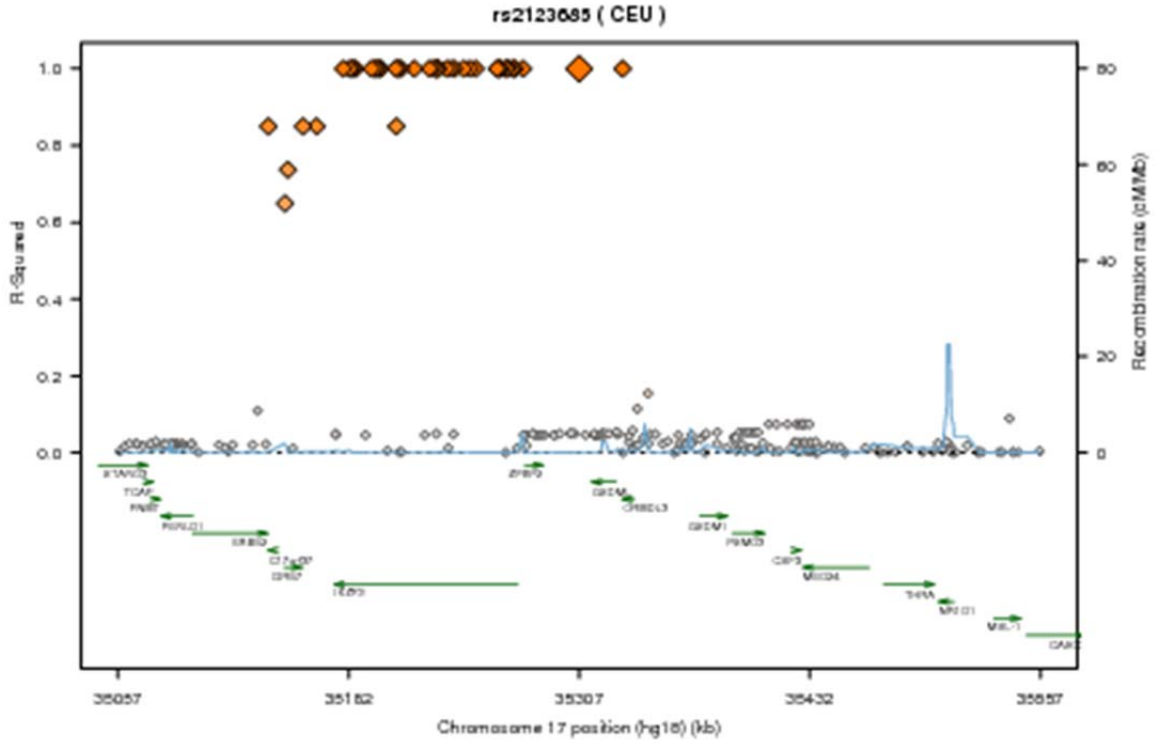

Supplementary Figure 3f. Linkage disequilibrium (LD) plots and genes within 500KB of rs2237199 (the index SNP at the *ATXN1* locus). LD information obtained from HapMap2 CEU (top) and YRI (bottom). SNAP[90] was used to create the LD plots and LD information was obtained from HapMap2.

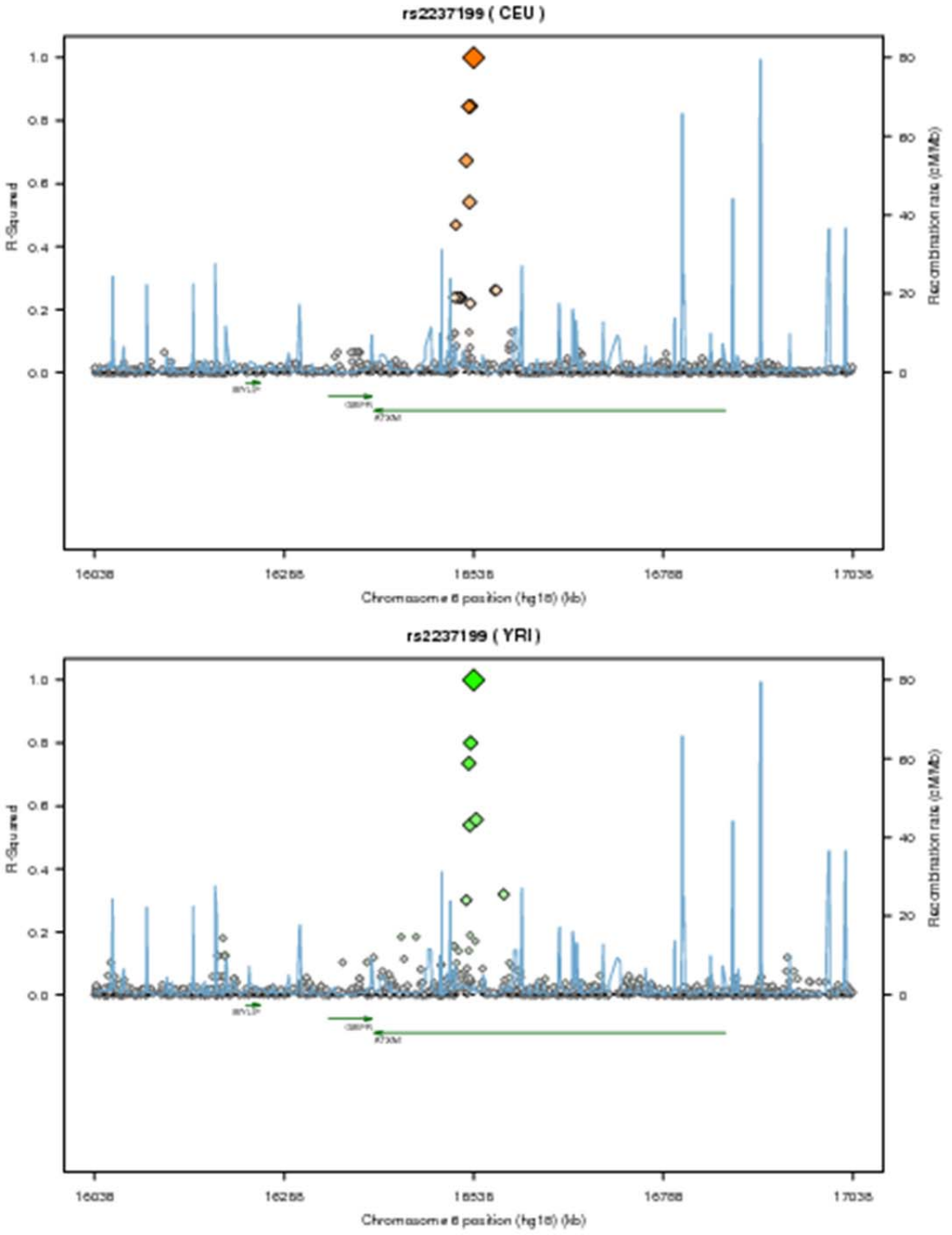

Supplementary Figure 3g. Linkage disequilibrium (LD) plots and genes within 500KB of rs7374732 (the index SNP at the *UBE2E2* locus). LD information obtained from HapMap2 CEU (top) and YRI (bottom). SNAP[90] was used to create the LD plots and LD information was obtained from HapMap2.

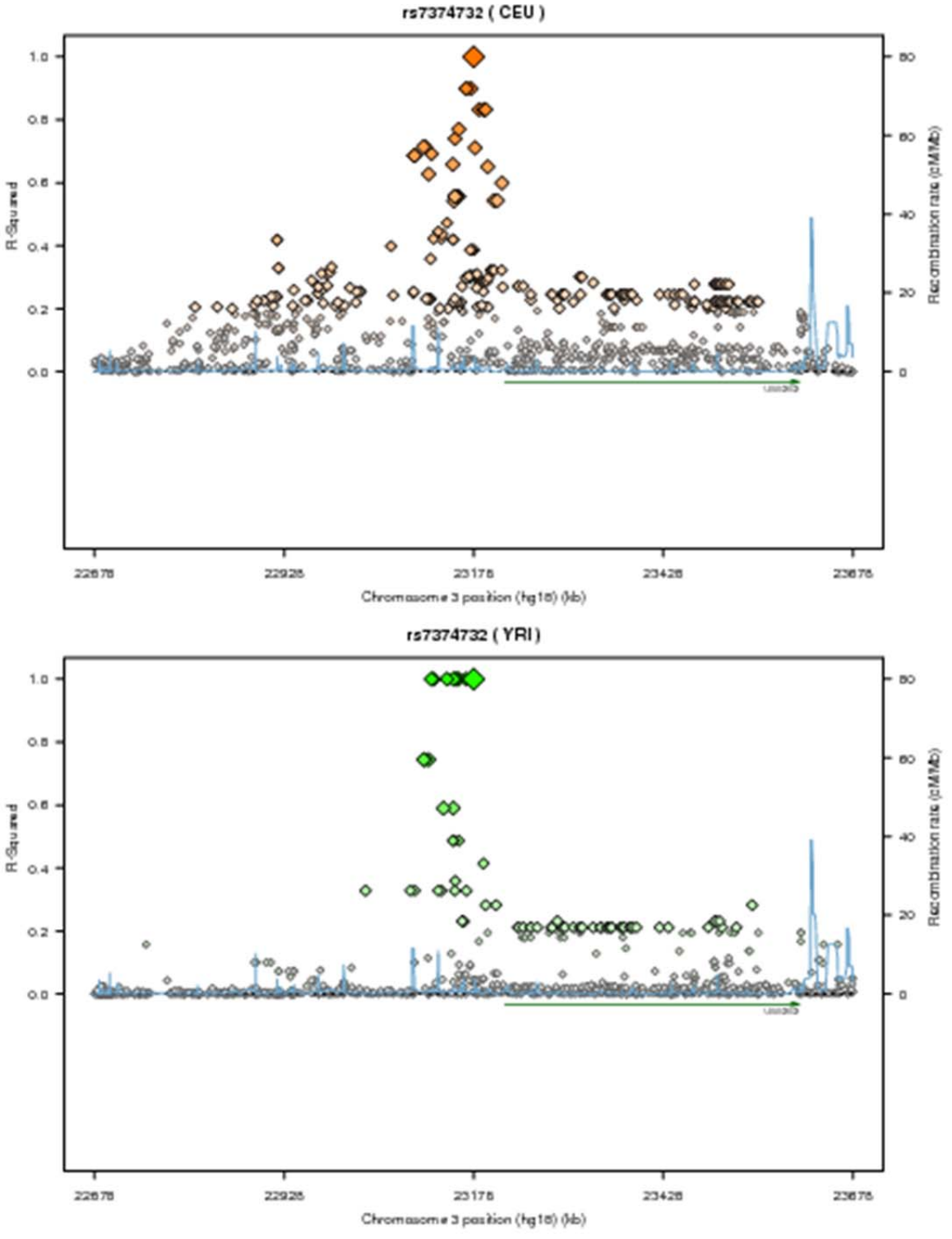

Supplementary Figure 4a. Manhattan plot and QQ plots for subcutaneous adipose tissue volume (SAT) analysis. P-values for association were obtained using a sample-size weighted fixed-effects meta-analysis implemented in METAL. [6,7] Order of analyses in panels is: a) OVERALL, N=18,247, b) WOMEN, N=9,562, c) MEN, N=8,685.

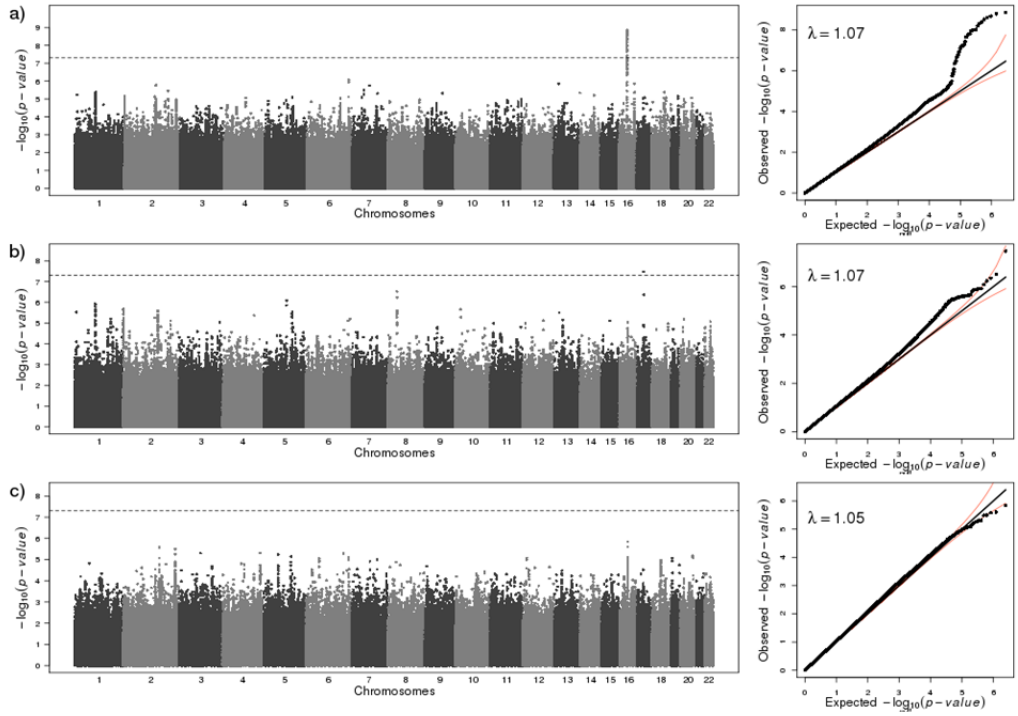

Supplementary Figure 4b. Manhattan plot and QQ plots for visceral adipose tissue volume (VAT). analysis. P-values for association were obtained using a sample-size weighted fixed-effects meta-analysis implemented in METAL.[6,7] Order of analyses in panels is: a) OVERALL, N=18,332, b) WOMEN, N=9,694, c) MEN, N=8,738.

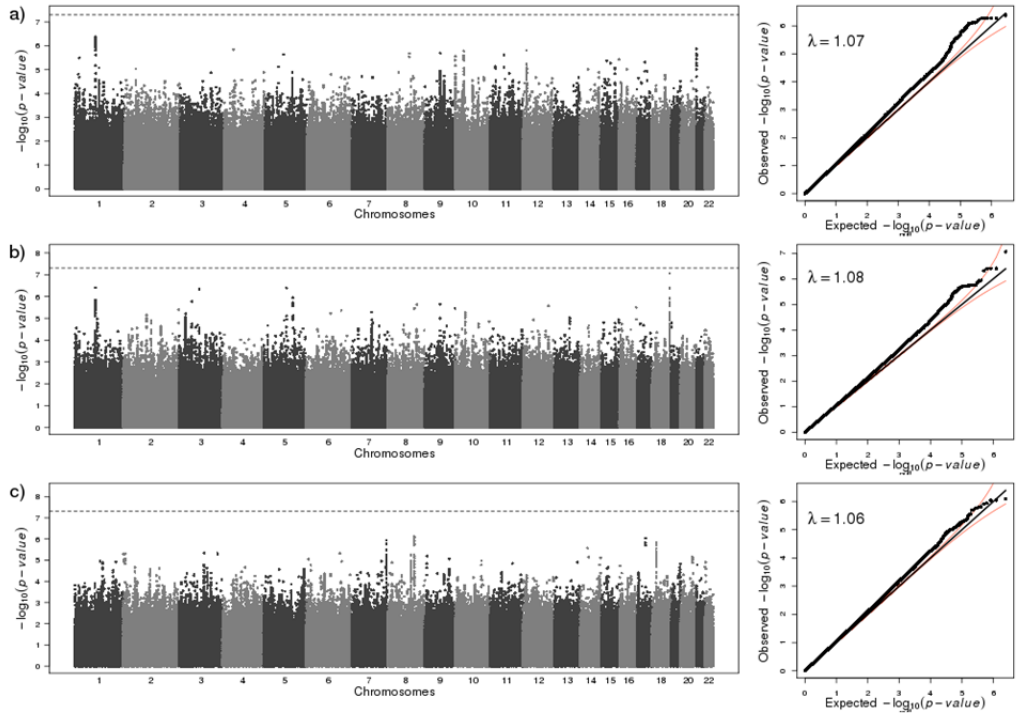

Supplementary Figure 4c. Manhattan plot and QQ plots for visceral adipose tissue volume adjusted for BMI (VATadjBMI) analysis. P-values for association were obtained using a sample-size weighted fixed-effects meta-analysis implemented in METAL.[6,7] Order of analyses in panels is: a) OVERALL, N=18,287, b) WOMEN, N=9,862, c) MEN, N=8,435.

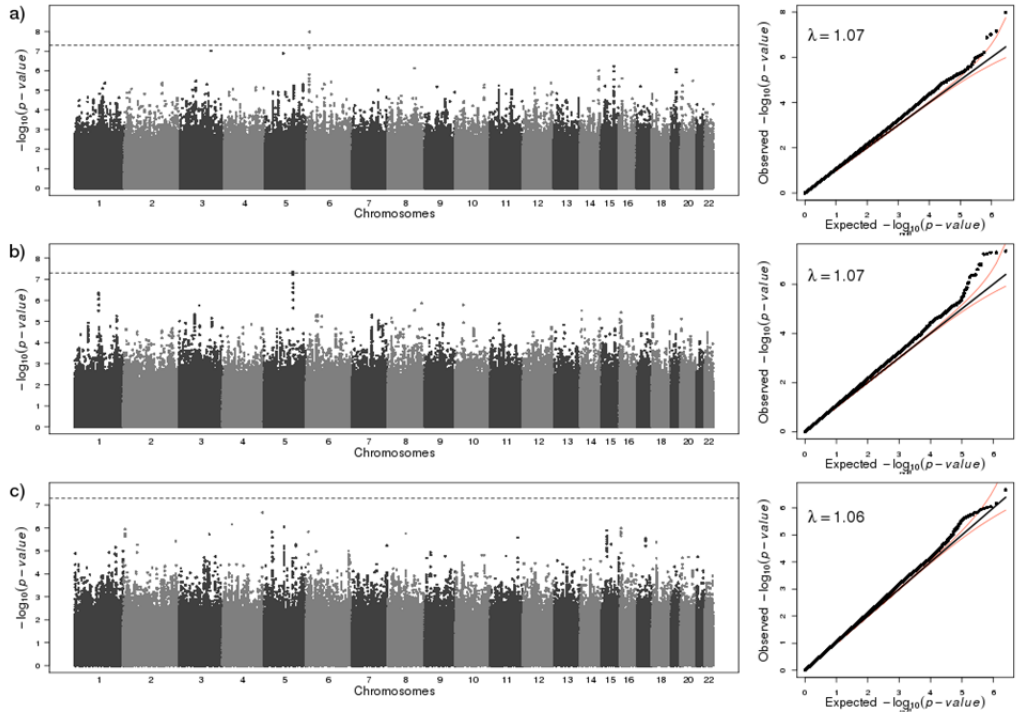

Supplementary Figure 4d. Manhattan plot and QQ plots for pericardial adipose tissue volume (PAT) analysis. P-values for association were obtained using a sample-size weighted fixed-effects meta-analysis implemented in METAL.[6,7] Order of analyses in panels is: a) OVERALL, N=12,204, b) WOMEN, N=6,362, c) MEN, N=5,842.

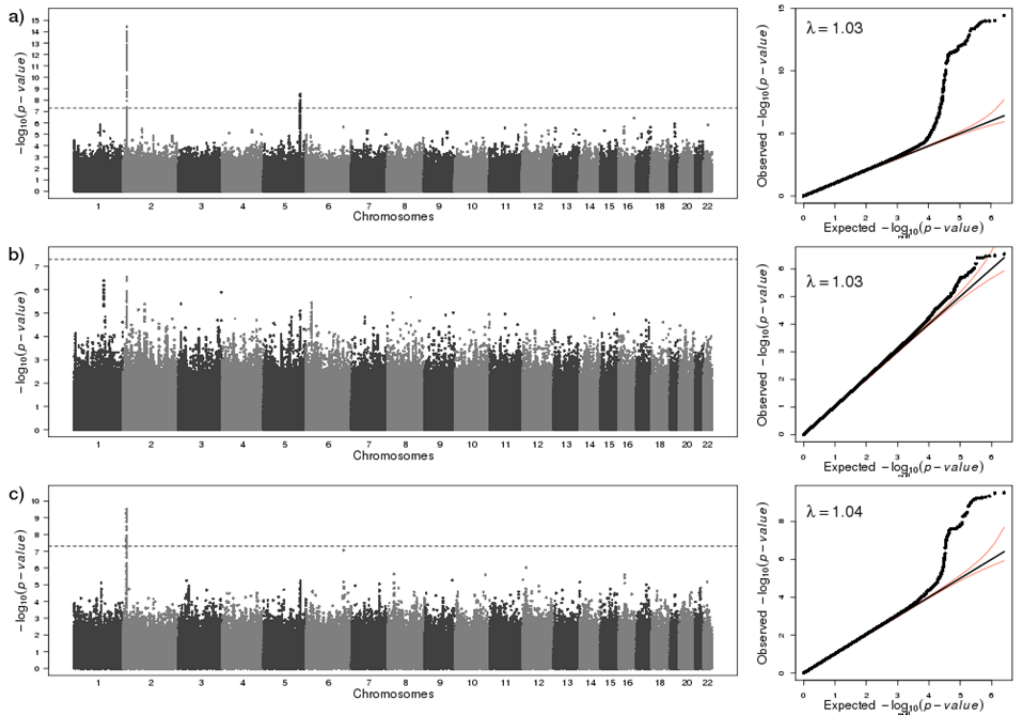

Supplementary Figure 4e. Manhattan plot and QQ plots for pericardial adipose tissue volume adjusted for Height and Weight (PATadjHtWt) analysis. P-values for association were obtained using a sample-size weighted fixed-effects meta-analysis implemented in METAL.[6,7] Order of analyses in panels is: a) OVERALL, N=11,583, b) WOMEN, N=6,110, c) MEN, N=5,473.

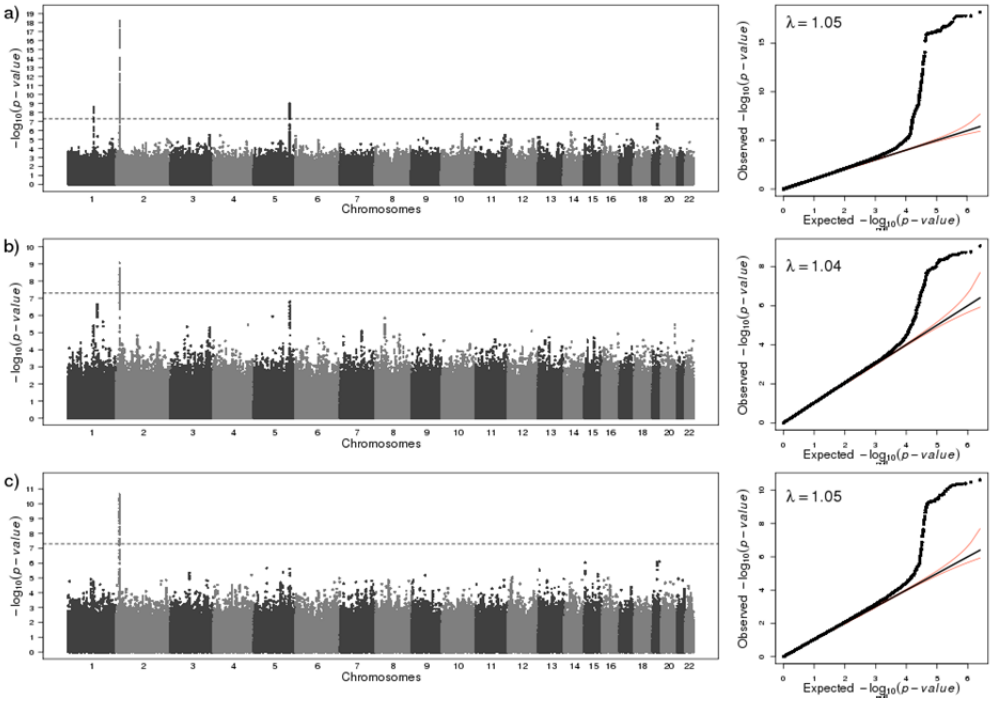

Supplementary Figure 4f. Manhattan plot and QQ plots for subcutaneous adipose tissue attenuation (SATHU) analysis. P-values for association were obtained using a sample-size weighted fixed-effects meta-analysis implemented in METAL.[6,7] Order of analyses in panels is: a) OVERALL, N=12,439, b) WOMEN, N=6,291, c) MEN, N=6,149.

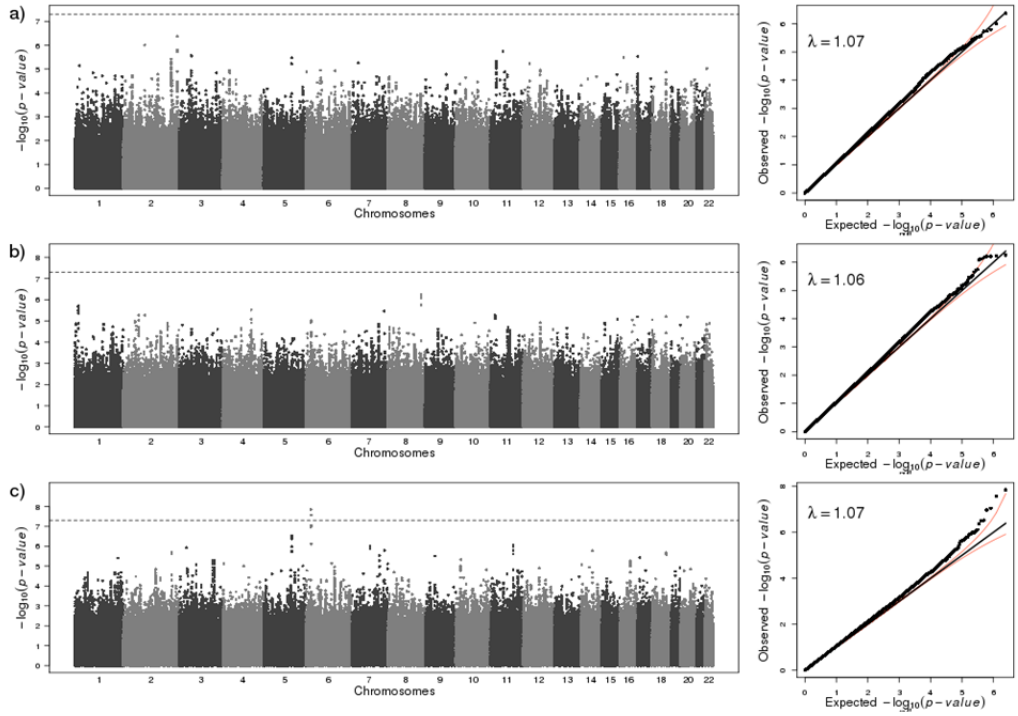

Supplementary Figure 4g. Manhattan plot and QQ plots for visceral adipose tissue attenuation (VATHU) analysis. P-values for association were obtained using a sample-size weighted fixed-effects meta-analysis implemented in METAL.[6,7] Order of analyses in panels is: a) OVERALL, N=12,519, b) WOMEN, N=6,321, c) MEN, N=6,199.

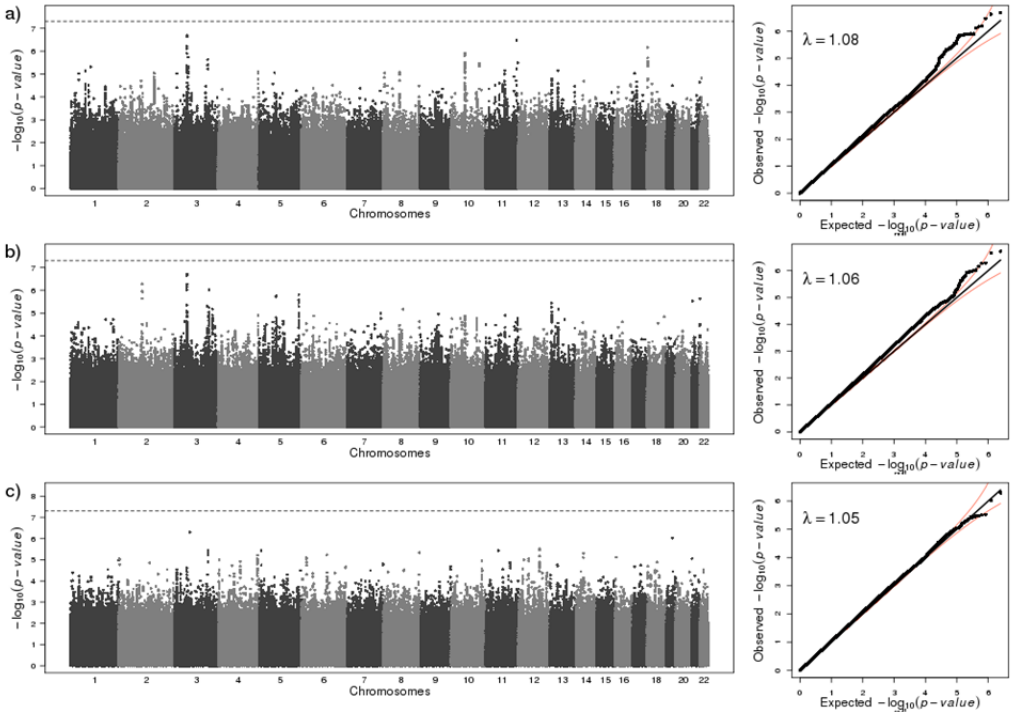

Supplementary Figure 4f. Manhattan plot and QQ plots for ratio of visceral adipose tissue volume to subcutaneous adipose tissue volume (VAT/SAT ratio). P-values for association were obtained using a sample-size weighted fixed-effects meta-analysis implemented in METAL.[6,7] Order of analyses in panels is: a) OVERALL, N=18,191, b) WOMEN, N=9,823, c) MEN, N=8,374.

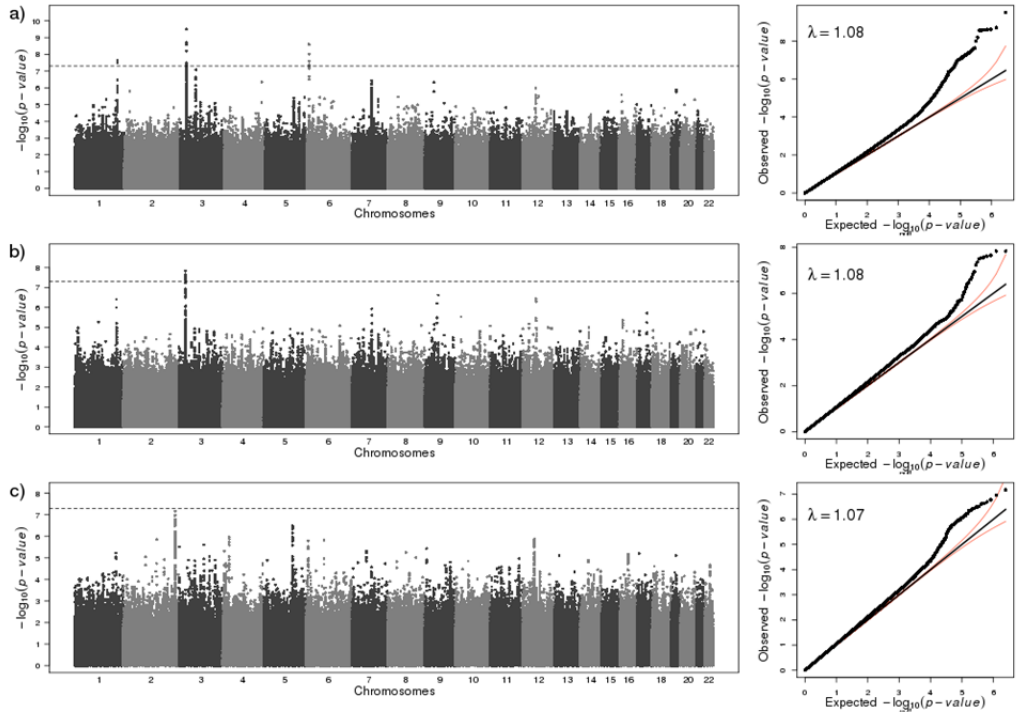

Supplementary Figure 4g Manhattan plot and QQ plots for ratio of visceral adipose tissue volume to subcutaneous adipose tissue volume adjusted for BMI (VAT/SAT ratio adj BMI). P-values for association were obtained using a sample-size weighted fixed-effects meta-analysis implemented in METAL.[6,7] Order of analyses in panels is: a) OVERALL, N=18,190, b) WOMEN, N=9,815, c) MEN, N=8,375.

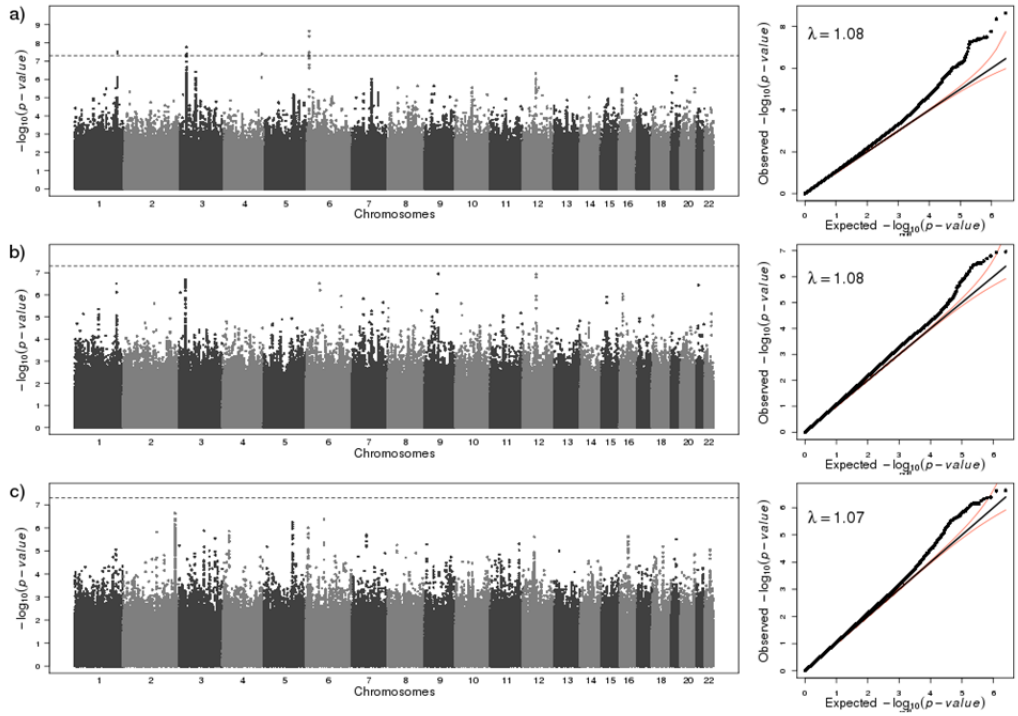

Supplementary Figure 5. Functional characterization of *Ebf1* and *Rreb1*.
Gene expression measured by qPCR in culture adipocyte progenitors isolated from the subcutaneous (SAT) or perigonadal visceral (VAT) depots (n=4). Cells were expanded to confluence and then collected at intervals after induction of adipogenic differentiation. Data was expressed as mean, error bar=s.e.m. Statistical significance was assessed using Kruskal-Wallis test and Dunn's correction for multiple comparisons.

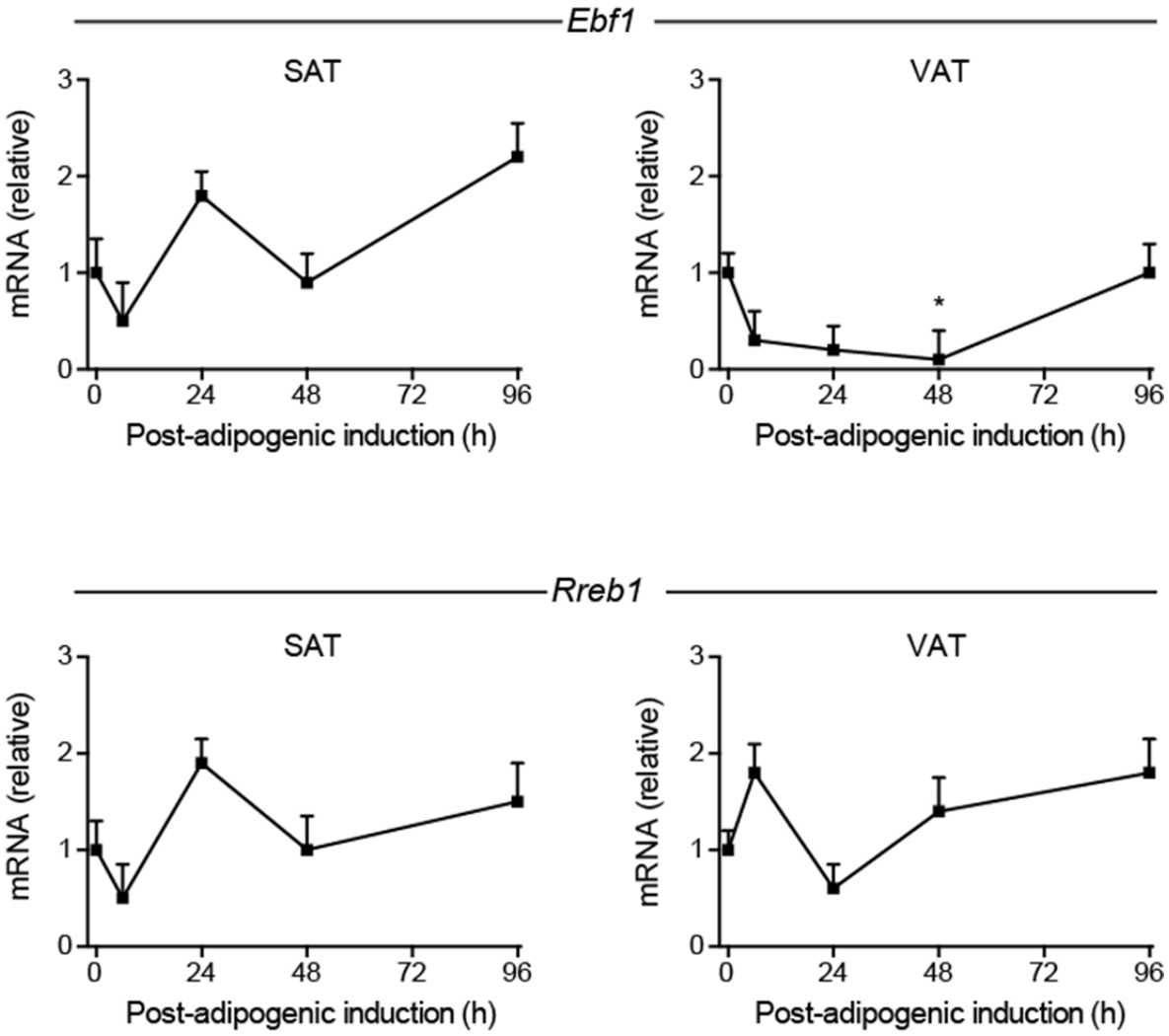

Supplementary Figure 6. Sex-specific expression of *Atxn1* in murine adipose tissue. Because the *ATXN1* association was confined to males, we considered the possibility that *Atxn1* expression in murine adipose tissue would be dependent on sex and measured its expression by qPCR in adipose depots of male and female mice (n=6). In the three analyzed depots, no sex-specific difference was observed. These data do not exclude a gender-specific expression pattern at other developmental time-points or in specific pathophysiologic contexts. Data is displayed as box/whisker plot where center line=median, box spans 25th-75th percentiles, whiskers span max/min values.

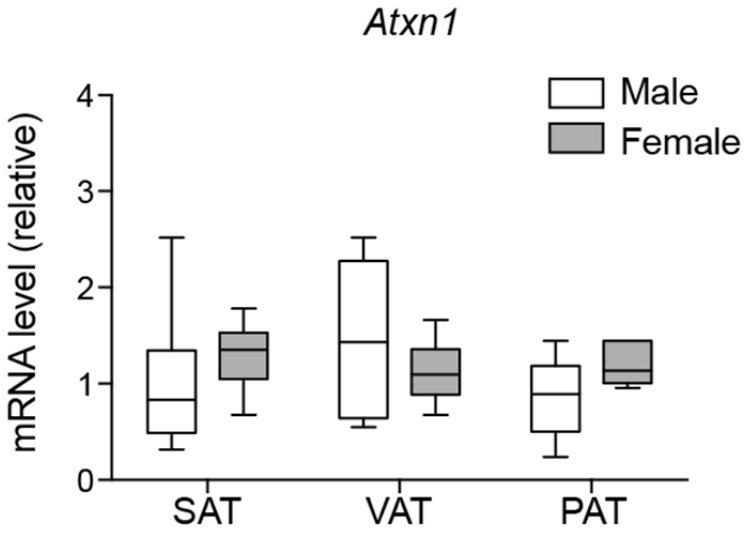

Supplementary Note

Cohort Specific Information and Protocols

AGES - The Age, Gene/Environment Susceptibility Reykjavik Study

AGES-Reykjavik Study. The Reykjavik Study cohort originally comprised a random sample of 30,795 men and women born in 1907-1935 and living in Reykjavik in 1967. A total of 19,381 people attended, resulting in 71% recruitment rate. The study sample was divided into six groups by birth year and birth date within month. One group was designated for longitudinal follow up and was examined in all stages. One group was designated a control group and was not included in examinations until 1991. Other groups were invited to participate in specific stages of the study. Between 2002 and 2006, the AGES-Reykjavik study[96] re-examined 5764 survivors of the original cohort who had participated before in the Reykjavik Study. The AGES-Reykjavik Study GWAS was approved by the National Bioethics Committee (VSN: 00-063) and the Data Protection Authority.

Abdominal adipose tissue measurements:
Computed tomography (CT) imaging of the abdomen at the L4/L5 vertebrae was performed with a 4-row detector system (Sensation; Siemens Medical Systems, Erlangen, Germany) as described previously.[97] Visceral adipose tissue (VAT) and abdominal subcutaneous adipose tissue (SAT) were estimated from a single 10-mm thick trans-axial section. Images were loaded into an AVS5 display environment. Visceral adipose tissue was distinguished from subcutaneous adipose tissue by tracing along the facial plane defining the internal abdominal wall. Adipose areas were calculated by multiplying the number of pixels by the pixel area using specialized software (University of California, San Francisco).

Amish

We included in this study individuals in whom CT scans were obtained to measure the quantity of coronary artery calcification. The scans were obtained using electron beam computed tomography (EBCT) on men aged 30 years and older and women aged 40 years and older recruited for studies of cardiovascular health (the Amish Family Calcification Study, 2002-2005 and the Amish Longevity Study, 2000-2008) from the Lancaster County, Pennsylvania Amish community. The design of these two studies has been previously described[98,99]. Study subjects were relatively healthy. The Amish Family Calcification Study was initiated to identify the determinants of vascular calcification and to evaluate the relationship between calcification of bone and vascular tissue in the Old Order Amish community. Participants were recruited based on their participation in an earlier study of bone mineral density; later the recruitment was open to their first and second-degree relatives. The longevity study was based on Amish who lived past the age of 90 years, their offspring, and the spouses of these offspring. All analyses were approved by the Institutional Review Board of University of Maryland, Baltimore.

Pericardial Fat Assessment
Non-contrast Electron Beam Computed Tomography (EBCT) scan was performed on an Imatron scanner (Imatron Inc. San Francisco, CA) in 3-mm thick contiguous slices with pixel size of 0.7813*0.7813 mm. Participants with complete scan from the root of major heart arteries to the apex of the heart and covered the full length of heart were included in the study.

Pericardial fat volume was defined as fat volume within the fibrous pericardium. We utilized the Medical Image Processing, Analysis, and Visualization (MIPAV) application for our volume measurements. Adipose tissue volumes (cm3) were measured without knowledge of the subject's coronary calcification score. Manual segmentation of the adipose tissue inside and outside of the pericardial sac was done by drawing regions-of-interest (ROIs) on every selected slice. A threshold of -190 to -30 Hounsfield units was applied to identify adipose tissue voxels. Our fat volume measurement has both high inter-observer and intra-observer reproducibility (0.92 and 0.96, respectively)

Imputation

Genotyping was performed using either the Affymetrix GeneChip Human Mapping 500K Array or 6.0 Array set (Affymetrix, Santa Clara, CA, USA) and included a total of 500,568 single nucleotide polymorphisms (SNPs). The Affymetrix GeneChip Genotyping Analysis Software and BRLMM genotype-calling algorithm (Affymetrix) were used to generate SNP data files. Mean sample call rate was 98.3% after filtered by relationship check and call rate (>95%). A total of 373, 825 SNPs that passed quality control (SNP call rate >95%, minor allele frequency (MAF) >0) and Hardy–Weinberg Equilibrium checks (at P>0.0001) were retained for analysis.

As a reference panel for imputation, we used Phase II CEU HapMap individuals for imputation and MACH v1.0.15/16 (http://www.sph.umich.edu/csg/abecasis/MACH/). A total of 338,598 autosomal SNPs were used for imputation after applying the filters: (1) not in HapMap, (2) frequency <0.01, (3) Hardy-Weinberg p<1 x 10¯6, and (4) missingness >0.05.

Statistical analysis

We performed genome-wide association of pericardial fat volume using a mixed model approach that models variation in pericardial fat volume as a function of SNP genotype, with adjustment for age, sex, and a polygenic component to account for the family relatedness among study subjects. We used the Mixed Model Analysis Program (MMAP) software program for analysis.

DHS - Diabetes Heart Study

All analyses were approved by the Institutional Review Board at Wake Forest University, School of Medicine.

The Abdominal CT scan series was performed on multi-dectector CT scanners (CTi, LIghtSpeed QXI, Pro16 and VCT, GE Medical Systems, Waukesha WI) in a helical scan mode, 120 KVP, 160 mAs, 2.5 mm slice collimation and standard reconstruction kernal.

Abdominal adipose tissue measurements

Abdominal fat volumes were measured from a 50 cm DFOV CT scan series with a 2.5 mm slice collimation to cover 60 mm (24 slices each 2.5 mm thick) of abdomen. Measurements were centered on the lumbar disk space centered at L4-L5. Subcutaneous and visceral adipose tissue volumes (SAT and VAT, respectively) were assessed with volume analysis software (Advantage Windows; GE Healthcare, Waukesha, WI). Fat volumes in the different compartments were measured by analysts using a semi-automatic segmentation technique. A tissue attenuation using a threshold of -190 to -30 Hounsfield Units (HU) was used to characterize each voxel as adipose tissue.

FamHS - Family Heart Study

The Family Heart Study (FamHS) is a multicenter, population-based, family study designed to investigate the determinants of cardiovascular disease. The collection of phenotypes and covariates as well as clinical examination have been previously described for the FamHS[100] (https://dsgweb.wustl.edu/fhscc/).

In brief, the FamHS recruited 1,200 families (approximately 6,000 individuals), half randomly sampled, and half selected because of an excess of CHD or risk factor abnormalities as compared with age- and sex-specific population rates. The participants were sampled from four population-based parent studies: the Framingham Heart Study, the Utah Family Tree Study, and two centers for the Atherosclerosis Risk in Communities study (ARIC: Minneapolis, and Forsyth County, NC). Between 2002 and 2003 about two-thirds of the largest families were invited to participate in a follow-up clinical examination that included measurement of the liver and abdomen with cardiac CT using standardized procedures and quality control methods developed in NHLBI's MESA and CARDIA studies[101]. Informed

consent was obtained from all participants and this project was approved by the Institutional Review Boards of all participating institutions. A total of 2,659 European descent subjects with CT measures participated in the GWA current study.

Family Heart Study CT exam:
Research CT exams of the chest for CAC and abdomen for measurement of abdominal body compensation were obtained from 5 field centers with one field center using 2 CT scan sites. The following CT scanner systems were used: GE LightSpeed Plus, Siemens Volume Zoom, GE LightSpeed Ultra, Marconi MX8000 and GE LightSpeed Plus, GE LIghtSpeed QXi. For the abdominal scan the following technique was utilized: helical (aka Spiral) scan, 120KVp, 150 mAs, gantry speed 0.8s, standard kernal, full reconstruction and pitch 3:1 (7.5 mm table travel over 2.5 mm slice). Images were reconstructed into both a 35 and 50 cm display field of view to include a calibration phantom (Image Analysis, Columbia, KY, USA) which was positioned under the abdomen of each subject.

Volumetric adipose tissue imaging
Participants underwent a cardiac MDCT exam with four detectors using a standardized protocol as described previously[101]. For participants weighing 100 kg (220 lbs) or greater, the mAs were increased by 25%. The effective radiation exposure for the average participant of each coronary scan was 1.5 mSv for men and 1.9 mSv for women. Participants received two sequential scans. CT images from all study centers were sent electronically to the central CT reading center located at Wake Forest University Health Sciences, Winston Salem, NC, USA.

Abdominal adipose tissue measurements
CT scans of the abdomen were reconstructed into 5 mm slices with the maximum 50 cm field-of-view to include the whole abdomen for body composition. Total and adipose tissues were measured volumetrically from two 5 mm contiguous slices located at the level of the lumbar disk between the 4th and 5th vertebra. Tissues with attenuation between -190 to -30 Hounsfield units were defined as adipose tissue. The Medical Image Processing, Analysis, and Visualization (MIPAV, [http://mipav.cit.nih.gov/index.php]) application was used by experienced analysts to segment the images based on anatomic boundaries (skin, subcutaneous fat-muscle interface and peritoneum) into the entire abdomen, abdominal wall and intra-abdominal compartments. In each compartment, we quantified total abdominal volume, total abdominal adipose tissue, subcutaneous adipose tissue and visceral adipose tissue contained within the 10 mm slice located at L4-5. Inter-observer variability based on the re-analysis of randomly selected 365 scans from the core study population by an expert observer showed an average correlation coefficient of 0.99. Intra-observer variability based on re-analysis of 45 scans by each of the four observers resulted in an average correlation coefficient of 0.99.

Pericardial Fat Assessment
Pericardial adipose tissue (PAT) volume in heart (cm3) was also performed on the CT images after segmentation of the heart and surrounding adipose tissue from the remainder of the thorax using specific anatomic landmarks. The PAT volume was the sum of all pericardial fat voxels over the 4.5-cm volume (cubic centimeters/ 4.5 cm)

Imputation
As a reference panel for imputation, we used Phase II CEU HapMap individuals; we imputed genotypes to nearly 2.5 million HapMap SNPs; further details are presented in Supplementary Table 3.

Statistical analysis
We performed linear regression modeling for SAT, VAT, VAT/SAT, and PAT.

FELS

The Fels Longitudinal Study began in 1929 and is the oldest continuous study of growth, development, and aging in the world[102] (ISBN 052137449). From its beginning, participants in the Fels Longitudinal Study have not been selected based on health status or any other obesity-, CVD-, or T2DM-related trait. Enrollment in the study began with some 10 newborns per year, increasing since the 1930s to 15 - 20 per year. The methodology and design have been described in Roche (ISBN 052137449). Each participant is followed from enrollment (usually birth) until death or infirmity rendering their continued participation impossible. Participants are not examined when menstruating, pregnant, or having other transient conditions (e.g., ill with infectious disease) that could affect specific data collected. All protocols were approved by the Institutional Review Board of the Boonshoft School of Medicine, Wright State University.

Currently, there are 1259 mostly white, non Hispanic, active participants in the Fels Longitudinal Study (HD012252, SA Czerwinski, PI), with the oldest participants with long-term serial data from birth now in their 80s. Since 2002, MRI assessment of abdominal obesity has been performed on a subset of Fels Longitudinal Study participants, initially as part of other research (DK064391, B Towne, PI). Currently, 635 active adult participants have had SAT and VAT data measured from a single MRI assessment of abdominal adiposity, and of these 578 have been SNP genotyped.

Principal components were calculated using 27, 966 cleaned Illumina SNPs that had minimal linkage disequilibrium ($r < 0.1$) across a 2Mb sliding window, and that had a relatively high minor allele frequency (15.5%) for our entire sample of SNP genotyped participants. From these participants, 452 unrelated participants were identified using the unrelate command in PEDSYS (http://www.txbiomed.org/departments/genetics/genetics-detail?r=42). Principal components analysis was performed on the 27,966 genotype scores of the 452 unrelated participants using prcomp in R (http://www.r-project.org). PC scores for all genotyped participants were calculated from the loadings using predict in R.

Volumetric adipose tissue imaging

Using a previously described protocols[103,104], MR Images were obtained using a research-dedicated Siemens Magnetom Avanto 1.5 Tesla whole body scanner, at Kettering Medical Center, Dayton, OH. Contiguous axial images were acquired across the entire abdominal region (T9 – S1). Slice thickness was 1 cm, and images were obtained every 1 cm. Depending on the height of the participant, the number of images ranged from 21 to 40 slices.

Abdominal adipose tissue measurements

SliceOmatic software (Tomovision Inc., Montreal, Canada) image analyses was performed to segment tissues and quantify VAT and SAT. First, trained technicians performed gray scale standardization to determine the best brightness settings to differentiate between different gray-level regions on each image. The gray level threshold for various tissues (i.e. VAT, and SAT) was then set and used to identify each tissue type. Each image was then reviewed and where necessary, segmentation was corrected. The area (cm2) of VAT and SAT in each image was then computed by summing the VAT and SAT tissue pixels and multiplying by the individual pixel surface area. The VAT and SAT tissue areas were then summed across all images to obtain volumes for VAT and SAT.

Imputation

As a reference panel for imputation, we used Phase II CEU HapMap individuals; we imputed genotypes to nearly 2.5 million HapMap SNPs; further details are presented in Supplementary Table 1. We used MACH v1.0 (http://www.sph.umich.edu/csg/abecasis/MACH/), and accounted for participant relatedness. We expressed imputed genotypes as allelic dosage (which is a fractional value ranging from 0-2).

Statistical analysis
We performed linear mixed effects regression modeling to account for pedigree structure using SOLAR.[1]

FHS - Framingham Heart Study

In 1948, the Framingham Heart Study began when the Original Cohort was enrolled.[105] Beginning in 1971, the Offspring Cohort was enrolled (5,124 participants); the methodology and design has been described. In 2002, the Third Generation cohort was enrolled (n=4095).[106] Participants for this study were drawn from the Framingham Heart Study Multi-detector Computed Tomography (MDCT) Study, a population-based sub-study of the community-based Framingham Heart Study Offspring and Third Generation cohorts. Participants for the current study were drawn from the MDCT sub-study. All protocols and analyses were approved by the Institutional Review Board at Boston University School of Public Health and National Heart, Lung and Blood Institute. Between June 2002 to April 2005, 3529 participants (2111 Third Generation, 1418 Offspring participants) underwent MDCT assessment of coronary and aortic calcium. Inclusion in this study was weighted towards participants from larger Framingham Heart Study families and those who resided in the Greater New England area. Men had to be at least 35 years of age, women had to be at least 40 years of age and non-pregnant, and all participants had to weigh less than 350 pounds. Of the total of 3529 subjects imaged, 3394 had interpretable CT measures, 3329 of whom had both SAT and VAT measured, and 3158 participated in the present GWAS study.

We observed association with the first principle components estimated using EIGENSTRAT;[107] this was accounted for in our analyses.

Volumetric adipose tissue imaging

Subjects underwent eight-slice MDCT imaging of the chest and abdomen in a supine position as previously described (LightSpeed Ultra, General Electric, Milwaukee, WI).[108] Briefly, twenty-five contiguous five mm thick slices (120 kVp, 400 mA, gantry rotation time 500 ms, table feed 3:1) were acquired covering 125 mm above the level of S1.

Abdominal adipose tissue measurements

Subcutaneous and visceral adipose tissue volumes (SAT and VAT) were assessed (Aquarius 3D Workstation, TeraRecon Inc., San Mateo, CA). In order to identify pixels containing fat, an image display window width of -195 to -45 Hounsfield Units (HU) and a window center of -120 HU were used. The abdominal muscular wall separating the visceral from the subcutaneous compartment was manually traced. Average HU per fat depot was recorded. Inter-reader reproducibility was assessed by two independent readers measuring VAT and SAT on a subset of 100 randomly selected participants.[108] Inter-class correlations for inter-reader comparisons were 0.992 for VAT and 0.997 for SAT. Similar high correlations were noted for intra-reader comparisons.

Pericardial Fat Assessment

Framingham Heart Study participants underwent MDCT utilizing 8-slice MDCT in a supine position (LightSpeed Ultra, General Electric, Milwaukee, WI). On average, 48 contiguous 2.5 mm slices of the heart were acquired with prospectively ECG triggered CT scanning protocol (120 kVp, 400 mA, temporal resolution 330 ms). We measured pericardial fat tissue volumes (cm3) with a dedicated offline workstation (Aquarius 3D Workstation, TeraRecon Inc., San Mateo, CA) based on the principle that absolute Hounsfield Units (HU) values correspond to tissue property. Thus, we set a predefined image display (window width -195 to -45 HU; window center -120 HU) to identify pixels that correspond with adipose tissue. Pericardial fat was measured across the complete available imaging volume in cm3. We used a semi-automatic segmentation technique which required the reader to manually trace the pericardium. We defined pericardial fat volume as adipose tissue located within the pericardial sac. Using a random sample of 100 participants, intra-reader (ICC 0.97) and inter-reader (ICC 0.95)

reproducibility was excellent.[109]

Imputation

As a reference panel for imputation, we used Phase II CEU HapMap individuals; we imputed genotypes to nearly 2.5 million HapMap SNPs; further details are presented in Supplementary Table 1. We used MACH v1.0.15/16 (http://www.sph.umich.edu/csg/abecasis/MACH/), and accounted for participant relatedness. We expressed imputed genotypes as allelic dosage (which is a fractional value ranging from 0-2).

Statistical analysis

We performed linear mixed effects regression modeling to account for pedigree structure (R kinship package).

GENOA - Genetic Epidemiology Network of Arteriopathy

GENOA is one of four networks in the NHLBI Family-Blood Pressure Program (FBPP).[110,111] GENOA's long-term objective is to elucidate the genetics of target organ complications of hypertension, including both atherosclerotic and arteriolosclerotic complications involving the heart, brain, kidneys, and peripheral arteries. The longitudinal GENOA Study recruited European-American and African-American sibships with at least 2 individuals with clinically diagnosed essential hypertension before age 60 years. All other members of the sibship were invited to participate regardless of their hypertension status. Participants were diagnosed with hypertension if they had either 1) a previous clinical diagnosis of hypertension by a physician with current anti-hypertensive treatment, or 2) an average systolic blood pressure ≥ 140 mm Hg or diastolic blood pressure ≥ 90 mm Hg based on the second and third readings at the time of their clinic visit. Exclusion criteria were secondary hypertension, alcoholism or drug abuse, pregnancy, insulin-dependent diabetes mellitus, or active malignancy. During the first exam (1995-2000), 1,583 European Americans from Rochester, MN and 1,854 African Americans from Jackson, MS were examined.

Between 2009 and 2011, 657 self-identified African American GENOA participants at the Jackson, Mississippi Field Center received computed tomography (CT) scans for coronary artery calcification, abdominal adipose tissue, and pericardial adipose tissue. Participants weighing more than 160 kg were excluded from the CT scan. The final sample included 552 GENOA participants with CT measures and GWAS data. Jackson Heart Study participants who also participated in GENOA were not included in the analyses as part of the Jackson Heart Study but were included as part of the GENOA Cohort. Study protocols were approved by the University of Mississippi and University of Michigan Institutional Review Boards and participants gave written informed consent.

Volumetric adipose tissue imaging

CT scans of the lower abdomen and heart were obtained with a GE LightSpeed Pro 16 multidetector scanner (GE Healthcare, Milwaukee, WI). The scans were reconstructed using display field-of-view (DFOV) of 35 cm and 50 cm and a Calcium QCT phantom was included in the images. For participants who weighed more than 100 kg, the tube current (i.e., mA) was adjusted upwards (25%). This adjustment was designed to maintain a more consistent image quality over the spectrum of body sizes. The estimated average whole-body effective dose for the entire protocol was 4 mSv. CT images were transmitted to the reading center at Wake Forest University.

Briefly, abdominal fat volumes were measured from a 50 cm DFOV CT scan series with a 2.5 mm slice collimation to cover 60 mm (24 slices each 2.5 mm thick) of abdomen from L3 to S1. Scanning was centered on the lumbar disk space centered at L4-L5.[112] Pericardial adipose tissue was measured from a 35 cm DFOV CT scan series of the heart with a 2.5 mm slice collimation starting 15 mm above and ending 30 mm below the superior extent of the left main coronary artery for coverage of 45 mm (18 slices each 2.5 mm thick) along the head-foot (z-axis) of the participant.[112]

Abdominal adipose tissue measurements

Subcutaneous and visceral adipose tissue volumes (SAT and VAT, respectively) were assessed with volume analysis software (Advantage Windows; GE Healthcare, Waukesha, WI). The abdominal muscular wall separating the visceral from the subcutaneous compartment was manually traced. Fat volumes in the different compartments were measured by a semiautomatic segmentation technique. A tissue attenuation using a threshold of -190 to -30 Hounsfield Units (HU) was used to characterize each voxel as fat.[113] Using this protocol, inter-class correlations for inter-reader comparisons were previously shown to be 0.95 for VAT and SAT.[113]

Pericardial Fat Assessment

Pericardial fat volume (PAT) was assessed with volume analysis software (Advantage Windows; GE Healthcare, Waukesha, WI). PAT was measured after segmentation of the heart and surrounding adipose tissue from the remainder of the thorax using specific landmarks. PAT was measured as a combination of pericardial and epicardial fat because it is difficult to distinguish the two fat measures on CT images. A tissue attenuation using a threshold of -190 to -30 Hounsfield Units (HU) was used to characterize each voxel as fat.[112] The PAT volume was the sum of all pericardial fat voxels over the 45 mm volume. Using this protocol, inter-class correlations for inter-reader comparisons were previously shown to be 0.96 for PAT.[112]

Imputation

A total of 1,263 African American GENOA participants were genotyped on the Affymetrix Genome-Wide Human SNP Array 6.0 at the Mayo Clinic in Rochester, Minnesota and an additional 269 were genotyped using the Illumina Human 1M-Duo BeadChip. Since the sibships for the GENOA study were identified using hypertensive participants from the ARIC Study as probands, we also obtained genotypes for 92 additional GENOA participants who were also in the ARIC Study and who could not be genotyped on either platform using the GENOA blood sample. Genotyping for the ARIC study was carried out at the Broad Institute on the Affymetrix 6.0 platform. For all genotyping platforms used, samples and SNPs with a call rate <95% were removed. Samples demonstrating sex mismatch, duplicate samples, and samples with low identity-by-state with all other samples were also removed. Imputation was performed with the single-step approach implemented in Markov Chain Haplotyper (MaCH) 1.0.16.[114] The reference panel was composed of the HapMap phased haplotypes (release 22) from 60 unrelated CEU and 60 unrelated YRI samples. Imputation was performed separately for participants genotyped on the Affymetrix 6.0 as part of the GENOA study, participants genotyped on the Illumina Human 1M-Duo BeadChip, and participants genotyped on the Affymetrix 6.0 as part of the ARIC Study. Since only a small number of directly genotyped SNPs overlap on the Affymetrix and Illumina platforms, imputed dosages were used for all.

Statistical analysis

We performed analyses with MMAP (Mixed Models Analysis for Pedigrees and Populations).[115] We adjusted for population stratification with the first four principal components estimated using EIGENSTRAT.[107]

HABC - Health Aging and Body Composition study

The Health ABC study is a prospective cohort study investigating the associations between body composition, weight-related health conditions, and incident functional limitation in older adults. Health ABC enrolled well-functioning, community-dwelling black (n=1281) and white (n=1794) men and women aged 70–79 years between April 1997 and June 1998. Participants were recruited from a random sample of white and all black Medicare eligible residents in the Pittsburgh, PA, and Memphis, TN, metropolitan areas. Participants have undergone annual exams and semi-annual phone interviews. The current study sample consists of 1559 white participants who attended the second exam in 1998–1999 with available genotyping and SAT/VAT data. All protocols and analyses were approved by the

Institutional Review Board at the University of Pittsburgh, University of Tennessee and the National Institutes on Aging.

Regional fat depots were assessed from CT scans obtained in Pittsburgh on a General Electric 9800 Advantage (General Electric, Milwaukee, WI) and in Memphis on a Siemens Somatron Plus 4 (Siemens, Erlangen, Germany) or Picker PQ2000S (Marconi Medical Systems, Cleveland, OH). A single axial scan (140 kVp, 300 to 360 mAs, 10-mm thickness) was taken at the disk space between the fourth and fifth lumbar vertebrae. Images were transferred to the Reading Center at the University of Colorado Health Sciences Center on optical disc or magnetic tape. Analyses were performed on a SPARC station II (Sun Microsystems, Mountain View, CA) using IDL development software (RSI Systems, Boulder, CO). An outline was traced surrounding the abdominal cavity. The adipose tissue density range was determined with a bimodal image distribution histogram for each participant. Visceral fat was defined as the area of all adipose tissue within the abdominal cavity with exclusion of the muscle region, calculated by multiplying the number of pixels within this range by a single pixel area. Abdominal subcutaneous fat was defined as the difference in the area between the entire adipose tissue in the scan and visceral fat. To assess the reproducibility of these measurements, 5% of the data was re-read in a blinded fashion. The intra-class correlation coefficients of reliability ranged from 0.93 to 1.000.

Genotyping and imputation.
Genomic DNA was extracted from buffy coat collected using PUREGENE DNA Purification Kit during the baseline exam. Genotyping was performed by the Center for Inherited Disease Research (CIDR) using the Illumina Human1M-Duo BeadChip system. Samples were excluded from the dataset for the reasons of sample failure, genotypic sex mismatch, and first-degree relative of an included individual based on genotype data. Genotyping was successful for 1,151,215 SNPs in 2,802 unrelated individuals (1663 Caucasians and 1139 African Americans). Imputation was done for the autosomes using the MACH software version 1.0.16. SNPs with minor allele frequency ≥1%, call rate ≥97% and HWE p≥10-6 were used for imputation. HapMap II phased haplotypes were used as reference panels. For EAs, genotypes were available on 914,263 high quality SNPs for imputation based on the HapMap CEPH reference panel (release 22, build 36). A total of 2,543,887 in EAs are available for analysis.

Statistical analysis.
We performed linear regression modeling for SAT, VAT, and the VAT/SAT ratio. We observed association with the first principal components estimated using EIGENSTRAT;[107] this was accounted for in our analyses.

JHS - Jackson Heart Study
The Jackson Heart Study is a single-site, prospective cohort study of the risk factors and causes of cardiovascular disease in adult African Americans. A probability sample of 5,301 African Americans, 21 to 84 years of age, residing in the three counties surrounding Jackson, MS, were recruited and examined at baseline (2000–2004) by trained and certified technicians according to standardized protocols. For all participants, the clinic visit included physical examination, anthropometry, survey of medical history and of cardiovascular risk factors, and collection of blood and urine for biological variables. Clinic visits and interviews occurred approximately every three years. Annual follow-up interviews and cohort surveillance are ongoing. All protocols and analyses were approved by the Institutional Review Board at Jackson Heart Study: Jackson State University, University of Mississippi Medical Center, and Tougaloo College

JHS Computed Tomography Protocol
CT-imaging slices of the chest and lower abdomen (L3-S1) were obtained by 16 slice multi-detector CT (GE Healthcare Lightspeed 16 Pro, Waukeshau, Wisconsin) during Exam 2 at the Jackson Medical Mall. Imaging consisted of a scout, prospective ECG gated series through the chest/heart and a helical

scan through the lower abdomen from L3-S1. The participants were scanned while lying on a rectangular 3 sample calcium calibration QCT Phantom (Image Analysis, Columbia, KY) long enough to extend from the top of the chest to the sacrum. The long axis of the QCT phantom paralleled the participant's spine. The phantom is made from tissue equivalent plastic and contains rods of hydroxyapatite of known radiographic densities: 0 for water, and 75 and 150 hydroxyapatite. Use of the QCT Phantom permits quantitative assessment of scans between patients (an internal standard). KV was 120 and gantry speed was 0.40 s. For participants weighing ≥220 lbs (100 Kg), the tube current (or mA) was increased by 25% from 400 mA to 500 mA. Participants received a one-time exposure of less than 6 mSv. Scans were analyzed centrally at the Wake Forest University School of Health Sciences (PI J. Jeffrey Carr). Calcified plaque in the coronary arteries and abdominal aorta were viewed and scored using a TeraRecon Aquarius Workstation (TeraRecon, Inc., San Mateo, CA).

Volumetric adipose tissue imaging

Briefly, abdominal fat volumes were measured from a 50 cm DFOV CT scan series with a 2.5 mm slice collimation to cover 60 mm (24 slices each 2.5 mm thick) of abdomen from L3 to S1. Scanning was centered on the lumbar disk space centered at L4-L5.[112] Pericardial adipose tissue was measured from a 35 cm DFOV CT scan series of the heart with a 2.5 mm slice collimation starting 15 mm above and ending 30 mm below the superior extent of the left main coronary artery for coverage of 45 mm (18 slices each 2.5 mm thick) along the head-foot (z-axis) of the participant.[112]

Abdominal adipose tissue measurements

Subcutaneous and visceral adipose tissue volumes (SAT and VAT, respectively) were assessed with volume analysis software (Advantage Windows; GE Healthcare, Waukesha, WI). The abdominal muscular wall separating the visceral from the subcutaneous compartment was manually traced. Fat volumes in the different compartments were measured by a semiautomatic segmentation technique. A tissue attenuation using a threshold of -190 to -30 Hounsfield Units (HU) was used to characterize each voxel as fat.[113] Using this protocol, inter-class correlations for inter-reader comparisons were previously shown to be 0.95 for VAT and SAT.[113]

MESA - Multi-Ethnic Study of Atherosclerosis

The Multi-Ethnic Study of Atherosclerosis (MESA) is a study of the characteristics of subclinical cardiovascular disease and the risk factors that predict progression to clinically overt cardiovascular disease or progression of the subclinical disease. MESA consisted of a diverse, population-based sample of an initial 6,814 asymptomatic men and women aged 45-84. 38 percent of the recruited participants were white, 28 percent African American, 22 percent Hispanic, and 12 percent Asian, predominantly of Chinese descent. Participants were recruited from six field centers across the United States: Wake Forest University, Columbia University, Johns Hopkins University, University of Minnesota, Northwestern University and University of California - Los Angeles.[116] All protocols and analyses were approved by the Institutional Review Boards of each participating university. Each participant received an extensive physical exam and determination of coronary calcification, ventricular mass and function, flow-mediated endothelial vasodilation, carotid intimal-medial wall thickness and presence of echogenic lucencies in the carotid artery, lower extremity vascular insufficiency, arterial wave forms, electrocardiographic (ECG) measures, standard coronary risk factors, sociodemographic factors, lifestyle factors, and psychosocial factors. Selected repetition of subclinical disease measures and risk factors at follow-up visits allowed study of the progression of disease. Participants are being followed for identification and characterization of cardiovascular disease events, including acute myocardial infarction and other forms of coronary heart disease (CHD), stroke, and congestive heart failure; for cardiovascular disease interventions; and for mortality. The first examination took place over two years, from July 2000 - July 2002. It was followed by four examination periods that were 17-20 months in length. Participants have been contacted every 9 to 12 months throughout the study to assess clinical morbidity and mortality.

For the Abdominal Body Composition, Inflammation, and Cardiovascular disease ancillary study, a subset of the baseline MESA cohort had abdominal CT scans performed at exams 2 or 3. Of these, a small number were rescanned at exam 4. As part of the MESA Body Composition ancillary study, selected abdominal slices from these scans were processed using MIPAV 4.1.2 software (provided by the NIH) that produced areas of fat, lean, and total tissue measured in square centimeters, as well as densities expressed in Hounsfield units (HU), for each specific tissue type and anatomic structure. The structures were defined as total abdomen area of interest (AOI), subcutaneous AOI and visceral AOI, plus 4 sets of muscles consisting of the right and left psoas, right and left rectus abdominis, right and left paraspinal muscle group, and right and left oblique muscle group. For this ancillary study, fat tissue was identified as being between -190 and -30 Hounsfield units (HU). Lean tissue was identified as being between 0 and 100 HU. Densities outside of these 2 ranges were labeled as undefined tissue type.

Measurement of pericardial fat volume by computed tomography (CT)
Consenting participants underwent CT scanning of the chest at Exam 1 (2000-2002) in MESA. Pericardial fat was measured in 18 2.5-mm slices, from 1.5 cm above to 3.0 cm below the superior extent of the left main coronary artery, using Volume Analysis software (GE Healthcare, Waukesha, WI). The anterior border of the volume was defined by the chest wall and the posterior border by the aorta and the bronchus. This volume includes the pericardial fat located around the proximal coronary arteries. Tissue with attenuation of -190 to -30 Hounsfield units was defined as fat. The pericardial fat volume was the sum of all voxels containing fat. The intrareader reproducibility was excellent in both studies (intraclass correlation coefficients, 0.99 in MESA). This measure of pericardial fat volume was highly correlated with total volume of pericardial fat as measured in the Diabetes Heart Study (correlation coefficient 0.93). All suitable CT scans in MESA were read for pericardial fat.

Imputation
IMPUTE version 2.1.0 was used to perform imputation for the MESA SHARe Caucasian participants (chromosomes 1-22) using HapMap Phase I and II - CEU as the reference panel (release #24 - NCBI Build 36 (dbSNP b126)). We imputed genotypes to nearly 2.5 million HapMap SNPs; further details are presented in Supplementary Table 1 Statistical analysis We performed linear regression modeling to account for covariates including age, gender, study sites, smoking status and PCs (SNPTEST).

MRCOB/TOPS - Metabolic Risk Complications of Obesity Genes/Take Off Pounds Sensibly, Inc
In 1993, the MRC-OB Family Study began with the initial recruitment based on the TOPS (Take Off Pounds Sensibly, Inc) membership (620 families of 3,007 Caucasian individuals). The design of recruitment and phenotype ascertainment has been described previously.[117] Beginning in year 1998, 506 individuals of 39 families were selected for phenotyping for a set of refined MetS traits that reflect not only clinical outcomes but also the biologic precursors including measurement of total body fat by DXA, measurement of abdominal subcutaneous and visceral fat masses (focus of this study) and acute insulin response by Minimal Model Analysis.[118]

Measurement of Body Fat Distribution by Computerized Tomography (CT)
Abdominal imaging to quantitate abdominal fat compartments[119-121] was performed using a General Electric (Waukesha, WI) 1.5-T whole-body MRI system using a GE Highspeed Advantage CT Scanner (GE Medical Systems, Waukesha WI). Scans were performed using a scan circle diameter of 48cm. Contiguous axial slices of 3 mm were obtained from the superior to inferior surfaces of the 3rd (L3) lumbar vertebra. The plane of the slices was parallel to the superior and inferior surfaces of the vertebra. Images were generated at 120 kV, one-second scanning and 150-240 mA. Images were displayed on a 512 x 512 matrix with CT numbers ranging from -1000 to +1000 (0 representing water). In addition, a trabecular bone constancy phantom consisting of three sections with known densities, was placed on the subject's abdomen during the abdominal scans.

Image Analysis. Phenotypes obtained from CT scans include total abdominal visceral fat volume (cmt), total abdominal subcutaneous fat volume (cmt) and total abdominal fat volume (cmt). The subcutaneous and intra-abdominal adipose tissue areas were differentiated by encircling the abdominal muscular wall. The number of volume elements in the scan containing fat was determined by thresholding techniques.[121,122] Computer software delineates tissue areas, from which quantitative estimates of the amounts of adipose tissue, muscle, or bone can be estimated.

SNP Genotyping and Data Cleaning

Genomic DNA was extracted and prepared from whole blood using commercial kits (Puregene, Minneapolis, MN). Genome-wide SNP genotyping was performed using Affymetrix Genome-Wide Human SNP 6.0 arrays and SNP calls were generated by Genotype Console 3.2. Individuals with fewer than 95% of all available markers called were excluded. 869,222 autosomal SNPs were prepared by Preswalk and checked for Mendelian consistency with SimWalk2. A SNP was eliminated if: 1) fewer than 95% of the cohort were typed successfully; 2) the SNP was monoallelic; 3) the SNP had more than two alleles; 4) fewer than five copies of the SNP existed in the current study cohort. Hardy-Weinberg equilibrium (HWE) was tested for each SNP using SOLAR;[1] SNPs with excessive deviation from HWE ($p < 10\text{-}8$) were excluded. Individuals who had missing data for individual SNPs had missing data imputed with MERLIN.[123]

Statistical analysis

Imputation

Annotations for the genotyped SNPs (strand and basepair location) were obtained from the official annotation files provided by Affymetrix (GenomeWideSNP_6.na30.annot.csv.zip) and used to revert dosages (see above) back to genotypes (A/B encoded alleles) and to identify SNPs to be flipped to the + strand. Then all genotyped individuals were coded as unrelateds and pre-phased into haplotypes using SHAPEIT.[124] Pre-phased haplotypes were then imputed using IMPUTE2,[125] a CEU panel, and windows of 5Mbp across each autosome. Autosomes were re-assembled after the imputation and the pedigree structure was restored. Using pedigree information, Mendelian inconsistencies in the imputed alleles were blanked and re-imputed with MERLIN. We expressed imputed genotypes as allelic dosage (weighted probabilities of number of copies of minor allele as a fractional value on range [0,2]).

Association tests

Analyses were performed using SOLAR.[1] Minor allele dosages were included as covariates in variance-components mixed models for measured genotype analyses;[126] all models incorporated the random effect of kinship and fixed effects such as age, age2, and smoking. Individual scores from a principal components analysis of representative SNPs were also included to correct for possible population stratification.[107] For each SNP covariate, maximum likelihood estimates of regression beta +/- standard error and percent of trait variance explained were obtained, and p-values were obtained from likelihood ratio tests against the null hypothesis of no association.

PIVUS - Prospective Investigation of the Vasculature in Uppsala Seniors

PIVUS is a community-based cohort of individuals living in Uppsala, Sweden with a primary aim of investigating vascular function in the elderly. All protocols and analyses were approved by the Ethics Committee of the University of Uppsala, and all participants provided informed consent. For cohort specific study protcols, please refer to: Lind L, Fors N, Hall J, Marttala K, Stenborg A. A comparison of three different methods to evaluate endothelium-dependent vasodilation in the elderly. The Prospective Investigation of the Vasculature in Uppsala Seniors (PIVUS) Study. Arterioscler Thromb Vasc Biol. 2005; 25:2368-75.[127,128]

SHIP-2 and SHIPTREND - Study of Health in Pomerania

The Study of Health in Pomerania (SHIP) is a population-based project in West Pomerania, the north-east area of Germany.[129,130] A sample from the population aged 20 to 79 years was drawn from

population registries. First, the three cities of the region (with 17,076 to 65,977 inhabitants) and the 12 towns (with 1,516 to 3,044 inhabitants) were selected. Then 17 out of 97 smaller towns (with less than 1,500 inhabitants) were drawn at random. From each of the selected communities, subjects were drawn at random, proportional to the population size of each community stratified by age and gender. Only individuals with German citizenship and main residency in the study area were included. Finally, 7,008 subjects were sampled, with 292 persons of each gender in each of the twelve five-year age strata. In order to minimize drop-outs by migration or death, subjects were selected in two waves. The net sample (without migrated or deceased persons) comprised 6,267 eligible subjects. Selected persons received a maximum of three written invitations. In case of non-response, letters were followed by a phone call or by home visits if contact by phone was not possible. The SHIP population finally comprised 4,308 participants (corresponding to a final response of 68.8%).

The SHIP-TREND is a longitudinal population based cohort study assessing the prevalence and incidence of common, population relevant diseases and their risk factors. Baseline examinations started in 2008 and were finished in 2012.[121] The sample was drawn randomly from population registries. The study region is essentially the same as the study region of the initial SHIP cohort.[129,130] The medical ethics committee of the University of Greifswald approved the study protocol. Oral and written informed consents were obtained from each of the study participants.

The SHIP samples were genotyped using the Affymetrix Genome-Wide Human SNP Array 6.0. Hybridisation of genomic DNA was done in accordance with the manufacturer's standard recommendations. The genetic data analysis workflow was created using the Software InforSense. Genetic data were stored in a Caché database (InterSystems). Genotypes were determined using the Birdseed2 clustering algorithm. For quality control purposes, several control samples were added. On the chip level, only subjects with a genotyping rate on QC probesets (QC callrate) of at least 86% were included. Finally, all arrays had a sample callrate > 92%. The overall genotyping efficiency of the GWA was 98.55 %. Imputation of genotypes in SHIP was performed with the software IMPUTE v0.5.0 based on HapMap II.

A subset of the SHIP-TREND samples was genotyped using the Illumina Human Omni 2.5 array. Hybridisation of genomic DNA was done in accordance with the manufacturer's standard recommendations at the Helmholtz Zentrum München. The genetic data analysis workflow was created using the Software InforSense. Genetic data were stored in a Caché database (InterSystems). Genotypes were determined using the GenomeStudio Genotyping Module v1.0 (GenCall algorithm). All 986 arrays included had a genotyping rate of at least 94%. The overall genotyping efficiency of the GWA was 99.67 %. Imputation of genotypes in SHIP was performed with the software IMPUTEv2 based on HapMap II (CEU v22, Build 36).

Acknowledgements and Funding Sources

AGES. The Age, Gene/Environment Susceptibility Reykjavik Study is funded by NIH contract N01-AG-12100, the NIA Intramural Research Program, Hjartavernd (the Icelandic Heart Association), and the Althingi (the Icelandic Parliament), in addition an Intramural Research Program Award (ZIAEY000401) from the National Eye Institute, an award from the National Institute on Deafness and Other Communication Disorders (NIDCD) Division of Scientific Programs (IAA Y2-DC_1004-02). The study is approved by the Icelandic National Bioethics Committee, VSN: 00-063. The researchers are indebted to the participants for their willingness to participate in the study.

Amish. The Amish sub-study was supported by NIH research grants R01 HL69313, R01 088119, R01 AR046838, U01 HL72515, and U01 HL084756, and with additional support from the University of Maryland General Clinical Research Center, Grant M01 RR 16500; the Mid-Atlantic Nutrition Obesity Research Center, Grant P30 DK072488; the General Clinical Research Centers Program, National Center for Research Resources (NCRR), NIH; and the Baltimore Veterans Administration Geriatric Research and Education Clinical Center (GRECC).

DHS. Grant support included General Clinical Research Center of Wake Forest School of Medicine M01 RR07122; NIH RO1 DK071891 (BIF); AR48797 (Carr, JJ); and HL67348 (DWB).

FamHS. This research was conducted using data and resources from the NHLBI Family Heart Study and Washington University School of Medicine. This work was partially supported by the NIDDK R01DK089256, NHLBI R01HL117078 and NHLBI U01HL67897 to Carr , JJ.

FELS. The study sample consisted of participants in the Fels Longitudinal Study, using data and resources funded by the National Institute of Child Health and Human Development (NICHD HD012252, HD053685), the National Institute of Diabetes and Digestive and Kidney Diseases (NIDDK DK064391), the National Institute of Arthritis and Musculoskeletal and Skin Diseases (NIAMS AR052147), and the Bill & Melinda Gates Foundation (OPP1135978). Most of the analyses utilized the AT&T Genomics Computing Center at the Texas Biomedical Research Institute (TBRI), and software developed by scientists at TBRI, which was partly funded by National Institutes of Health.

FHS. This research was conducted in part using data and resources from the Framingham Heart Study of the National Heart, Lung, and Blood Institute of the National Institutes of Health and Boston University School of Medicine. This work was partially supported by the National Heart, Lung and Blood Institute's Framingham Heart Study (Contract No. N01-HC-25195 and Contract No. HHSN268201500001I) and its contract with Affymetrix, Inc for genotyping services (Contract No. N02-HL-6-4278). A portion of this research utilized the Linux Cluster for Genetic Analysis (LinGA-II) funded by the Robert Dawson Evans Endowment of the Department of Medicine at Boston University School of Medicine and Boston Medical Center. This research was partially supported by grant R01-DK089256 from the National Institute of Diabetes and Digestive and Kidney Diseases (MPIs: I.B. Borecki, L.A. Cupples, K. North).

GENOA. Support for the Genetic Epidemiology Network of Arteriopathy (GENOA) was provided by the National Institutes of Health, grant numbers HL085571 and HL087660 from National Heart, Lung, Blood Institute. Genotyping was performed at the Mayo Clinic (Stephen T. Turner, MD, Mariza de Andrade PhD, Julie Cunningham, PhD). We thank Eric Boerwinkle, PhD and Megan L. Grove from the Human Genetics Center and Institute of Molecular Medicine and Division of Epidemiology, University of Texas Health Science Center, Houston, Texas, USA for their help with genotyping. We would also like to thank the families that participated in the GENOA study.

HABC. Health ABC Study acknowledgements (VAT): This research was supported by NIA contracts N01AG62101, N01AG62103, N01AG62106, and R01 AG028288. The Genome-Wide Association Study was funded by NIA grant 1R01AG032098-01A1 to Wake Forest University Health Sciences and genotyping services were provided by the Center for Inherited Disease Research (CIDR). CIDR is fully funded through a federal contract from the National Institutes of Health to The Johns Hopkins University, contract number HHSN268200782096C. This research was supported in part by the Intramural Research Program of the NIH, National Institute on Aging.

JHS. The Jackson Heart Study is supported by contracts HHSN268201300046C, HHSN268201300047C, HHSN268201300048C, HHSN268201300049C, HHSN268201300050C from the National Heart, Lung, and Blood Institute and the National Institute on Minority Health and Health Disparities.

MESA. MESA and the MESA SHARe project are conducted and supported by the National Heart, Lung, and Blood Institute (NHLBI) in collaboration with MESA investigators. Support for MESA is provided by grants R01-HL-085323 and R01-HL-071205 and by contracts N01-HC-95159, N01-HC-95160, N01-HC-95161, N01-HC-95162, N01-HC-95163, N01-HC-95164, N01-HC-95165, N01-HC-95166, N01-HC-95167, N01-HC-95168, N01-HC-95169, UL1-TR-001079, UL1-TR-000040, DK063491, and RR-024156. Funding for SHARe genotyping was provided by NHLBI Contract N02-HL-64278. Genotyping was performed using the Affymetrix Genome-Wide Human SNP Array 6.0. Funding for CARe genotyping was provided by NHLBI Contract N01-HC-65226. Funding support for the abdominal aortic CT dataset was provided by grant 1R01HL088451-01A1. The provision of genotyping data was supported in part by the National Center for Advancing Translational Sciences, CTSI grant UL1TR001881, and the National Institute of Diabetes and Digestive and Kidney Disease Diabetes Research Center (DRC) grant DK063491 to the Southern California Diabetes Endocrinology Research Center. The funders had no role in study design, data collection and analysis, decision to publish, or preparation of the manuscript.

MRCOB/TOPS. This research was conducted in part using data and resources from the Metabolic Risk and Complications of Obesity Genes (MRC-OB) project. The analyses reflect intellectual input and resource development from the TOPS Center for Obesity and Metabolic Research investigators and our collaborators at the Texas Biomedical Research Institute. This work was made possible by funding (stated below) provided by the National Institute of Health and TOPS Club, Inc. The recruitment of the subjects studied here and the SNP genotyping were partially supported by the National Institute of Diabetes and Digestive and Kidney Disease (RO1-DK071895-03, RO1-DK65598-01, and RO1-DK54026), the National Heart, Lung and Blood Institute (RO1-HL34989 and R01-HL74168), the National genome Research Institute (P50-HG4952), and TOPS Club, Inc.

PIVUS. This project was supported by Knut and Alice Wallenberg Foundation (Wallenberg Academy Fellow), European Research Council (ERC Starting Grant), Swedish Diabetes Foundation (2013-024), Swedish Research Council (2012-1397, 2012-1727, 2012-2215, and 2012-2330), Marianne and Marcus Wallenberg Foundation, County Council of Dalarna, Dalarna University, and Swedish Heart-Lung Foundation (20120197). The computations were performed on resources provided by SNIC through Uppsala Multidisciplinary Center for Advanced Computational Science (UPPMAX) under Project b2011036. Genotyping was funded by the Wellcome Trust under award WT064890. Analysis of genetic data was funded by the Wellcome Trust under awards WT098017 and WT090532. We thank the SNP&SEQ Technology Platform in Uppsala (www.genotyping.se) for excellent genotyping. Andrew P Morris is a Wellcome Trust Senior Fellow in Basic Biomedical Science (grant number WT098017).

SHIP-2 and SHIPTREND. SHIP is part of the Community Medicine Research net of the University of Greifswald, Germany, which is funded by the Federal Ministry of Education and Research (grants no. 01ZZ9603, 01ZZ0103, and 01ZZ0403), the Ministry of Cultural Affairs as well as the Social Ministry of

the Federal State of Mecklenburg-West Pomerania, and the network ‘Greifswald Approach to Individualized Medicine (GANI_MED)’ funded by the Federal Ministry of Education and Research (grant 03IS2061A). Whole-body MR imaging was supported by a joint grant from Siemens Healthcare, Erlangen, Germany and the Federal State of Mecklenburg West Pomerania. The University of Greifswald is a member of the 'Center of Knowledge Interchange' program of the Siemens AG and the Caché Campus program of the InterSystems GmbH. The SHIP authors are grateful to Mario Stanke for the opportunity to use his Server Cluster for the SNP imputation as well as to Holger Prokisch and Thomas Meitinger (Helmholtz Zentrum München) for the genotyping of the SHIP-TREND cohort.

Matthew L. Steinhauser was supported by grants from the National Institute of Diabetes and Digestive and Kidney Disease (K08DK090147 and RO3DK106477).

Supplement Only References

1. Almasy, L. & Blangero, J. Multipoint quantitative-trait linkage analysis in general pedigrees. *Am. J. Hum. Genet.* **62**, 1198-1211, doi:10.1086/301844 (1998).
2. Rosenquist, K. J. *et al.* Visceral and subcutaneous fat quality and cardiometabolic risk. *JACC Cardiovasc. Imaging* **6**, 762-771, doi:10.1016/j.jcmg.2012.11.021 (2013).
3. Fox, C. S. *et al.* Abdominal visceral and subcutaneous adipose tissue compartments: association with metabolic risk factors in the Framingham Heart Study. *Circulation* **116**, 39-48, doi:10.1161/CIRCULATIONAHA.106.675355 (2007).
4. Kaess, B. M. *et al.* The ratio of visceral to subcutaneous fat, a metric of body fat distribution, is a unique correlate of cardiometabolic risk. *Diabetologia* **55**, 2622-2630, doi:10.1007/s00125-012-2639-5 (2012).
5. Yeoh, A. J., Pedley, A., Rosenquist, K. J., Hoffmann, U. & Fox, C. S. The Association Between Subcutaneous Fat Density and the Propensity to Store Fat Viscerally. *J. Clin. Endocrinol. Metab.* **100**, E1056-1064, doi:10.1210/jc.2014-4032 (2015).
6. Willer, C. J., Li, Y. & Abecasis, G. R. METAL: fast and efficient meta-analysis of genomewide association scans. *Bioinformatics* **26**, 2190-2191, doi:10.1093/bioinformatics/btq340 (2010).
7. Stouffer, S. A., Suchman, E. A., DeVinney, L. C., Star, S. A. & Williams, R. M. J. *Adjustment During Army Life*. (Princeton University Press, 1949).
8. Shungin, D. *et al.* New genetic loci link adipose and insulin biology to body fat distribution. *Nature* **518**, 187-196, doi:10.1038/nature14132 (2015).
9. Locke, A. E. *et al.* Genetic studies of body mass index yield new insights for obesity biology. *Nature* **518**, 197-206, doi:10.1038/nature14177 (2015).
10. Manning, A. K. *et al.* A genome-wide approach accounting for body mass index identifies genetic variants influencing fasting glycemic traits and insulin resistance. *Nat. Genet.* **44**, 659-669, doi:10.1038/ng.2274 (2012).
11. Replication, D. I. G. *et al.* Genome-wide trans-ancestry meta-analysis provides insight into the genetic architecture of type 2 diabetes susceptibility. *Nat. Genet.* **46**, 234-244, doi:10.1038/ng.2897 (2014).
12. Global Lipids Genetics, C. *et al.* Discovery and refinement of loci associated with lipid levels. *Nat. Genet.* **45**, 1274-1283, doi:10.1038/ng.2797 (2013).
13. International Consortium for Blood Pressure Genome-Wide Association, S. *et al.* Genetic variants in novel pathways influence blood pressure and cardiovascular disease risk. *Nature* **478**, 103-109, doi:10.1038/nature10405 (2011).
14. Ward, L. D. & Kellis, M. HaploReg: a resource for exploring chromatin states, conservation, and regulatory motif alterations within sets of genetically linked variants. *Nucleic Acids Res.* **40**, D930-934, doi:10.1093/nar/gkr917 (2012).
15. Boyle, A. P. *et al.* Annotation of functional variation in personal genomes using RegulomeDB. *Genome Res.* **22**, 1790-1797, doi:10.1101/gr.137323.112 (2012).
16. Gabrielsson, B. G. *et al.* Molecular characterization of a local sulfonylurea system in human adipose tissue. *Mol. Cell. Biochem.* **258**, 65-71 (2004).
17. Naour, N. *et al.* Cathepsins in human obesity: changes in energy balance predominantly affect cathepsin s in adipose tissue and in circulation. *J. Clin. Endocrinol. Metab.* **95**, 1861-1868, doi:10.1210/jc.2009-1894 (2010).
18. Xiao, Y. *et al.* Cathepsin K in adipocyte differentiation and its potential role in the pathogenesis of obesity. *J. Clin. Endocrinol. Metab.* **91**, 4520-4527, doi:10.1210/jc.2005-2486 (2006).
19. Pei, Y. F. *et al.* Meta-analysis of genome-wide association data identifies novel susceptibility loci for obesity. *Hum. Mol. Genet.* **23**, 820-830, doi:10.1093/hmg/ddt464 (2014).
20. Winkler, T. W. *et al.* The Influence of Age and Sex on Genetic Associations with Adult Body Size and Shape: A Large-Scale Genome-Wide Interaction Study. *PLoS genetics* **11**, e1005378, doi:10.1371/journal.pgen.1005378 (2015).

21. Wood, A. R. *et al.* Defining the role of common variation in the genomic and biological architecture of adult human height. *Nat. Genet.* **46**, 1173-1186, doi:10.1038/ng.3097 (2014).
22. Al Olama, A. A. *et al.* A meta-analysis of 87,040 individuals identifies 23 new susceptibility loci for prostate cancer. *Nat. Genet.* **46**, 1103-1109, doi:10.1038/ng.3094 (2014).
23. Macgregor, S. *et al.* Genome-wide association study identifies a new melanoma susceptibility locus at 1q21.3. *Nat. Genet.* **43**, 1114-1118, doi:10.1038/ng.958 (2011).
24. Kirin, M. *et al.* Genome-wide association study identifies genetic risk underlying primary rhegmatogenous retinal detachment. *Hum. Mol. Genet.* **22**, 3174-3185, doi:10.1093/hmg/ddt169 (2013).
25. Kottgen, A. *et al.* New loci associated with kidney function and chronic kidney disease. *Nat. Genet.* **42**, 376-384, doi:10.1038/ng.568 (2010).
26. Guo, Y. *et al.* Genome-wide association study identifies ALDH7A1 as a novel susceptibility gene for osteoporosis. *PLoS genetics* **6**, e1000806, doi:10.1371/journal.pgen.1000806 (2010).
27. Grassi, M. A. *et al.* Genome-wide meta-analysis for severe diabetic retinopathy. *Hum. Mol. Genet.* **20**, 2472-2481, doi:10.1093/hmg/ddr121 (2011).
28. Smith, J. G. *et al.* Impact of ancestry and common genetic variants on QT interval in African Americans. *Circ. Cardiovasc. Genet.* **5**, 647-655, doi:10.1161/CIRCGENETICS.112.962787 (2012).
29. Chung, S. J. *et al.* Genomic determinants of motor and cognitive outcomes in Parkinson's disease. *Parkinsonism Relat. Disord.* **18**, 881-886, doi:10.1016/j.parkreldis.2012.04.025 (2012).
30. Cirulli, E. T. *et al.* Common genetic variation and performance on standardized cognitive tests. *Eur. J. Hum. Genet.* **18**, 815-820, doi:10.1038/ejhg.2010.2 (2010).
31. Hagman, J., Ramirez, J. & Lukin, K. B lymphocyte lineage specification, commitment and epigenetic control of transcription by early B cell factor 1. *Curr. Top. Microbiol. Immunol.* **356**, 17-38, doi:10.1007/82_2011_139 (2012).
32. Milatovich, A., Qiu, R. G., Grosschedl, R. & Francke, U. Gene for a tissue-specific transcriptional activator (EBF or Olf-1), expressed in early B lymphocytes, adipocytes, and olfactory neurons, is located on human chromosome 5, band q34, and proximal mouse chromosome 11. *Mamm. Genome* **5**, 211-215 (1994).
33. Le, T. P., Sun, M., Luo, X., Kraus, W. L. & Greene, G. L. Mapping ERbeta genomic binding sites reveals unique genomic features and identifies EBF1 as an ERbeta interactor. *PLoS One* **8**, e71355, doi:10.1371/journal.pone.0071355 (2013).
34. Singh, A. *et al.* Gene by stress genome-wide interaction analysis and path analysis identify EBF1 as a cardiovascular and metabolic risk gene. *Eur. J. Hum. Genet.* **23**, 854-862, doi:10.1038/ejhg.2014.189 (2015).
35. Wain, L. V. *et al.* Genome-wide association study identifies six new loci influencing pulse pressure and mean arterial pressure. *Nat. Genet.* **43**, 1005-1011, doi:10.1038/ng.922 (2011).
36. Deelen, J. *et al.* Genome-wide association meta-analysis of human longevity identifies a novel locus conferring survival beyond 90 years of age. *Hum. Mol. Genet.* **23**, 4420-4432, doi:10.1093/hmg/ddu139 (2014).
37. Michailidou, K. *et al.* Large-scale genotyping identifies 41 new loci associated with breast cancer risk. *Nat. Genet.* **45**, 353-361, 361e351-352, doi:10.1038/ng.2563 (2013).
38. Low, S. K. *et al.* Genome-wide association study of chemotherapeutic agent-induced severe neutropenia/leucopenia for patients in Biobank Japan. *Cancer Sci.* **104**, 1074-1082, doi:10.1111/cas.12186 (2013).
39. Geller, F. *et al.* Genome-wide association analyses identify variants in developmental genes associated with hypospadias. *Nat. Genet.* **46**, 957-963, doi:10.1038/ng.3063 (2014).
40. Yu, B. *et al.* Genome-wide association study of a heart failure related metabolomic profile among African Americans in the Atherosclerosis Risk in Communities (ARIC) study. *Genet. Epidemiol.* **37**, 840-845, doi:10.1002/gepi.21752 (2013).

41. Fox, C. S. *et al.* Genome-wide association for abdominal subcutaneous and visceral adipose reveals a novel locus for visceral fat in women. *PLoS genetics* **8**, e1002695, doi:10.1371/journal.pgen.1002695 (2012).
42. Berndt, S. I. *et al.* Genome-wide meta-analysis identifies 11 new loci for anthropometric traits and provides insights into genetic architecture. *Nat. Genet.* **45**, 501-512, doi:10.1038/ng.2606 (2013).
43. Heid, I. M. *et al.* Meta-analysis identifies 13 new loci associated with waist-hip ratio and reveals sexual dimorphism in the genetic basis of fat distribution. *Nat. Genet.* **42**, 949-960, doi:10.1038/ng.685 (2010).
44. Liu, C. T. *et al.* Genome-wide association of body fat distribution in African ancestry populations suggests new loci. *PLoS genetics* **9**, e1003681, doi:10.1371/journal.pgen.1003681 (2013).
45. Scott, R. A. *et al.* Large-scale association analyses identify new loci influencing glycemic traits and provide insight into the underlying biological pathways. *Nat. Genet.* **44**, 991-1005, doi:10.1038/ng.2385 (2012).
46. Fingerlin, T. E. *et al.* Genome-wide association study identifies multiple susceptibility loci for pulmonary fibrosis. *Nat. Genet.* **45**, 613-620, doi:10.1038/ng.2609 (2013).
47. Kottgen, A. *et al.* Genome-wide association analyses identify 18 new loci associated with serum urate concentrations. *Nat. Genet.* **45**, 145-154, doi:10.1038/ng.2500 (2013).
48. Yang, Q. *et al.* Multiple genetic loci influence serum urate levels and their relationship with gout and cardiovascular disease risk factors. *Circ. Cardiovasc. Genet.* **3**, 523-530, doi:10.1161/CIRCGENETICS.109.934455 (2010).
49. International Multiple Sclerosis Genetics, C. *et al.* Genetic risk and a primary role for cell-mediated immune mechanisms in multiple sclerosis. *Nature* **476**, 214-219, doi:10.1038/nature10251 (2011).
50. Neale, B. M. *et al.* Genome-wide association study of advanced age-related macular degeneration identifies a role of the hepatic lipase gene (LIPC). *Proc. Natl. Acad. Sci. U. S. A.* **107**, 7395-7400, doi:10.1073/pnas.0912019107 (2010).
51. Lindstrom, S. *et al.* Genome-wide association study identifies multiple loci associated with both mammographic density and breast cancer risk. *Nature communications* **5**, 5303, doi:10.1038/ncomms6303 (2014).
52. Shyn, S. I. *et al.* Novel loci for major depression identified by genome-wide association study of Sequenced Treatment Alternatives to Relieve Depression and meta-analysis of three studies. *Mol. Psychiatry* **16**, 202-215, doi:10.1038/mp.2009.125 (2011).
53. Beltowski, J. & Jazmroz-Wisniewska, A. Transactivation of ErbB receptors by leptin in the cardiovascular system: mechanisms, consequences and target for therapy. *Curr. Pharm. Des.* **20**, 616-624 (2014).
54. Fontaine, C. *et al.* The orphan nuclear receptor Rev-Erbalpha is a peroxisome proliferator-activated receptor (PPAR) gamma target gene and promotes PPARgamma-induced adipocyte differentiation. *J. Biol. Chem.* **278**, 37672-37680, doi:10.1074/jbc.M304664200 (2003).
55. Wang, J. & Lazar, M. A. Bifunctional role of Rev-erbalpha in adipocyte differentiation. *Mol. Cell. Biol.* **28**, 2213-2220, doi:10.1128/MCB.01608-07 (2008).
56. Fernandez-Real, J. M. *et al.* Thyroid hormone receptor alpha gene variants increase the risk of developing obesity and show gene-diet interactions. *Int. J. Obes. (Lond.)* **37**, 1499-1505, doi:10.1038/ijo.2013.11 (2013).
57. Ortega, F. J. *et al.* Subcutaneous fat shows higher thyroid hormone receptor-alpha1 gene expression than omental fat. *Obesity* **17**, 2134-2141, doi:10.1038/oby.2009.110 (2009).
58. Zhu, X. G., Kim, D. W., Goodson, M. L., Privalsky, M. L. & Cheng, S. Y. NCoR1 regulates thyroid hormone receptor isoform-dependent adipogenesis. *J. Mol. Endocrinol.* **46**, 233-244, doi:10.1530/JME-10-0163 (2011).
59. Redonnet, A. *et al.* Relationship between peroxisome proliferator-activated receptor gamma and retinoic acid receptor alpha gene expression in obese human adipose tissue. *Int. J. Obes. Relat. Metab. Disord.* **26**, 920-927, doi:10.1038/sj.ijo.0802025 (2002).

60. Chen, W., Yang, Q. & Roeder, R. G. Dynamic interactions and cooperative functions of PGC-1alpha and MED1 in TRalpha-mediated activation of the brown-fat-specific UCP-1 gene. *Mol. Cell* **35**, 755-768, doi:10.1016/j.molcel.2009.09.015 (2009).
61. Ge, K. *et al.* Transcription coactivator TRAP220 is required for PPAR gamma 2-stimulated adipogenesis. *Nature* **417**, 563-567, doi:10.1038/417563a (2002).
62. Bonnelykke, K. *et al.* A genome-wide association study identifies CDHR3 as a susceptibility locus for early childhood asthma with severe exacerbations. *Nat. Genet.* **46**, 51-55, doi:10.1038/ng.2830 (2014).
63. Torgerson, D. G. *et al.* Meta-analysis of genome-wide association studies of asthma in ethnically diverse North American populations. *Nat. Genet.* **43**, 887-892, doi:10.1038/ng.888 (2011).
64. van der Valk, R. J. *et al.* Fraction of exhaled nitric oxide values in childhood are associated with 17q11.2-q12 and 17q12-q21 variants. *J. Allergy Clin. Immunol.* **134**, 46-55, doi:10.1016/j.jaci.2013.08.053 (2014).
65. Hinds, D. A. *et al.* A genome-wide association meta-analysis of self-reported allergy identifies shared and allergy-specific susceptibility loci. *Nat. Genet.* **45**, 907-911, doi:10.1038/ng.2686 (2013).
66. Barrett, J. C. *et al.* Genome-wide association defines more than 30 distinct susceptibility loci for Crohn's disease. *Nat. Genet.* **40**, 955-962, doi:10.1038/ng.175 (2008).
67. Franke, A. *et al.* Genome-wide meta-analysis increases to 71 the number of confirmed Crohn's disease susceptibility loci. *Nat. Genet.* **42**, 1118-1125, doi:10.1038/ng.717 (2010).
68. Barrett, J. C. *et al.* Genome-wide association study and meta-analysis find that over 40 loci affect risk of type 1 diabetes. *Nat. Genet.* **41**, 703-707, doi:10.1038/ng.381 (2009).
69. Anderson, C. A. *et al.* Meta-analysis identifies 29 additional ulcerative colitis risk loci, increasing the number of confirmed associations to 47. *Nat. Genet.* **43**, 246-252, doi:10.1038/ng.764 (2011).
70. McGovern, D. P. *et al.* Genome-wide association identifies multiple ulcerative colitis susceptibility loci. *Nat. Genet.* **42**, 332-337, doi:10.1038/ng.549 (2010).
71. Okada, Y. *et al.* Genetics of rheumatoid arthritis contributes to biology and drug discovery. *Nature* **506**, 376-381, doi:10.1038/nature12873 (2014).
72. Liu, X. *et al.* Genome-wide meta-analyses identify three loci associated with primary biliary cirrhosis. *Nat. Genet.* **42**, 658-660, doi:10.1038/ng.627 (2010).
73. Nakamura, M. *et al.* Genome-wide association study identifies TNFSF15 and POU2AF1 as susceptibility loci for primary biliary cirrhosis in the Japanese population. *Am. J. Hum. Genet.* **91**, 721-728, doi:10.1016/j.ajhg.2012.08.010 (2012).
74. Jostins, L. *et al.* Host-microbe interactions have shaped the genetic architecture of inflammatory bowel disease. *Nature* **491**, 119-124, doi:10.1038/nature11582 (2012).
75. Shi, Y. *et al.* A genome-wide association study identifies two new cervical cancer susceptibility loci at 4q12 and 17q12. *Nat. Genet.* **45**, 918-922, doi:10.1038/ng.2687 (2013).
76. Crosslin, D. R. *et al.* Genetic variants associated with the white blood cell count in 13,923 subjects in the eMERGE Network. *Hum. Genet.* **131**, 639-652, doi:10.1007/s00439-011-1103-9 (2012).
77. Kamatani, Y. *et al.* Genome-wide association study of hematological and biochemical traits in a Japanese population. *Nat. Genet.* **42**, 210-215, doi:10.1038/ng.531 (2010).
78. Nalls, M. A. *et al.* Multiple loci are associated with white blood cell phenotypes. *PLoS genetics* **7**, e1002113, doi:10.1371/journal.pgen.1002113 (2011).
79. Soranzo, N. *et al.* A genome-wide meta-analysis identifies 22 loci associated with eight hematological parameters in the HaemGen consortium. *Nat. Genet.* **41**, 1182-1190, doi:10.1038/ng.467 (2009).
80. Shin, S. Y. *et al.* An atlas of genetic influences on human blood metabolites. *Nat. Genet.* **46**, 543-550, doi:10.1038/ng.2982 (2014).

81. Arking, D. E. *et al.* Genetic association study of QT interval highlights role for calcium signaling pathways in myocardial repolarization. *Nat. Genet.* **46**, 826-836, doi:10.1038/ng.3014 (2014).
82. Lind, P. A. *et al.* Genome-wide association study of a quantitative disordered gambling trait. *Addict. Biol.* **18**, 511-522, doi:10.1111/j.1369-1600.2012.00463.x (2013).
83. Investigators, G., Investigators, M. & Investigators, S. D. Common genetic variation and antidepressant efficacy in major depressive disorder: a meta-analysis of three genome-wide pharmacogenetic studies. *Am. J. Psychiatry* **170**, 207-217, doi:10.1176/appi.ajp.2012.12020237 (2013).
84. Landers, J. E. *et al.* Reduced expression of the Kinesin-Associated Protein 3 (KIFAP3) gene increases survival in sporadic amyotrophic lateral sclerosis. *Proc. Natl. Acad. Sci. U. S. A.* **106**, 9004-9009, doi:10.1073/pnas.0812937106 (2009).
85. Yamauchi, T. *et al.* A genome-wide association study in the Japanese population identifies susceptibility loci for type 2 diabetes at UBE2E2 and C2CD4A-C2CD4B. *Nat. Genet.* **42**, 864-868, doi:10.1038/ng.660 (2010).
86. Hara, K. *et al.* Genome-wide association study identifies three novel loci for type 2 diabetes. *Hum. Mol. Genet.* **23**, 239-246, doi:10.1093/hmg/ddt399 (2014).
87. Kanazawa, T. *et al.* Genome-wide association study of atypical psychosis. *Am. J. Med. Genet. B Neuropsychiatr. Genet.* **162B**, 679-686, doi:10.1002/ajmg.b.32164 (2013).
88. Jiao, S. *et al.* Genome-wide search for gene-gene interactions in colorectal cancer. *PLoS One* **7**, e52535, doi:10.1371/journal.pone.0052535 (2012).
89. Gudbjartsson, D. F. *et al.* Association of variants at UMOD with chronic kidney disease and kidney stones-role of age and comorbid diseases. *PLoS genetics* **6**, e1001039, doi:10.1371/journal.pgen.1001039 (2010).
90. Johnson, A. D. *et al.* SNAP: a web-based tool for identification and annotation of proxy SNPs using HapMap. *Bioinformatics* **24**, 2938-2939, doi:10.1093/bioinformatics/btn564 (2008).
91. Emilsson, V. *et al.* Genetics of gene expression and its effect on disease. *Nature* **452**, 423-428, doi:10.1038/nature06758 (2008).
92. Greenawalt, D. M. *et al.* A survey of the genetics of stomach, liver, and adipose gene expression from a morbidly obese cohort. *Genome Res.* **21**, 1008-1016, doi:10.1101/gr.112821.110 (2011).
93. Grundberg, E. *et al.* Mapping cis- and trans-regulatory effects across multiple tissues in twins. *Nat. Genet.* **44**, 1084-1089, doi:10.1038/ng.2394 (2012).
94. Consortium, G. T. The Genotype-Tissue Expression (GTEx) project. *Nat. Genet.* **45**, 580-585, doi:10.1038/ng.2653 (2013).
95. Foroughi Asl, H. *et al.* Expression quantitative trait Loci acting across multiple tissues are enriched in inherited risk for coronary artery disease. *Circ. Cardiovasc. Genet.* **8**, 305-315, doi:10.1161/CIRCGENETICS.114.000640 (2015).
96. Harris, T. B. *et al.* Age, Gene/Environment Susceptibility-Reykjavik Study: multidisciplinary applied phenomics. *Am. J. Epidemiol.* **165**, 1076-1087, doi:10.1093/aje/kwk115 (2007).
97. Koster, A. *et al.* Fat distribution and mortality: the AGES-Reykjavik Study. *Obesity* **23**, 893-897, doi:10.1002/oby.21028 (2015).
98. Sorkin, J. *et al.* Exploring the genetics of longevity in the Old Order Amish. *Mech. Ageing Dev.* **126**, 347-350, doi:10.1016/j.mad.2004.08.027 (2005).
99. Post, W. *et al.* Determinants of coronary artery and aortic calcification in the Old Order Amish. *Circulation* **115**, 717-724, doi:10.1161/CIRCULATIONAHA.106.637512 (2007).
100. Higgins, M. *et al.* NHLBI Family Heart Study: objectives and design. *Am. J. Epidemiol.* **143**, 1219-1228 (1996).
101. Carr, J. J. *et al.* Calcified coronary artery plaque measurement with cardiac CT in population-based studies: standardized protocol of Multi-Ethnic Study of Atherosclerosis (MESA) and Coronary Artery Risk Development in Young Adults (CARDIA) study. *Radiology* **234**, 35-43, doi:10.1148/radiol.2341040439 (2005).

102. Chumlea, W. C. *et al.* The first seriatim study into old age for weight, stature and BMI: the Fels Longitudinal Study. *J. Nutr. Health Aging* **13**, 3-5 (2009).
103. Demerath, E. W. *et al.* Validity of a new automated software program for visceral adipose tissue estimation. *Int. J. Obes. (Lond.)* **31**, 285-291, doi:10.1038/sj.ijo.0803409 (2007).
104. Demerath, E. W. *et al.* Approximation of total visceral adipose tissue with a single magnetic resonance image. *Am. J. Clin. Nutr.* **85**, 362-368 (2007).
105. Dawber, T. R., Meadors, G. F. & Moore, F. E., Jr. Epidemiological approaches to heart disease: the Framingham Study. *Am. J. Public Health Nations Health* **41**, 279-281 (1951).
106. Splansky, G. L. *et al.* The Third Generation Cohort of the National Heart, Lung, and Blood Institute's Framingham Heart Study: design, recruitment, and initial examination. *Am. J. Epidemiol.* **165**, 1328-1335, doi:10.1093/aje/kwm021 (2007).
107. Price, A. L. *et al.* Principal components analysis corrects for stratification in genome-wide association studies. *Nat. Genet.* **38**, 904-909, doi:10.1038/ng1847 (2006).
108. Maurovich-Horvat, P. *et al.* Comparison of anthropometric, area- and volume-based assessment of abdominal subcutaneous and visceral adipose tissue volumes using multi-detector computed tomography. *Int. J. Obes. (Lond.)* **31**, 500-506, doi:10.1038/sj.ijo.0803454 (2007).
109. Rosito, G. A. *et al.* Pericardial fat, visceral abdominal fat, cardiovascular disease risk factors, and vascular calcification in a community-based sample: the Framingham Heart Study. *Circulation* **117**, 605-613, doi:10.1161/CIRCULATIONAHA.107.743062 (2008).
110. Daniels, P. R. *et al.* Familial aggregation of hypertension treatment and control in the Genetic Epidemiology Network of Arteriopathy (GENOA) study. *Am. J. Med.* **116**, 676-681, doi:10.1016/j.amjmed.2003.12.032 (2004).
111. Investigators, F. Multi-center genetic study of hypertension: The Family Blood Pressure Program (FBPP). *Hypertension* **39**, 3-9 (2002).
112. Liu, J. *et al.* Pericardial adipose tissue, atherosclerosis, and cardiovascular disease risk factors: the Jackson heart study. *Diabetes Care* **33**, 1635-1639, doi:10.2337/dc10-0245 (2010).
113. Liu, J. *et al.* Impact of abdominal visceral and subcutaneous adipose tissue on cardiometabolic risk factors: the Jackson Heart Study. *J. Clin. Endocrinol. Metab.* **95**, 5419-5426, doi:10.1210/jc.2010-1378 (2010).
114. Li, Y., Willer, C. J., Ding, J., Scheet, P. & Abecasis, G. R. MaCH: using sequence and genotype data to estimate haplotypes and unobserved genotypes. *Genet. Epidemiol.* **34**, 816-834, doi:10.1002/gepi.20533 (2010).
115. O'Connell, J. in *63th Annual Meeting of The American Society of Human Genetics* (Boston MA USA, 2013).
116. Bild, D. E. *et al.* Multi-Ethnic Study of Atherosclerosis: objectives and design. *Am. J. Epidemiol.* **156**, 871-881 (2002).
117. Kissebah, A. H. *et al.* Quantitative trait loci on chromosomes 3 and 17 influence phenotypes of the metabolic syndrome. *Proc. Natl. Acad. Sci. U. S. A.* **97**, 14478-14483, doi:10.1073/pnas.97.26.14478 (2000).
118. Zhang, Y. *et al.* Obesity-related dyslipidemia associated with FAAH, independent of insulin response, in multigenerational families of Northern European descent. *Pharmacogenomics* **10**, 1929-1939, doi:10.2217/pgs.09.122 (2009).
119. Peiris, A. N. *et al.* Relationship of anthropometric measurements of body fat distribution to metabolic profile in premenopausal women. *Acta Med. Scand. Suppl.* **723**, 179-188 (1988).
120. Tokunaga, K., Matsuzawa, Y., Ishikawa, K. & Tarui, S. A novel technique for the determination of body fat by computed tomography. *Int. J. Obes.* **7**, 437-445 (1983).
121. Borkan, G. A. *et al.* Assessment of abdominal fat content by computed tomography. *Am. J. Clin. Nutr.* **36**, 172-177 (1982).
122. Kvist, H., Chowdhury, B., Grangard, U., Tylen, U. & Sjostrom, L. Total and visceral adipose-tissue volumes derived from measurements with computed tomography in adult men and women: predictive equations. *Am. J. Clin. Nutr.* **48**, 1351-1361 (1988).

123. Abecasis, G. R., Cherny, S. S., Cookson, W. O. & Cardon, L. R. Merlin--rapid analysis of dense genetic maps using sparse gene flow trees. *Nat. Genet.* **30**, 97-101, doi:10.1038/ng786 (2002).
124. Delaneau, O., Marchini, J. & Zagury, J. F. A linear complexity phasing method for thousands of genomes. *Nature methods* **9**, 179-181, doi:10.1038/nmeth.1785 (2012).
125. Howie, B., Marchini, J. & Stephens, M. Genotype imputation with thousands of genomes. *G3* **1**, 457-470, doi:10.1534/g3.111.001198 (2011).
126. Boerwinkle, E. & Sing, C. F. The use of measured genotype information in the analysis of quantitative phenotypes in man. III. Simultaneous estimation of the frequencies and effects of the apolipoprotein E polymorphism and residual polygenetic effects on cholesterol, betalipoprotein and triglyceride levels. *Ann. Hum. Genet.* **51**, 211-226 (1987).
127. Lind, L., Fors, N., Hall, J., Marttala, K. & Stenborg, A. A comparison of three different methods to evaluate endothelium-dependent vasodilation in the elderly: the Prospective Investigation of the Vasculature in Uppsala Seniors (PIVUS) study. *Arterioscler. Thromb. Vasc. Biol.* **25**, 2368-2375, doi:10.1161/01.ATV.0000184769.22061.da (2005).
128. Kullberg, J. *et al.* Practical approach for estimation of subcutaneous and visceral adipose tissue. *Clin. Physiol. Funct. Imaging* **27**, 148-153, doi:10.1111/j.1475-097X.2007.00728.x (2007).
129. John, U. *et al.* Study of Health In Pomerania (SHIP): a health examination survey in an east German region: objectives and design. *Soz. Praventivmed.* **46**, 186-194 (2001).
130. Volzke, H. *et al.* Cohort profile: the study of health in Pomerania. *Int. J. Epidemiol.* **40**, 294-307, doi:10.1093/ije/dyp394 (2011).